

GAS PHASE EXTRACTION OF VANADIUM FROM SPENT VANADIUM CATALYST AND TANTALUM FROM TANTALUM OXIDE



Dissertation submitted to the faculty of Engineering and the Built Environment, University of the Witwatersrand in fulfilment of the requirements for the degree of Master of Science in Engineering

by

**Author: Obakeng Daniel Olehile
(0709312J)**

Supervised by: Prof. Lizelle van Dyk

Metals Extraction and Recovery Group (MERG)
School of Chemical and Metallurgical Engineering

October 2017

DECLARATION

1. I know that plagiarism is wrong. Plagiarism is to use another's work and to pretend that it is one's own.
2. I have used the Harvard referencing system for citation and referencing. Each significant contribution to, and quotation in, this report from the work, or works, of other people has been attributed, and has been cited and referenced.
3. This dissertation is my own work.

Name.....

Signature.....

ABSTRACT

Gas phase extraction of metals using volatile organic reagents can be applied to metal bearing sources such as metal oxides, iron ore fines and fly ash. The process has the potential of having a smaller environmental impact compared with conventional extraction processes and the possibility also exists to recover and recycle the extractant. The research was directed to extend the application of gas phase extraction to two new metal systems, namely spent vanadium catalysts and a synthetic low grade tantalum oxide “ore”.

A literature review revealed that acetylacetone, trifluoro-acetylacetone and hexafluoro-acetylacetone were suitable extractants for vanadium and tantalum in a gas phase process. Due to safety considerations the fluorinated acetylacetone derivatives were not applied in the process and acetylacetone was the only extractant under investigation. The influence of the process parameters, temperature, particle size, acetylacetone flowrate and bed weight of the solid, on the extraction extent was studied for each system.

The sulphuric acid spent catalyst contained 49.03 mg vanadium/ g catalyst and the process was capable of extracting up to 60.3% of vanadium after contacting 15 g of catalyst (particle size +250 μ m to -500 μ m) with 7 mL/min of acetylacetone at a reaction temperature of 190 °C after 7 hours. It was also found that the reaction temperature, acetylacetone flowrate, and the interaction effects between particle size, ligand flowrate and catalyst bed loading, had a significant influence on the extraction degree of vanadium at 95% confidence level. Furthermore, a kinetic analysis revealed that the gas phase extraction was either mixed controlled or diffusion controlled.

The preliminary tantalum extraction study conducted here shows that gas phase extraction can be successfully applied to a synthetic tantalum oxide-silica sand mixture. The highest tantalum extraction of 93.4% was achieved at 150 °C after 5 hours of extraction at an acetylacetone flowrate of 7 mL/min for a 15 g bed (2 wt% Ta₂O₅). The solid-gas reaction between tantalum oxide and acetylacetone fluidised bed reactor were significantly influenced by the joint interaction effect of tantalum oxide concentration, acetylacetone flowrate and bed weight of the synthetic tantalum oxide mixture at 95% confidence level. The kinetic study showed that the gas phase extraction reaction of tantalum was governed by diffusion.

ACKNOWLEDGEMENTS

LORD Jesus Christ, thank you for the gift of life. I got hit by a car (2015) and ran over by another (2016) within the period of this project, and as though that was not enough, I was attacked by robbers 3 times in a row (2016 & 2017). But LORD, you proved to be my absolute shield and strength because I sustained no harm from all the incidences either physically or emotionally, and you made it possible for me to successfully finish and close this stormy chapter of my life. Praise and Glory be unto your name LORD, I will forever be at awe of your works, and in you I will always be satisfied.

I would also like to extend my most sincere appreciation and gratitude to my most awesome supervisor Prof. Lizelle van Dyk. Prof. Van Dyk, thank you for your guidance, wisdom, encouragement and absolute patience. You are truly amazing and I would still choose to have you as my supervisor. I will always be grateful for having been in the midst of a non-compromising high calibre supervisor like you.

Once again, Prof. Van Dyk and the National Research Foundation (NRF), thank you for the financial support that enabled the purchasing of the research materials and equipment, as well as covering costs for accommodation, I really appreciate it, all these made it easier to successfully conduct the research project. Furthermore, thanks to Mr Doctor Mbese, I really appreciate your help with AAS sample analysis throughout the entire period; your assistance will never be forgotten, and of course thanks to the School of Chemical and Metallurgical Engineering for the research facilities and amazing staff members.

To my friends: Phasha Motshamonyane, Morapeli Matjoi, Andries Coetsee, Collin Nelson, Pauline Kern-Nelson, Wesley Neutt, Navern Naidoo, Keenan Heynes, Khanyiso Vuyelwa, Benjamin Mhantando, Mlungisi Dlamini and my special friend Veleshia Govender thanks for lending me your ear, every one of you played their own unique role. My dearest brother, Kealeboga Motitswe, as for you, I'm at loss for words, you've helped me throughout the years and you are an absolute blessing, words cannot express my gratitude to you honestly!

Lastly, but certainly not least, I would like to give thanks to my family, without your love and support, I would never have made it this far. Indeed, after my LORD and Saviour Jesus Christ, you are without a doubt, my most cherished treasure in this life. Thank you for always being there, and to my late grandmother Ebbie Motitswe, thanks for your words of encouragements and for the lessons you taught me through your character and of course Mama, Johanna Olehile, only God knows how grateful I am for you, Papa, Benjamin Olehile, Tshepiso Modise, Mmane Wabiki, I will always cherish and love all of you. Modimo a le tshegofatse ka dinako tsotlhe!!!

TABLE OF CONTENTS

DECLARATION	i
ABSTRACT	ii
ACKNOWLEDGEMENTS.....	iii
TABLE OF CONTENTS.....	iv
LIST OF FIGURES.....	vi
LIST OF TABLES	ix
NOMENCLATURE.....	xii
1 INTRODUCTION	1
1.1 Background	1
1.2 Problem statement	2
1.3 Objectives.....	3
1.4 Dissertation Structure	3
2 LITERATURE REVIEW	4
2.1 Conventional Recovery Routes of Metals from Industrial Waste	4
2.2 Gas-phase Extraction Process using Volatile Chelating Ligands	6
2.2.1 Kinetic analysis for the gas-solid reactions in the gas phase extraction process	8
2.2.2 Recent studies on the selective extraction of metals using gaseous organic extractants	11
2.3 Formation and Typical Composition of Spent Vanadium Catalyst used in the Contact Process	13
2.3.1 Studies on the recovery of vanadium from vanadium spent catalyst	14
2.4 Sources of Tantalum Scrap and Recovery Methods	15
2.5 Polydentate chelating reagents complexing with Vanadium and Tantalum .	18
2.5.1 Introduction.....	18
2.5.2 Studies of vanadium chelates.....	19

2.5.3	Studies of tantalum chelates.....	20
2.5.4	Selected chelating reagents for vanadium and tantalum experiments..	20
3	EXPERIMENTAL.....	21
3.1	Materials.....	21
3.2	Experimental Setup	21
3.3	Experimental procedure	24
3.3.1	Sample preparation	24
3.3.2	Process start-up and operation procedure.....	24
3.3.3	Process shut-down procedure	25
3.4	Experimental methods.....	25
4	RESULTS AND DISCUSION OF RESULTS.....	29
4.1	Vanadium extraction from spent vanadium catalyst	29
4.1.1	Determination of significant experimental factors	29
4.1.2	Kinetic analysis of vanadium extraction experiments	42
4.1.3	Optimization experiments	45
4.2	Tantalum extraction from tantalum oxide -silica sand mixture	46
4.2.1	Determination of significant parameters	46
4.2.2	Kinetic analysis of tantalum extraction experiments	54
4.2.3	Additional Experiments.....	55
5	CONCLUSIONS	57
6	RECOMMENDATIONS	58
7	REFERENCES	59
	APPENDIX A: EXPERIMENTAL Data OF EXTRACTION EXPERIMENTS.....	67
	APPENDIX B: STATISTICAL ANALYSIS CALCULATIONS.....	83
	APPENDIX C: KINETIC ANALYSIS - VANADIUM EXTRACTION EXPERIMENTS	90
	APPENDIX D: KINETIC ANALYSIS –TANTALUM EXTRACTION EXPERIMENTS	99

LIST OF FIGURES

Figure 2-1:	Basic flowsheet of hydrometallurgical process (Adapted from Gupta, 2006).....	5
Figure 2-2:	Industrial and laboratory scale application of bio-hydrometallurgical processing technique for metal recovery (Adapted from Willner et al., 2015).....	6
Figure 2-3:	Gas-phase extraction process flowsheet (Adapted from Allimann-Lecourt et al., 2002).	8
Figure 2-4:	Schematic representation of the shrinking unreacted core particle (Levenspiel, 1972).....	10
Figure 2-5:	Flowsheet for the recovery of vanadium from leached solution of spent V_2O_5 catalyst using Cyanex 272 (Painuly, 2015).	15
Figure 2-6:	Flowsheet for commercial tin slag processing for tantalum recovery and proposed treatment method for processing tantalum capacitor scrap (Gupta, 2006; Mineta & Okabe, 2005).	16
Figure 2-7:	Types of ligands by the manner in which they bind to the central metal ion from their respective complexes-Monodentate (a) and polydentate ligands (b-c). Common organic ligands- acac, o-phen and bbip (Van der Put, 1998).	18
Figure 3-1:	The gas phase extraction schematic diagram.	22
Figure 3-2:	Extractant pre-heater.	22
Figure 3-3:	Evaporation unit consisting of heating mantle and evaporation flask. .	23
Figure 3-4:	Column reactor used in the gas phase extraction process.....	23
Figure 3-5:	Condenser Column.	24
Figure 4-1:	Vanadium extraction with time (5 g bed loading and acetylacetone flowrate of 1 mL/min).....	32
Figure 4-2:	Vanadium extraction with time (15 g bed loading and acetylacetone flowrate of 1 mL/min).....	32
Figure 4-3:	Vanadium extraction with time (5 g bed loading and acetylacetone flowrate of 5 mL/min).....	33
Figure 4-4:	Vanadium extraction with time (15 g bed loading and acetylacetone flowrate of 5 mL/min).....	33
Figure 4-5:	Normal probability plot of factor effects on vanadium extraction response.	34

Figure 4-6: Effect of temperature on the extraction extent of vanadium from spent vanadium catalyst, using acetylacetone as a volatile ligand.	36
Figure 4-7: Effect of acetylacetone flowrate on the extraction extent of vanadium from spent vanadium catalyst.....	36
Figure 4-8: Influence of BCD interaction effect on the extraction extent of vanadium from spent vanadium catalyst, using acetylacetone as a volatile ligand.	37
Figure 4-9: Vanadium extraction with time (15 g bed loading and reaction temperature of 200 °C).....	39
Figure 4-10: Vanadium extraction with time (50 g bed loading and reaction temperature of 200 °C).....	39
Figure 4-11: Normal probability plot of factor effects on the vanadium extraction response.	40
Figure 4-12: Effect of flowrate on the extraction extent of vanadium from spent vanadium catalyst.	41
Figure 4-13: Effect of bed loading on the extraction extent of vanadium from spent vanadium catalyst	41
Figure 4-14: Influence of BCD interaction effect on the extraction extent of vanadium from spent vanadium catalyst.....	42
Figure 4-15: Influence of BC interaction effect on the extraction extent of vanadium from spent vanadium catalyst.....	42
Figure 4-16: Optimization experiments for vanadium extraction from spent vanadium catalyst over the duration of 7 hours.	46
Figure 4-17: Tantalum extraction with time (15 g bed loading and acetylacetone flowrate of 5 mL/min).....	48
Figure 4-18: Tantalum extraction with time (50 g bed loading and acetylacetone flowrate of 5 mL/min).....	48
Figure 4-19: Tantalum extraction with time (15 g bed loading and acetylacetone flowrate of 7 mL/min).....	49
Figure 4-20: Tantalum extraction with time (50 g bed loading and acetylacetone flowrate of 7 mL/min).....	49
Figure 4-21: Normal probability plot of factor effects on tantalum extraction results.	50
Figure 4-22: Effect of tantalum oxide concentration on the extraction extent.	51
Figure 4-23: Effect of acetylacetone flowrate on the extraction extent of tantalum from tantalum oxide/silica mixture.	52

Figure 4-24: Influence of bed load on the extraction extent of tantalum from tantalum oxide/silica mixture.	52
Figure 4-25: Influence of AC interaction effect on the extraction extent of tantalum from tantalum oxide/silica mixture.	52
Figure 4-26: Influence of AD interaction effect on the extraction extent of tantalum from tantalum oxide/silica mixture, using acetylacetone as a volatile ligand.	53
Figure 4-27: Influence of CD interaction effect on the extraction extent of tantalum from tantalum oxide/silica mixture, using acetylacetone as a volatile ligand.	53
Figure 4-28: Influence of ACD interaction effect on the extraction extent of tantalum from tantalum oxide/silica mixture, using acetylacetone as a volatile ligand.	53
Figure 4-29: Additional experiments for tantalum extraction from synthetic tantalum containing mixture.	56
Figure C-1: Kinetic model regression curves for vanadium extraction experiments at 5 g and 1 mL/min.	96
Figure C-2: Kinetic model regression curves for vanadium extraction experiments at 15 g and 1 mL/min.	96
Figure C-3: Kinetic model regression curves for vanadium extraction experiments at 5 g and 5 mL/min.	97
Figure C-4: Kinetic model regression curves for vanadium extraction experiments at 15 g and 5 mL/min.	97
Figure C-5: Kinetic model regression curves for additional experiments at 15 g and 7 mL/min.	98
Figure C-6: Kinetic model regression curves for additional experiments at 50 g and 7 mL/min.	98
Figure D-1: Kinetic model regression curves for tantalum extraction experiments at 15 g and 3 mL/min.	103
Figure D-2: Kinetic model regression curves for tantalum extraction experiments at 50 g and 3 mL/min.	103
Figure D-3: Kinetic model regression curves for tantalum extraction experiments at 15 g and 5 mL/min.	104
FigureD-4: Kinetic model regression curves for tantalum extraction experiments at 50 g and 5 mL/min.	104

LIST OF TABLES

Table 2-1: Summary of Non-Catalytic Gas-Solid Reaction-Diffusion Kinetic Models (Leib & Pereira, 2008).....	9
Table 2-2: Recoveries of metals from their respective metal oxides at optimum operational conditions (Potgieter et al., 2006).	12
Table 2-3: Chemical composition of vanadium spent catalyst from contact process (adapted from Mazurek, 2010).	13
Table 3-1: Properties of acetylacetone used for vanadium and tantalum extraction experiments.	21
Table 3-2: The metal source matrixes charged in the reaction column for extraction experiments.	21
Table 3-3: Factorial design experiments for vanadium extraction case study, using acetylacetone.	26
Table 3-4: Optimization experiments for vanadium extraction experiments.....	26
Table 3-5: Factorial design experiments for vanadium extraction case study.....	27
Table 3-6: Criteria used to estimate k at different values of σ^2 (Szekely et al., 1976).	28
Table 4-1: Summary results of 2^4 factorial design experiments for vanadium extraction.	31
Table 4-2: <i>Analysis of variance for vanadium extraction factorial design experiments</i>	34
Table 4-3: Summary results of 2^3 factorial design experiments for vanadium extraction.	38
Table 4-4: Analysis of variance for the design.	40
Table 4-5: Kinetic rate constants and effective diffusivities of initial vanadium experiments.	44
Table 4-6: Kinetic rate constants and effective diffusivities of initial vanadium experiments.	45
Table 4-7: The design matrix and summary results for vanadium extraction experiments, using acetylacetone as extractant.	47
Table 4-8: Analysis of variance for tantalum extraction results.	50
Table 4-9: Summary of the attained shrinking core-reaction modulus and kinetic rate constants for tantalum extraction experiments.	55
Table A-1: Legend for variable experimental parameters at 2-level conditions.....	68
TableA-2: Experimental design matrix for vanadium extraction experiments.....	68

Table A-3: Raw data for vanadium extraction experiments: Experimental design experiment 1-4.....	69
Table A-4: Raw data for vanadium extraction experiments: Experimental design experiment 5-8.....	70
Table A-5: Raw data for vanadium extraction experiments: Experimental design experiment 9-12.....	71
Table A-6: Raw data for vanadium extraction experiments: Experimental design experiment 13-16.....	72
Table A-7: Legend for variable experimental parameters at 2-level conditions: additional vanadium experiments.	73
TableA-8: Experimental design matrix for additional vanadium extraction experiments.	73
Table A-9: Raw data for vanadium extraction experiments: Experimental design experiment 1-4.....	74
Table A-10:Raw data for vanadium extraction experiments: Experimental design experiment 5-8.....	75
Table A-11:Vanadium extraction optimisation experiments.	76
Table A-12:Additional vanadium extraction experiment.	77
Table A-13:Legend for variable experimental parameters at 2-level conditions.	78
Table A-14:Experimental design matrix for tantalum extraction experiments.....	78
Table A-15:Raw data for tantalum extraction experiments: Experimental design experiment 1-4.....	79
Table A-16:Raw data for tantalum extraction experiments: Experimental design experiment 5-6.....	80
Table A-17:Raw data for tantalum extraction experiments: Experimental design experiment 9-12.....	81
Table A-18:Raw data for tantalum extraction experiments: Experimental design experiment 13-16.....	82
Table B-1: Algebraic signs for calculating the factor effects in the 2^4 design: Vanadium extraction experiments.....	83
Table B-2: Algebraic signs for calculating the factor effects in the 2^3 design: Additional vanadium extraction experiments	84
Table B-3: Algebraic signs for calculating the factor effects in the 2^4 design: Tantalum extraction experiments.....	85
Table B-4: Normal probability table for vanadium extraction experiments.	88

Table B-5: Normal probability table for additional vanadium extraction experiments.	88
Table B-6: Normal probability table for vanadium extraction experiments.	89
Table C-1: Regression results of kinetic model fitting for vanadium response curves 5 g and 1 mL/min.	90
Table C-2: Regression results of kinetic model fitting for vanadium response curves 15 g and 1 mL/min.	91
Table C-3: Regression results of kinetic model fitting for vanadium response curves 5 g and 5 mL/min.	92
Table C-4: Regression results of kinetic model fitting for vanadium response curves at 15 g and 5 mL/min.	93
Table C-5: Kinetic model regression results for additional vanadium extraction experiments at 15 g and 5 mL/min.	94
Table C-6: Kinetic model regression results for additional vanadium extraction experiments at 50 g and 5 mL/min.	95
Table D-1: Regression results of kinetic model fitting for tantalum extraction experiments at 15 g and 3 mL/min.	99
Table D-2: Regression results of kinetic model fitting for tantalum extraction experiments at 50 g and 3 mL/min.	100
Table D-3: Regression results of kinetic model fitting for tantalum extraction experiments at 15 g and 5 mL/min.	101
Table D-4: Regression results of kinetic model fitting for tantalum extraction experiments at 50 g and 5 mL/min.	102

NOMENCLATURE

Analytical Equipment

ASS	Atomic adsorption spectroscopy
ICP-OES	Inductively coupled plasma optical emission spectroscopy

Elements and Compounds

Cr	Chromium
Co	Cobalt
Ni	Nickel
V	Vanadium
W	Tungsten
Ag	Silver
Ta	Tantalum
Mo	Molybdenum
SO ₂	Sulphur dioxide
SO ₃	Sulphur trioxide
Al ₂ O ₃	Alumina
SiO ₂	Silica
V ₂ O ₅	Vanadium pentoxide
K ₂ O	Potassium oxide
H ₂ SO ₄	Sulphuric acid
NaOH	Sodium hydroxide
K ₂ TaF ₇	Potassium heptafluorotantalate
TaO ₅	Tantalum pentoxide
Ta(OCH ₃) ₅	Tantalum penta-methoxide
Ta(OEt) ₅	Tantalum penta-ethoxide
HF	Hydrofluoric acid

HCl

Hydrochloric acid

Organic Extractants

Hacac	acetylacetone, 2, 4-pentanedione
Hbis-dmap	1,3-bis(dimethylamino)-2-propoxide
Hbzac	benzoylacetone, 1-phenyl-1,3-butanedione
Hdbm	dibenzoylmethane, 1,3-diphenyl-1,3-propanedione
Hdmae	N,N-dimethylaminoethoxide
Hhdod	1,1,1,2,2,3,3-heptafluoro-7,7-dimethyloctane-4,6-dione
Htdhd	1, 1, 1-trifluoro-5,5-dimethylhexane-2,4-dione
Htmhd	dipivaloylmethane, 2,2,6,6-tetramethyl-3,5-heptanedione
Htpd=Htfac	trifluoroacetylacetone, 1,1,1-trifluoropentane-2,4-dione
Hpdhd	1,1,1,2,2-pentafluoro-6,6-dimethylheptane-3,5-dione
Httfacac	2-thinoyltrifluoroacetone

Vanadium and Tantalum Complexes

[Ta(OCH ₃) ₄ (tmhd)]	
[Ta(OCH ₃) ₄ (acac)]	
[Ta(OCH ₃) ₄ (dmae)]	
[Ta(OCH ₃) ₄ (bis-dmap)]	
[VO(acac) ₂]	bis(acetylacetonato)oxovanadium (IV)
[VO (bzac) ₂]	bis(acetylacetonato)oxovanadium (IV)
[VO(dbm) ₂]	bis(dibenzoylmethanato)oxovanadium (IV)
[VO(tfacac) ₂]	bis(trifluoroacetylacetonato)oxovanadium (IV)
[VO(ttfacac) ₂]	bis(2-thinoyltrifluoroacetonato)oxovanadium (IV)

1 INTRODUCTION

1.1 BACKGROUND

The majority of industrial processes use catalysts in order to improve the process efficiency. Examples include petroleum refineries, pharmaceutical, polymer and chemical companies. The catalysts used in these processes deactivate with time and regeneration methods are used to prolong the catalyst life. However, regeneration is not always possible, and after a few cycles of regeneration and reuse the catalyst activity may decrease significantly such that it becomes uneconomical to regenerate (Marafi & Stanislaus, 2008). The spent catalysts are then discarded as solid waste (Dufresne, 2007). Disposal of spent catalysts in landfill sites raises concerns due to pollution from the leaching of heavy metals into the environment. Typical heavy metals contained in these spent catalysts include Ni, V, Co and Mo (Jadhav, 2012; Ognyanova et al., 2009). These metals are highly valuable and are used extensively in the manufacturing of alloys and steel (Ognyanova et al., 2009). Therefore, these waste spent catalysts which are causing serious environmental problems, can act as cheap secondary sources for such heavy metals.

The vanadium based catalyst ($V_2O_5/SiO_2 - \gamma Al_2O_3$) has been widely used for catalytic oxidation of SO_2 to SO_3 , to commercially produce sulphuric acid. The active phase of ($V_2O_5/SiO_2 - \gamma Al_2O_3$) usually contains up to 5 – 9 % of V_2O_5 and 8-12 % of K_2O , modified by the addition of Na and Ce (Ksibi et al., 2003). However, the catalyst deactivates with the continued operation of the production process. Grzesiak (2005) highlighted that tons of spent catalyst are discarded annually, and since there is substantial value for the metals contained, there is a need for metal recovery methods, to recover largest possible fractions of vanadium (Moskalyk & Alfantazi, 2003). As a result, Ognyanova et al. (2009), Mazurek et al. (2010), Mazurek (2013) and Painuly (2015) conducted studies on the recovery of vanadium from spent vanadium catalyst used in contact process. The aforementioned studies involved the use of a two-step process which included, roasting (pyro-metallurgical process) and leaching (hydro-metallurgical process) of vanadium spent catalyst using H_2SO_4 , NaOH, urea oxalic acid and aqua-regia.

Secondly, the electronics industry currently consumes more than 70 % of tantalum (Ta) produced globally, for manufacturing reliable electronic capacitors (Espinoza, 2012). In addition, aerospace industry makes use of this metal to manufacture jet engine super alloys, whereas other fraction is used in chemical industries, manufacture of turbines for electricity generation, cemented carbides and spattering targets (Polinares Consortium, 2012). However, this rare metal is not found in a free state, but always occurs in the oxidised state in combination with niobium. The primary sources of tantalum include tin slag and tantalum-niobium minerals such as,

tantalite and columbite, while secondary sources include waste scrap generated during the manufacture of tantalum containing compounds and unrecovered tantalum contained in tailings.

Ta and Nb have comparable chemical properties; therefore it is a challenge to separate them. Hydrometallurgical processes are commonly used to recover both Ta and Nb from mineral ores. The current commercial solvent extraction processes involves the use of concentrated HF, commonly in a mixture of mineral acids such as hydrochloric and sulphuric acid, for dissolving Ta and Nb. The solvents used in these systems are, MIBX, TBP, CHN and 2-OCL (Zhu & Cheng, 2011). However, due to the stringent environmental regulations, the use of HF needs to be eliminated or reduced, consequently solvent extraction systems for separating tantalum and niobium without use of HF are being investigated (Zhu & Cheng, 2011).

Matsuoka et al. (2004) indicated that although a large amount of off-spec tantalum capacitors are generated during the manufacturing process, an efficient recycling technique or process has not yet been established to recover the tantalum from them. It is therefore essential to establish a new recycling technique to recover tantalum from capacitor scrap or other tantalum waste scrap.

Pyro-metallurgical treatment processes are energy intensive and generate toxic gases whereas hydro-metallurgical processes generate large volumes of potentially hazardous liquid waste. Therefore, environmental regulations demand eco-friendly technologies to recover metals.

It has been shown from previous studies that the gas-phase extraction processes offer an eco-friendly technique for metal recovery from low grade metal-containing matrixes (Allimann-Lecourt et al., 2002; Allimann-Lecourt, 2004; Potgieter et al., 2006; Van Dyk et al., 2010; Van Dyk et al., 2011; Van Dyk et al., 2012) and industrial waste (Mpana, 2011). The process offers a potential alternative technique to metal extraction which might present a solution to the limitations encountered during conventional metal recovery processing. Amongst other advantages is the regeneration of the organic extractants, absence of bulky fluid transportation and good metal selectivity (Chen et al., 2011)

1.2 PROBLEM STATEMENT

It has previously been shown that the gas phase extraction process can be applied to synthetic metal oxide systems and the extraction of aluminium from fly ash. The intention of this research is to apply this technique, with a suitable organic extractant(s) to extract vanadium from spent vanadium catalyst used in the production of sulphuric acid. In addition, a preliminary study will also be conducted to investigate its applicability in the extraction of tantalum from tantalum oxide as a step in the development of an alternative process to recover tantalum from low grade ore sources.

1.3 OBJECTIVES

The central objective of this study is to further explore the gas-phase extraction process and apply it to recover vanadium from vanadium spent catalyst and tantalum from synthetic low grade tantalum oxide matrix. This objective is divided into the following sub-aims:

- i. To perform a literature review to identify suitable volatile organic ligands that can chelate with vanadium and tantalum and be used in the gas phase extraction process.
- ii. To improve the design of the gas phase extraction experimental setup.
- iii. To investigate the leach potential of the identified extractant(s) in the gas phase extraction process, and identify the significant process parameters that influence the degree of extraction of tantalum and vanadium from their respective matrixes.
- iv. To model the kinetics and optimize the gas phase extraction by adjusting the identified significant experimental parameters.

1.4 DISSERTATION STRUCTURE

This dissertation comprises of six chapters. Chapter 1 describes the background and motivation of the study, as well as the problem statement and the objectives. Chapter 2 is literature review which encapsulates key details regarding the gas phase extraction process. Its initial focus is directed towards understanding the pros and cons of conventional metal recovery techniques and in the latter sections it examines possible leaching agents forming complexes with vanadium and tantalum from previous studies. Chapter 3 provides a detailed description of the materials used, a description of the experimental apparatus/set-up, and experimental procedures and methods applied to achieve the research objectives. Chapters 4 presents the experimental results, coupled with discussions. An in-depth statistical analysis of the determination of the significant extraction parameters is given, followed by kinetic modelling of the extraction process. In Chapter 5 the conclusions of the study is given followed by recommendations in Chapter 6. The calculations, experimental raw data and detailed regression analysis are presented in the Appendixes.

2 LITERATURE REVIEW

This chapter aims to further demonstrate the need for this research and provides in-depth insight concerning the gas phase extraction process and previous research conducted in the field.

2.1 CONVENTIONAL RECOVERY ROUTES OF METALS FROM INDUSTRIAL WASTE

The value metals contained in various industrial wastes such as petroleum spent catalysts, electronic scraps, fly ash etc., are commercially recovered through pyro-, hydro-and bio-hydrometallurgical processing routes.

Pyro-metallurgical processing

Pyro-metallurgical processing involves subjecting a metal-bearing matrix to thermal treatment carried out in high temperature units such as furnaces, so as to effect transformation on the physical and chemical properties of the metal-bearing matrix, to allow for the recovery of value metals. The key advantages of this processing route include high production rates due to rapid reactions at high temperatures and ease of separation of metals from gangue via melting or vaporization. Nevertheless, pyro-metallurgical processes are very expensive due to their high energy demand, and they give rise to harmful gaseous emissions, dust and generation of slags. Refining, roasting, smelting and metallorhetic reduction are classical examples of pyro-metallurgical processes used for metal recovery (Ghosh & Shanker, 1991).

Hydro-metallurgical processing

The hydrometallurgical processing route is traditionally used to extract valuable metals from low grade and complex ore matrix (Gupta, 2006). The process mainly involves the leaching of valuable metal from the ore or waste matrix using appropriate aqueous leaching agent, followed by concentration and purification of the leach liquor; with subsequent recovery of value metals (Ghosh & Shanker, 1991; Jadhav & Hocheng, 2012). A basic flowsheet of the process is presented in Figure 2-1.

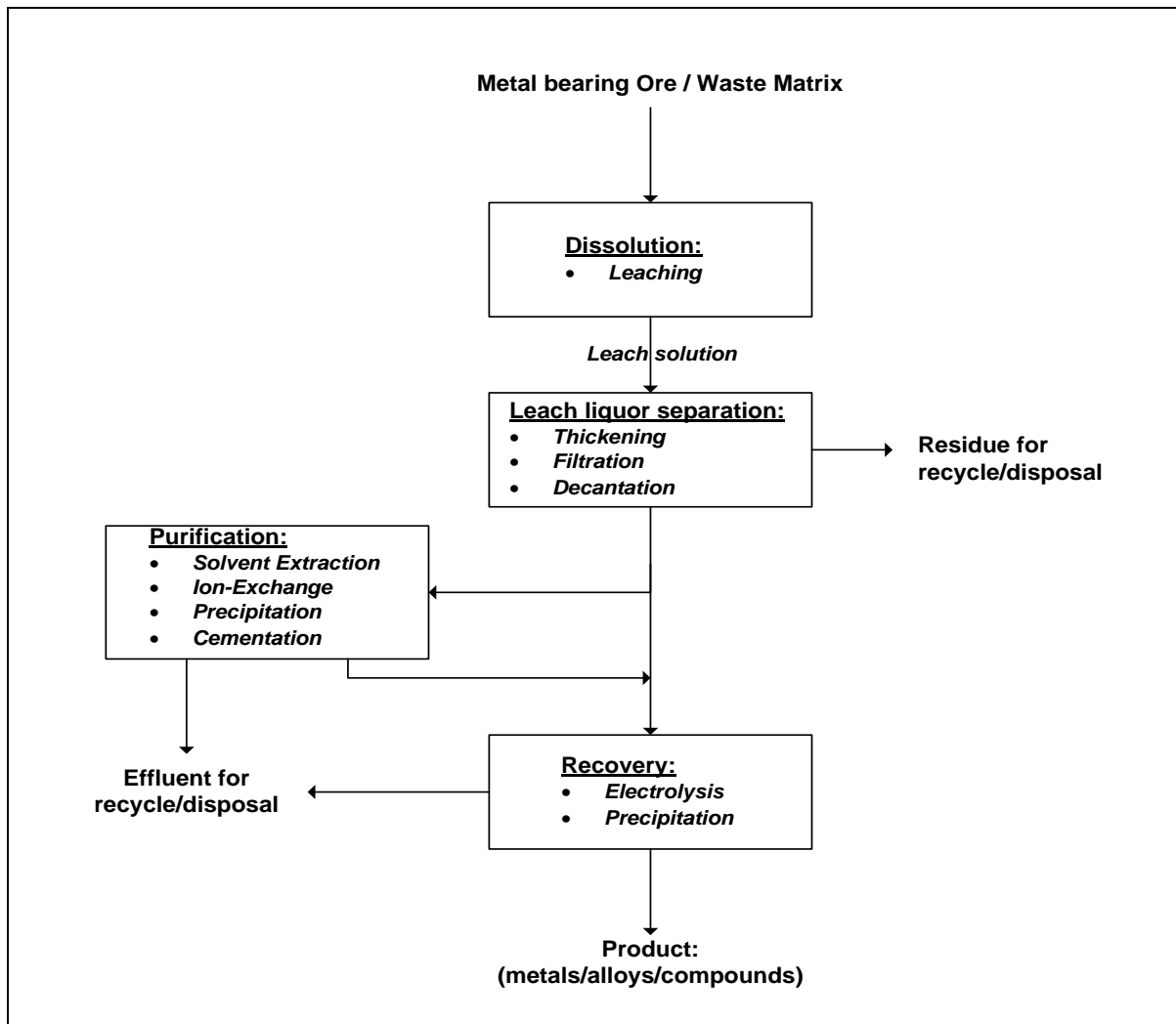


Figure 2-1: Basic flowsheet of hydrometallurgical process (Adapted from Gupta, 2006).

The key advantages of hydrometallurgical processing include its suitability to treat low grade and complex ore matrix at moderate temperatures, with minimal gas emissions. However, hydrometallurgical process involves the use of acids in large scale operations; as a result, large volumes of potentially hazardous waste streams are generated (Gupta, 2006).

As a result of strict environmental regulations and depletion of high grade ore bodies, concerted efforts have been focused on developing economical and eco-friendly processes for the recovery of metals from industrial waste and lean ore matrixes. Consequently, microbial leaching processes are being considered for their low cost and environment friendly nature (Akcil & Gahan, 2015).

Bio-hydrometallurgical processing

Bio-hydrometallurgical processing route involves the utilization of microorganisms and bio-reagents for recovery of heavy metals. This process has been successfully applied commercially. A summary of commercial and laboratory applications of bio-hydrometallurgy is presented in Figure 2-2.

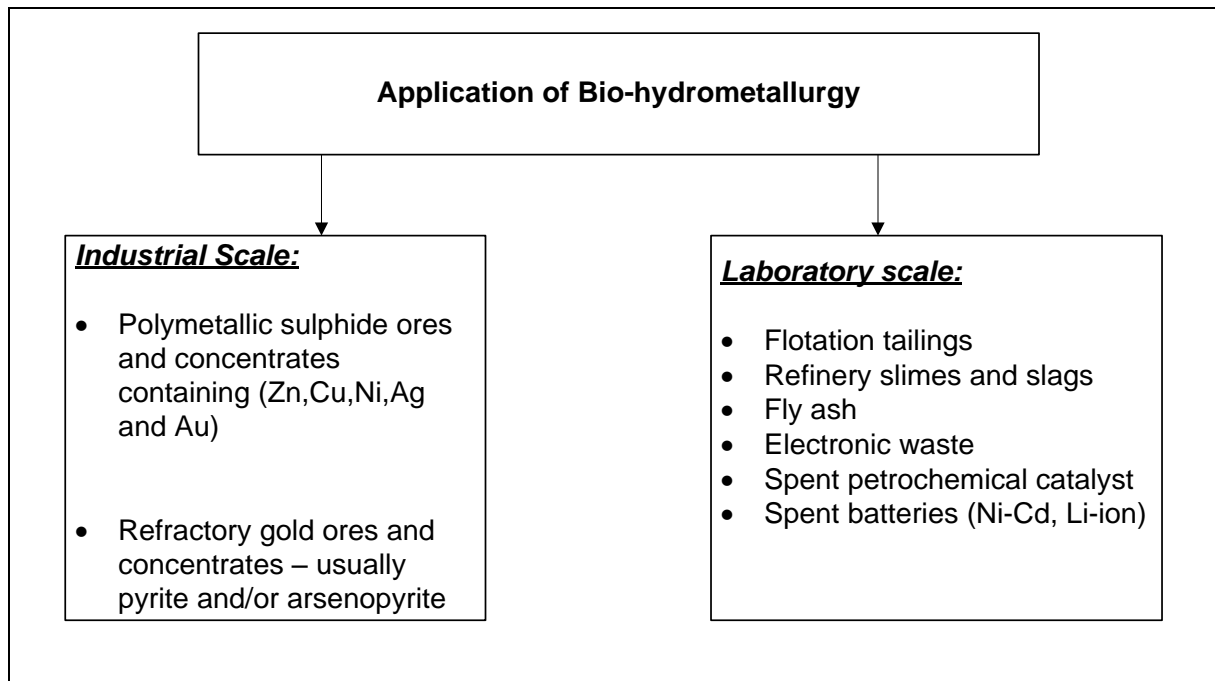


Figure 2-2: Industrial and laboratory scale application of bio-hydrometallurgical processing technique for metal recovery (Adapted from Willner et al., 2015).

The process is energy efficient, eco-friendly, cost effective and the harmful chemicals used in conventional hydrometallurgical processing are replaced with bio-degradable and metal specific biological reagents (Natarajan, 2013). Despite numerous advantages of bio-hydrometallurgical processes, it is recognised that the main limitation is long leaching time required, and operation at high pulp densities (> 20% solids), and relatively high cost for stirred tank reactors have limited the process for use only with high grade metal containing minerals. High pulp densities (>20 wt%) causes deficiencies in gas transfer and microbial damage of the cells as a result of shear force caused by the impellers of the stirred tank reactors (Pandey, 2015).

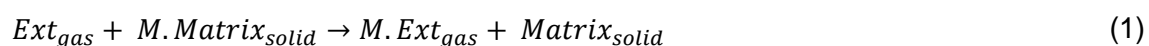
2.2 GAS-PHASE EXTRACTION PROCESS USING VOLATILE CHELATING LIGANDS

Cox et al. (1985) developed a gas-phase extraction process known as the Selective Extraction and Recovery using Volatile Organic compounds (SERVO) as alternative process for the extractive metallurgy of low grade ores. The selective extraction of a metal from the metal-bearing matrix is achieved by subjecting a metal-bearing ore or solid waste to a gaseous feed of volatile organic polydentate reagent, in a heated fluidized bed reactor. The metal of interest contained in the metal-bearing matrix must be present in an oxide, hydroxide or sulphide form because organic polydentate reagents are weak acids (Allimann-Lecourt et al., 2002).

The rigorous selection process of organic chelating reagent considers factors such as coordination chemistry, ease of volatilization, transport of complexing reagent, and formation of stable metal complexes with minimal or no decomposition (Chen et al., 2011).

The chelating reagent should ideally be tetradentate. The latter encompasses reagents such as, a porphyrin, a phthalocyanine, a Schiff base reagent or a hydroxyoxime (Cox et al., 1985).

Equation (1) describes the selective heterogeneous reaction occurring when the metal-bearing matrix is contacted with the suitable volatilised organic chelating reagent.



The products resulting from the reaction comprise of volatile metal complexes and residual gangue. Metal complexes can be removed from the residual gangue by the carrier gas flow and condensation (Potgieter et al., 2006). Subsequently, the metal complexes can be reduced in vapour phase by hydrogen (Equation 2) or the reduction can occur after condensation of vapour phase to yield a metal product, and regenerate the organic extractant for recycling (Allimann-Lecourt et al., 2002; Potgieter et al., 2006).



Alternatively, these metal complexes can be captured in an organic solvent and the organic solution can be treated with mineral acid to decompose the metal complex. The metal of interest and the chelating reagent can then be recovered using appropriate separation techniques (Allimann-Lecourt et al., 2002).

The gas-phase extraction process has been successfully applied to extract heavy metals from contaminated soil, fly ash and metal oxide compounds (Allimann-Lecourt et al., 2002; Allimann-Lecourt, 2004; Potgieter et al., 2006; Van Dyk et al., 2010; Shemi et al., 2012) with potential application to the recovery of valuable metals from slag, spent catalysts or low grade ores. The process presents potential advantages in terms of good metal selectivity, pure metal recovery, eco-friendly waste residue, low energy costs, absence of bulky transport of solution, low operational temperature, low operation pressure and recycling of chelating reagent (Chen et al., 2011).

A generalised process flowsheet of the gas phase extraction process is shown in Figure 2-3.

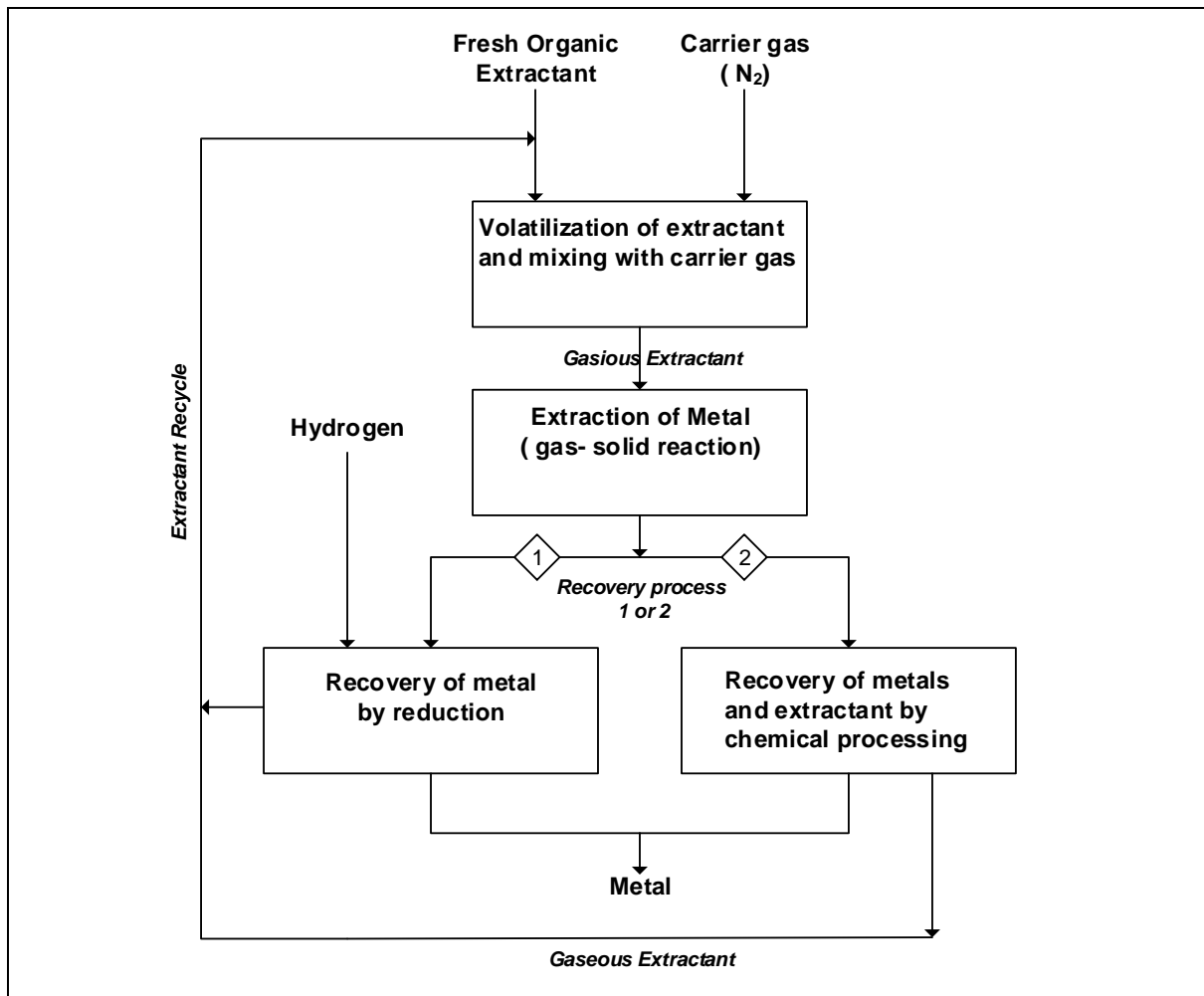


Figure 2-3: Gas-phase extraction process flowsheet (Adapted from Allimann-Lecourt et al., 2002).

2.2.1 Kinetic analysis for the gas-solid reactions in the gas phase extraction process

Seetharaman (2005) indicated that the overall gas-solid reaction process involves the combination of the following mechanisms:

1. Transfer of gaseous reactants and products between the bulk gas and external surface of the solid particle.
2. Diffusion of gaseous reactants and products within the solid pores, if the solid is porous.
3. Chemical reaction between the solid and reactant gas at the gas-solid interface.
4. Transfer of heat within the solid.
5. Convective and radiation transfer of heat between the external surface of particle and surroundings
6. Structural changes of solid particle as a result of heat and chemical reaction.

On these grounds, concerted efforts by numerous researchers have enabled the development of models which incorporate the aforementioned mechanisms, so as to determine the rate controlling step(s) under a given set of reaction conditions. Thus, several models used in literature to describe non-catalytic gas-solid reactions are presented in Table 2-1, coupled with the main features for each.

Table 2-1: Summary of Non-Catalytic Gas-Solid Reaction-Diffusion Kinetic Models (Leib & Pereira, 2008).

Model	Main Characteristics
<i>Shrinking Unreacted Core Model</i>	<ul style="list-style-type: none"> • Reacting solid is non-porous. • Reacting solid ash is porous. • Reaction occurs at the ash-unreacted solid interface.
<i>Volume reaction model</i>	<ul style="list-style-type: none"> • Reacting solid is porous. • Reaction occurs throughout the particle at all time
<i>Grain model</i>	<ul style="list-style-type: none"> • Particle is divided into identical solid spherical grains • Each grain reacts according to the shrinking unreacted core model
<i>Crackling core model</i>	<ul style="list-style-type: none"> • Combination of shrinking unreacted core model and grain model
<i>Nucleation model</i>	<ul style="list-style-type: none"> • Nucleation of metals in metal reduction reactions

Szekely (1976) highlighted that the unreacted core model approximates most real gas-solid reactions, and is attractive for its mathematical and conceptual simplicity.

Shrinking-unreacted core model

The visualisation of gas-solid reaction described by the equation (5), for the system defined by the shrinking –unreacted core model, is shown in Figure 2-4. In view of the fact that, mass transfer and reaction processes occur in succession, the resistances associated with external mass transfer, diffusion through the ash layer and reaction at the sharp unreacted solid/ash interface are additive. As a result, Szekely et al. (1976) derived the model described by equation (3), which exactly combines these resistances to define the fractional conversion of the reacting solid.

Fractional conversion of non-porous reacting solid:

$$t^* = g_{Fp}(X) + \sigma_s^2 [p_{Fp}(X) + 2X/Sh^*] \quad (3)$$

$$t^* \equiv (bk/\rho_s)(A_p/F_p V_p)(C_{Ab}^n - C_{Cb}^m/K_E)t \quad (4)$$

The terms $g_{Fp}(X)$ and $p_{Fp}(X)$ in equation (3), are functions describing surface reaction at solid-ash interface and diffusion through the ash layer, respectively. These terms are correspondingly defined by equations (6) and (7-9) for kinetic and transport controlled reactions.

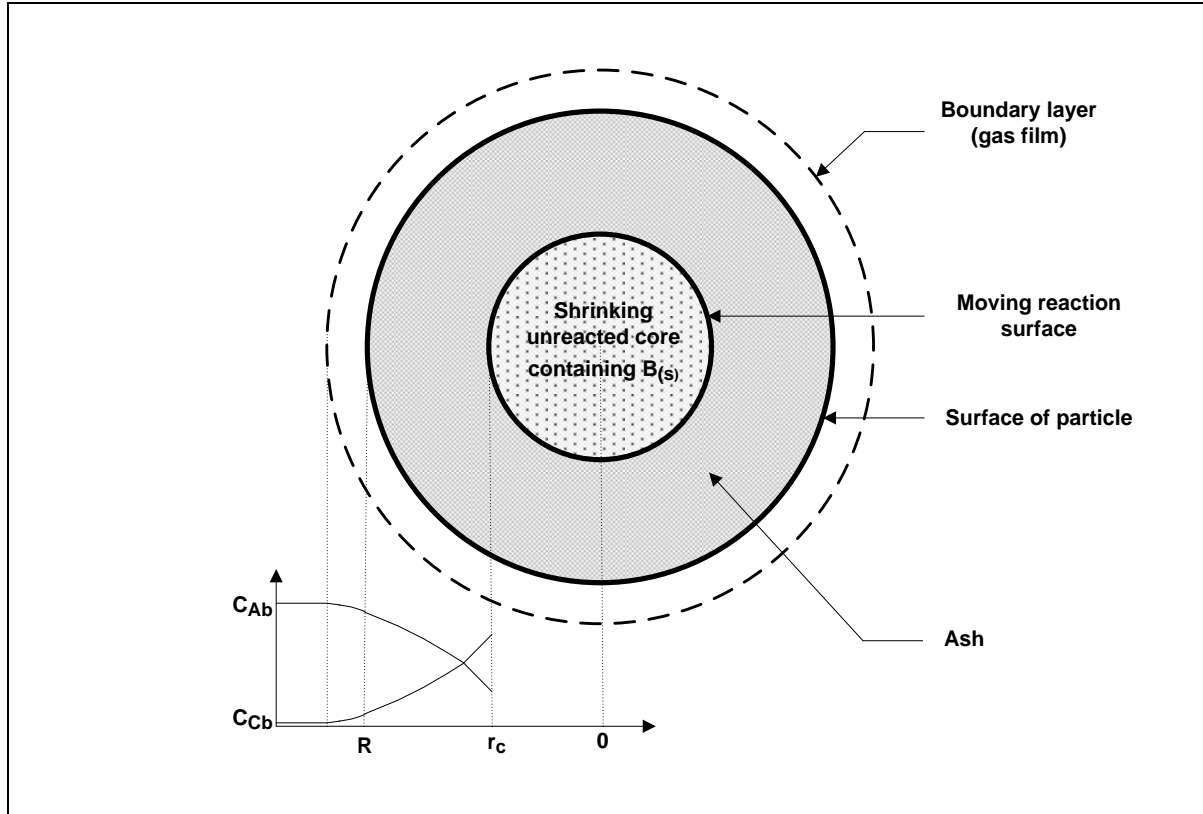


Figure 2-4: Schematic representation of the shrinking unreacted core particle (Levenspiel, 1972).

Conversion function when chemical reaction controls:

$$g_{Fp}(X) \equiv 1 - (1 - X)^{F_p} \quad (6)$$

Conversion function when mass transport controls:

$$p_{Fp}(X) \equiv X^2 \quad \text{for} \quad F_p = 1 \quad \text{slab} \quad (7)$$

$$\equiv X + (1 - X) \ln(1 - X) \quad \text{for} \quad F_p = 2 \quad \text{cylinder} \quad (8)$$

$$\equiv 1 - 3(1 - X)^{2/3} + 2(1 - X) \quad \text{for} \quad F_p = 3 \quad \text{sphere} \quad (9)$$

Additionally, the term σ_s^2 is mathematically defined in equation (10), and it is known as the shrinking core-reaction modulus.

Shrinking-core reaction modulus:

$$\sigma_s^2 \equiv (k/2D_{eA})(V_p/A_p)(1 + 1/K_E) \quad (10)$$

This parameter is very useful in determining whether the reaction is mixed controlled, chemical or diffusion controlled, and the criteria used to classify the regimes is that, for $\sigma_s^2 < 0.1$, the process can be regarded as being governed by chemical reaction, whilst at $\sigma_s^2 > 10$ the controlling process can be attributed to mass transfer, thus, at $0.1 < \sigma_s^2 < 10$ both chemical and mass transfer mechanisms have comparable resistances, and the reaction can be regarded as being mixed/intermediate controlled.

Furthermore, the external mass transfer is taken into account by the incorporation of the Sh^* term, mathematically defined by equation (11), which in essence represents the modified ratio of the mass transfer time constant (k_{dA}/d_p) and diffusion time constant (D_A/d_p^2) known as the Sherwood number; it compares the rate of mass transfer to diffusion rate. When Sh is large, the mass transfer is controlled by diffusion in the porous ash/product, but at small Sh the diffusion through the gas film controls the overall mass transfer.

Modified Sherwood number:

$$Sh^* \equiv (h_D/D_{eA})(F_p V_p/A_p) = (D_A/D_{eA})(k_{dA}d_p/D_A) = (D_A/D_{eA})Sh \quad (11)$$

2.2.2 Recent studies on the selective extraction of metals using gaseous organic extractants

Allimann-Lecourt and co-workers (2002) applied the gas phase extraction process to selectively extract value metals such as Zn, Pb, Cd, Mo, V, Co, Fe and Ni from combustion ashes using β -diketones, β -diketodiimines and tetra-alkyldithiophosphoramides, followed by volatility and thermal stability tests. The study revealed that the extraction depended on metal speciation, and it was observed that complexes of tetra-alkyldithiophosphoramides were more thermally stable than the others investigated.

Potgieter et al. (2006) studied the feasibility of recovering value metals from their respective oxides by gas phase extraction process using acetylacetone as a volatile ligand in a laboratory scale fluidized bed reactor. The results indicated that the gas phase extraction process could be successfully applied to recover aluminium, chromium, vanadium and iron with acetylacetone from their respective oxides. The recoveries of the aforementioned metals are presented in Table 2-2.

Table 2-2: Recoveries of metals from their respective metal oxides at optimum operational conditions (Potgieter et al., 2006).

Metal Oxide	Conditions	Metal complex	Recovery
Al ₂ O ₃	180°C / 105 min	Al(acac) ₃	63.7 %
Cr ₂ O ₃	210°C / 150 min	Cr(acac) ₃	48.2 %
V ₂ O ₅	190°C / 120min	VO(acac) ₂	63.0 %
Fe ₂ O ₃	180°C / 45 min	Fe(acac) ₃	75.2 %

The concerted effort of Van Dyk and co-workers (2010) was aimed at investigating the effect of temperature, and acetylacetone and metal oxide concentration on the gas phase extraction of iron from its oxide. The study revealed that the extraction process was influenced by all of the aforementioned parameters, and Fe extractions above 80 % were achieved after 4 hours for low metal oxide charge. Furthermore, recommendation of addressing the question as to how the variables interact and the relationship for predicting the extractions was suggested for future studies.

The former investigation conducted by Potgieter et al. (2006), showed that metals such as Al can successfully be extracted from their respective oxide form, using the gas phase extraction process with acetylacetone as a chelating ligand. As a result, Van Dyk and co-workers (Shemi et al., 2012) further conducted a comparative study for the recovery of Al from coal fly ash using the gas phase extraction process, and conventional sulphuric acid leaching. The results showed that extractions using acetylacetone in a gas phase were comparatively lower than acid leaching, but presented advantages of reduced extraction time. Moreover, the study revealed that the minerology of the mineral containing matrixes also plays a key role on the extraction process.

In addition, Tshofu (2015) applied this process to recover iron from iron ore fines using acetylacetone ligand, but as a result of possible passivation layer formation with reaction progress, highest extractions of 3.88% were achieved after subjecting the iron ore fines to 9 mL/min of acetylacetone for 6 hours. Thus, the experiments were then conducted using conventional liquid phase leaching to overcome the passivation phenomenon.

However, the gas phase extraction process has not yet been applied to spent catalysts, and since Potgieter and co-workers (2006), established that it was possible to extract vanadium from its pentoxide form using acetylacetone; it is thus the basis of this study to further apply this process to recover vanadium from industrial spent vanadium catalyst. Furthermore, since there is rapid growth and development of electronic devices, electronic waste is also of great concern to the environment, hence the other aspect of this project will be to investigate the possibility of extracting tantalum (component in electronic circuits) from its oxide form, before it can be applied to electronic or other forms of scrap. The next sections (2.3 & 2.4) are therefore aimed at understanding how these waste matrix (spent vanadium catalyst and tantalum waste) are formed, and also to understand

the typical compositions of these waste matrix, followed by an overview as to what has been done to date regarding its treatment for recovery.

2.3 FORMATION AND TYPICAL COMPOSITION OF SPENT VANADIUM CATALYST USED IN THE CONTACT PROCESS

Catalysts are substances that enhance the rate of chemical reaction by establishing an alternative pathway which lowers activation energy for the making and breaking of bonds (Lieb & Pereira, 2008). Good catalysts are typically made from transition elements and their compounds because they have the ability to assume a wide variety of oxidation states (Sharma, 2000). Most industrial processes are catalysed and these include chemical, pharmaceutical, materials, energy and polymer industries.

The vanadium based catalyst ($V_2O_5/SiO_2 - \gamma Al_2O_3$) has been widely used for catalytic oxidation of SO_2 to SO_3 , to commercially produce sulphuric acid. The $V_2O_5/SiO_2 - \gamma Al_2O_3$ catalyst deactivates via three mechanisms, these are chemical, thermal and physical deactivation mechanisms. The chemical deactivation is caused by the infiltration of impurities such as arsenic, iron sulphates, halogen and selenium onto the catalyst active sites (Ksibi, 2003). In addition, vanadyl (IV) sulphates such as $Na_2VO(SO_4)$, $Na_4(VO)_2O(SO_4)_4$ and $K_4(VO)_3(SO_4)$ precipitate significantly onto the catalyst surface at low temperatures (Charry & González, 2011). The $V_2O_5/SiO_2 - \gamma Al_2O_3$ catalyst is known to be active at temperatures between 400 and 600 °C. However, the support properties are altered at the temperature of 575 °C (Ksibi, 2003). This alteration in the support properties decreases catalyst activity. The physical deactivation process of $V_2O_5/SiO_2 - \gamma Al_2O_3$ results from the blockage of catalyst pores by fine powder (Ksibi, 2003), consequently reducing the active catalytic sites. The typical composition of vanadium spent catalyst is shown Table 2-3.

Table 2-3: Chemical composition of vanadium spent catalyst from contact process (adapted from Mazurek, 2010).

V_2O_5 (%)	SiO_2 (%)	K_2O (%)	Fe_2O_3 (%)	References
4.80	49.50	5.80	2.10	Aniol, (1997)
6.18	48.70	10.03	1.43	Ksibi, (2003)
4.67	59.11	4.96	3.36	Stanchewa & Makedonski, (2003)
4.68	57.31	8.70	2.56	Mazurek, (2010)

The spent catalysts cause serious environmental concerns as a result of the presence of heavy metals and hence they are classified as hazardous waste. There is therefore a need for metal containment or, processing prior to waste disposal for

metal recovery. The recovery of value metals such as vanadium will help both in the mitigation of environmental hazards and improvement in the economy of the country (Painuly, 2015). Hence, research has also moved towards finding economical and environmentally benign techniques to extract vanadium from spent vanadium pentoxide catalysts. The efforts of various researchers to develop effective vanadium recovery methods are presented in the next section.

2.3.1 Studies on the recovery of vanadium from vanadium spent catalyst

In pursuit of an effective vanadium recovery method, Ognyanova et al. (2009) conducted alkaline leaching experiments to recover vanadium from industrial spent catalyst used in the contact process. According to a study conducted by Ho et al. (1994) an alkaline leaching method is very selective towards vanadium over iron, with potential limitations attributed to the dissolution of silica and the high costs of reagents. Nevertheless, the highest vanadium extraction yield of 78% were achieved after roasting the spent catalyst at 400 °C and leaching at 80 °C for 2h using 4 M NaOH at liquid to solid ratio of 10 mL/g.

Mazurek and co-workers (2010) conducted leaching experiments using urea as leaching agent, for the recovery of vanadium, potassium and iron from spent vanadium catalyst used in the contact process. The study achieved its highest extraction yields of 78% (V), 90% (K) and 29% (Fe), after contacting urea leach solution with spent vanadium catalyst (particle size 180 – 250 µm) at 20 °C for 1h at a liquid to solid ratio of 10 mL: 1 g.

Furthermore, with the anticipation of further improving the latter observations and investigating leaching potential of other extractants, Mazurek (2013) carried out additional leaching experiments with oxalic acid as a leaching agent, and managed to attain highest extraction yields of 91% (V), 92% (K) and 63% (Fe), after leaching [180 – 250 µm] spent vanadium catalyst at 50 °C for 4 h in presence of oxalic acid solution at a liquid to solid ratio of 25 mL: 1 g.

More recently, Painuly (2015) developed an elegant processing technique for recovering vanadium from spent vanadium catalyst, and achieved quantitative yields of approximately 99%, a brief but detailed flowsheet of the proposed recovery technique is presented in Figure 2-5. As discussed in section 2.1, pyro- and hydro-metallurgical processing routes pose an environmental burden due to their effluent streams, and as can be seen in Figure 2-5, reagents such as Aqua-regia (a very strong acid) are applied in this process. Therefore handling the waste will require additional costs and sophisticated equipment. As a result, a search for effective but eco-friendly processing method is still ongoing.

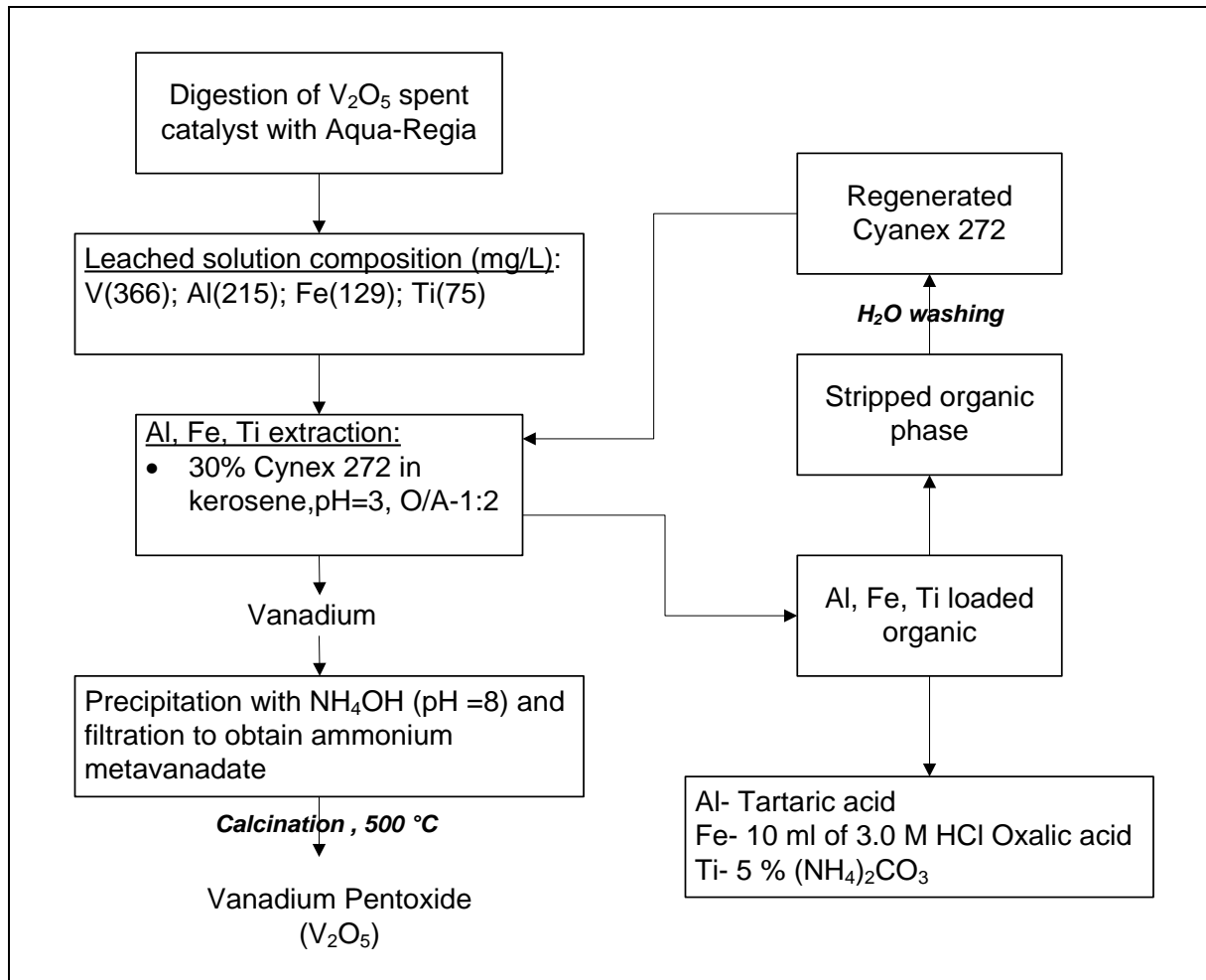


Figure 2-5: Flowsheet for the recovery of vanadium from leached solution of spent V_2O_5 catalyst using Cyanex 272 (Painuly, 2015).

2.4 SOURCES OF TANTALUM SCRAP AND RECOVERY METHODS

Tantalum is mainly used in the manufacture of reliable electronic capacitors, super alloys, cemented carbides and sputtering targets, with more than 70 % consumed in electronics industry (Espinoza, 2012). A considerable amount of tantalum scrap is generated during the manufacturing process of tantalum based capacitors, but since an effective recycling process has not yet been fully developed (Matsuoka et al., 2004), these off spec capacitors are reclaimed back to the refining processes, and consequently treated along with virgin tantalum ores (Cunningham, 2003). On the other hand, tin slag is amongst one of the major sources of tantalum; about 20 % of the total supply of tantalum derives from the utilization of this type of waste (Polinares Consortium, 2012). The commercial treatment process of tin slag for the recovery of tantalum is presented in Figure 2-6a (Gupta, 2006), whereas the proposed treatment process for tantalum capacitor scrap is presented in Figure 2-6b (Mineta & Okabe, 2005).

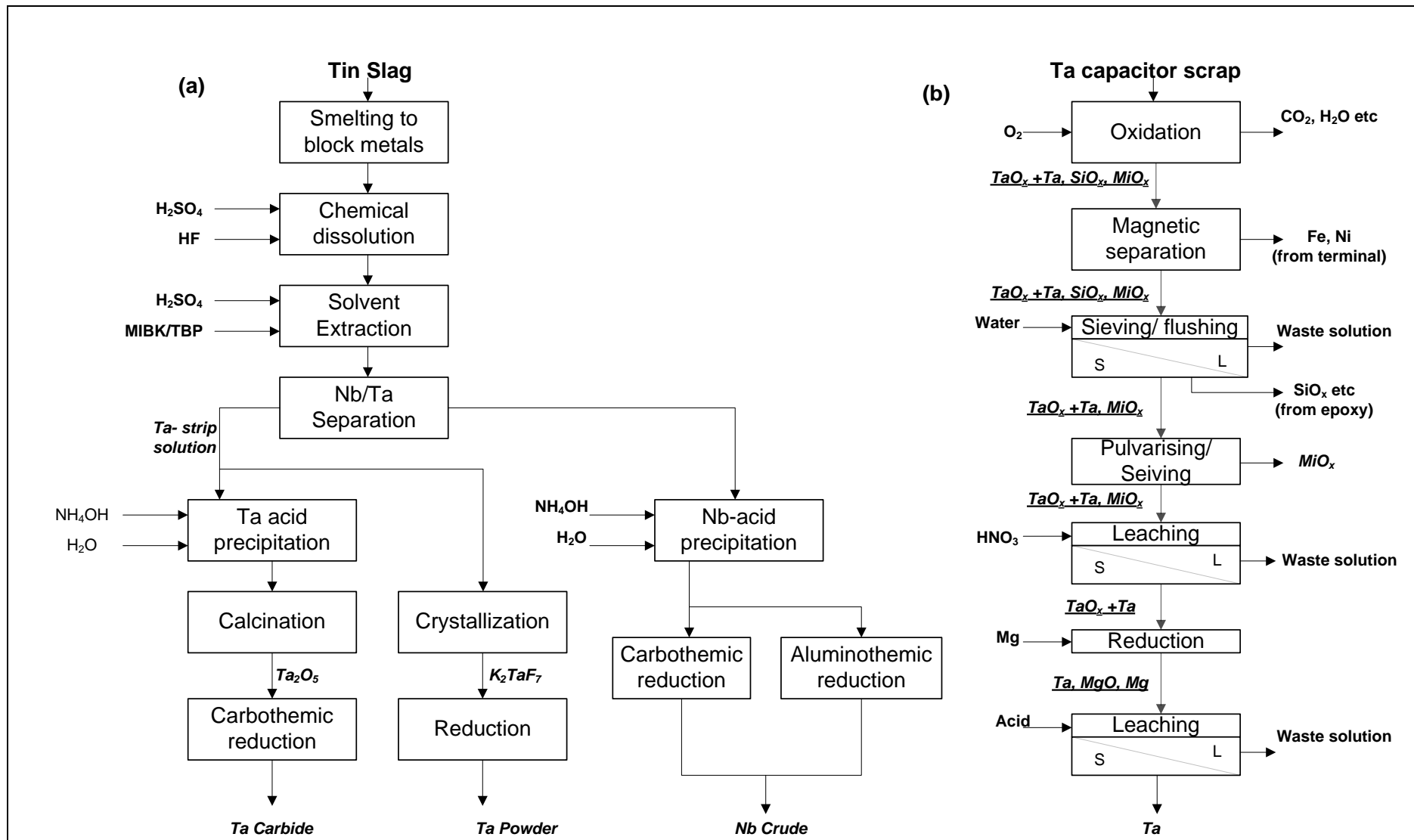


Figure 2-6: Flowsheet for commercial tin slag processing for tantalum recovery and proposed treatment method for processing tantalum capacitor scrap (Gupta, 2006; Mineta & Okabe, 2005).

This tin slag treatment process (Figure 2-6a) involves chemical treatment, or an acid digestion step, where it is digested at elevated temperatures, using concentrated HF or a concentrated binary acid, HF-H₂SO₄, to dissolve Ta and Nb, thereby producing complex fluoride complexes. The reaction of oxides with HF is described by equations below:



These solvent extraction processes, are operated in the presence of fluoride ions, in the mixture with mineral acid such as H₂SO₄. However, environmental regulations demands minimization or rather elimination of harmful fluorides (Zhu & Cheng, 2011).

On the other hand, the proposed Ta capacitor scraps treatment process (Figure 2-6b) produced 99 wt% tantalum powder through the magnesiothermic reduction of tantalum oxide powder. This process follows the conventional extraction techniques, which are rendered to pose environmental risk due to the nature of the effluent waste streams. Therefore, there is a need for cost effective and eco-friendly processes to recover tantalum from tantalum capacitor scrap and tin slag.

Concluding remarks

In conjunction with the previous sections (2.1 to 2.3), it can be seen that the development of an efficient but environmentally friendly process for the recovery of metals such as tantalum and vanadium from their respective waste matrixes, would bring about a partial halt on the deterioration of the ecosystem, and a boost to the economy of the country. Thus, it might be beneficial to test and apply the promising, eco-friendly and evolving gas phase extraction process to the aforementioned waste matrixes of tantalum and vanadium, and to explore its potential to attain plausible extractions of these metals, with the aim of commercially establishing a process in future.

2.5 POLYDENTATE CHELATING REAGENTS COMPLEXING WITH VANADIUM AND TANTALUM

The study conducted by Potgieter and co-workers (2006) confirmed that the extraction of vanadium from its pentoxide form using acetylacetone ligand in a gas phase extraction process is plausible (63.0%), making acetylacetone a potential ligand of choice. This section aims to examine other possible chelating ligands that form complexes with vanadium and tantalum metals, through the review of experimental findings by various researchers. The selection process of organic chelating reagent considers factors such as coordination chemistry, ease of volatilization, and formation of stable metal complexes with minimal or no decomposition (Chen et al., 2011).

2.5.1 Introduction

In coordination chemistry a ligand is described as being an atom or molecule that donates one or more electron pair through binding to the central atom to form a coordination complex. Ligands are attached to the metal ion in a complex through electron pairing.

A ligand may be a molecule often having an electric dipole moment, such as pyridine and ammonia. They can also be negative ions such as the acetylacetonate ion. If a number of donor atoms of one ligand molecule are bound simultaneously to the same metal ion, the ligand is said to be a polydentate or a chelate. A summary of some common organic ligands and the types of ligands are shown in Figure 2-7.

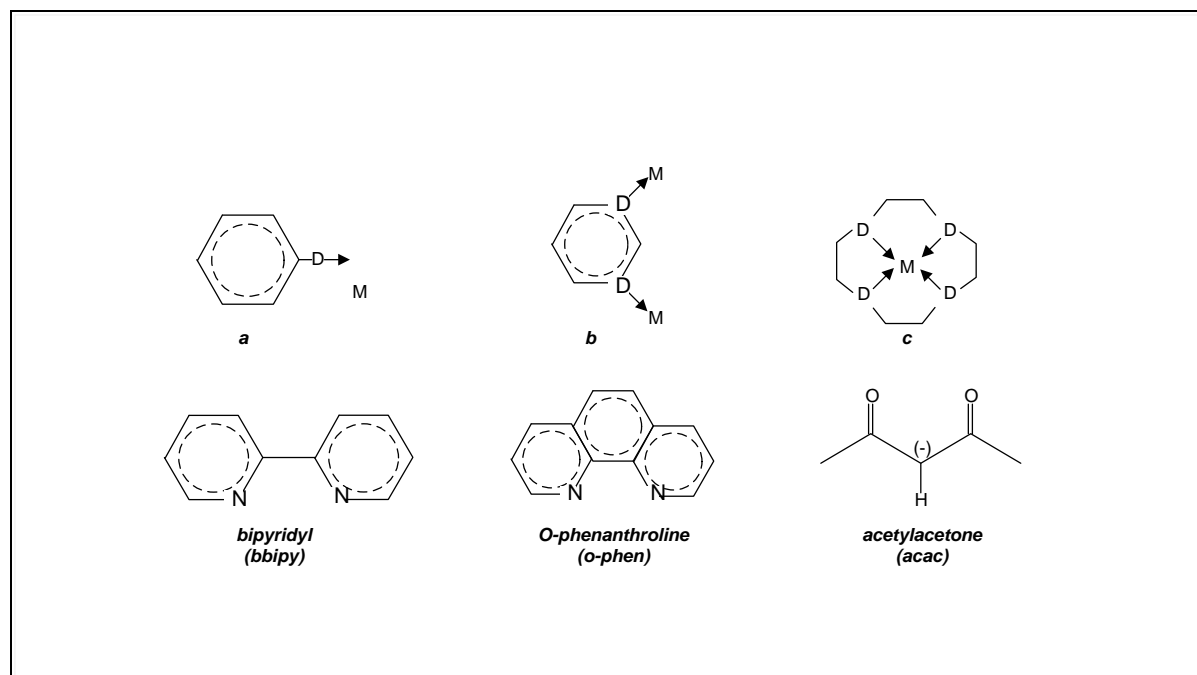


Figure 2-7: Types of ligands by the manner in which they bind to the central metal ion from their respective complexes-Monodentate (a) and polydentate ligands (b-c). Common organic ligands- acac, o-phen and bbip (Van der Put, 1998).

A variety of β -diketones and fluorinated derivatives have been suggested as being useful for the extraction of metals such as vanadium, iron(III), nickel(II), zirconium lithium and others, from their aqueous solutions (MacKay & Sudderth, 1977). Belcher (1973) and Crompton (1987) highlighted that a number of thermogravimetric studies show that the fluorinated β -diketonates chelates are more volatile than non-fluorinated β -diketonates.

2.5.2 Studies of vanadium chelates

Dilli and Patsalides (1976), prepared complexes of vanadium(III) and oxovanadium(IV) with fluorinated and non-fluorinated β -diketones, namely Hacac, Htpd, Htmhd, Htdhd, Hpdhd and Hhdod, followed by volatility and thermal studies of the resulting chelates. The thermogravimetric studies showed that V^{3+} chelates of fluorinated β -diketones volatilized with little evidence of decomposition at temperatures of 280-320 °C. However, the light green VO^{2+} chelates completely decomposed over the temperature range 180-240 °C, forming a brown solution. A bluish-green $VO(acac)_2$ decomposed at temperature of 251 °C whereas $VO(hpd)_2$ decomposed from 180 °C and $VO(tdhd)_2$ decomposed rapidly at 226-230 °C, fusing at 231-232 °C.

Dilli and Patsalides (1981) conducted a stability and volatility study of transition metal chelates of tetradentate Schiff Bases. The ligands were derived from ethane-1,2-diamine and propane-1,2-diamine containing alkyl, branched alkyl, trifluoromethyl and phenyl substituents. The results showed that Schiff base chelates of VO^{2+} , Cu^{2+} , Ni^{2+} and Pd^{2+} were less volatile but more thermally stable than corresponding β -diketonates.

Additionally, Aliyu and Mustapha (2009), prepared oxovanadium(IV) complexes of, $[VO(acac)_2]$, $[VO(dbm)_2]$, $[VO(tfacac)_2]$, $[VO(ttfacac)_2]$ and $[VO(bzac)_2]$ by treating V_2O_5 with H_2O , $EtOH$ and H_2SO_4 to generate VO^{2+} , and adding acetylacetone, dibenzoylmethane, 2-thionyltrifluoroacetone, trifluoroacetylacetone and benzoylacetone. The complexes decomposed in the temperature range of 212 °C and 285 °C. It is also noted that, another principal chelating polydentate reagent, other than the acetylacetonates and its fluorinated derivatives that complexes with vanadium, is Etioporphyrin (Crompton, 1987).

2.5.3 Studies of tantalum chelates

Narula et al. (1983) carried out reactions of tantalum pentaethoxide with p-haloaryl substituted β -diketones as well as 2-thenoyltrifluoroacetone using different molar ratios. Complexes of the type $[\text{Ta}(\text{OEt})_{5-n}(\text{L})_n]$ were prepared and characterised (L= p-fluoro-, p-chloro, 2-thenoyltrifluoro-acetonate and p-bromobenzoylacetonate; n=1, 2, 3).

In 1999, Davies and co-workers repeated the work of Narula et al. (1983) and Kapoor et al. (1965), substituting the parent methoxide for the parent ethoxide, and synthesised $[\text{Ta}(\text{OCH}_3)_4(\text{tmhd})]$, $[\text{Ta}(\text{OCH}_3)_4(\text{acac})]$ complexes from the reaction of tantalum penta-methoxide with Htmhd and Hacac in hexane. These complexes formed were found to be relatively stable.

Additionally, $[\text{Ta}(\text{OCH}_3)_4(\text{dmae})]$ and $[\text{Ta}(\text{OCH}_3)_4(\text{bis-dmap})]$ complexes were prepared from the reactions of tantalum penta-methoxide with the nitrogen containing donors dmaeH and bis-dmapH. The reaction between TaCl_5 with non-fluorinated β -diketones (tmhdH or acacH) in absolute methanol yielded complexes of the type trans, cis- $\text{TaCl}_2(\text{OCH}_3)_2(\beta\text{-diketonate})$. Kepert and Trigwell (1976), highlighted that fluorinated ditertiary arsines such as 1,2-bis(dimethylarsio)-3,3,4,4,5,5-hexafluorocyclopentene (hfas) and 1,2-bis(dimethylarsio)-4-fluorobenzene (fas) react with TaCl_5 and TaBr_5 to form $\text{MX}_5(\text{diarsine})$ (M=Metal, X=Cl or Br). Lopez (2006) synthesized $[(3,5\text{-Cl}_2\text{C}_6\text{H}_3\text{NCH}_2\text{CH}_2)_3\text{N}]\text{TaCl}_2$ from the reaction between $\text{H}_3[(3,5\text{-Cl}_2\text{C}_6\text{H}_3\text{NCH}_2\text{CH}_2)_3\text{N}]$ and TaCl_5 in presence of trimethylamine.

2.5.4 Selected chelating reagents for vanadium and tantalum experiments

The studies presented in section 2.5.2 and 2.5.3, indicate that β -diketones and their fluorinated derivatives form stable complexes with tantalum and vanadium metals. The reoccurring bidentate ligand used to form complexes with both metals is acetylacetone and as indicated by Dilli and Patsalides (1981), this ligand gives preference to metals ions having a charge of +2 coordination number of 4, with square-planar or square-pyramidal coordination geometry for greater selectivity, of which both metals possess. Therefore, for this reason it is chosen as a ligand of choice, while it is acknowledged that its fluorinated derivatives, namely, trifluoro-acetylacetone and hexafluoro-acetylacetone are also potential extractants for the gas phase extraction process. Due to some safety considerations the two last mentioned derivatives were not considered in this study. Furthermore, the fluorinated derivatives were in solid form and the gas phase extraction experimental setup was designed to handle liquid extractants, and would require considerable changes to the process design.

3 EXPERIMENTAL

Gas phase extraction experiments were performed to determine the extraction kinetics of vanadium from spent vanadium catalyst and tantalum from tantalum oxide. The experimental methods and procedures are described below.

3.1 MATERIALS

1. Reagents

Acetylacetone used in this study was purchased from Sigma-Aldrich and it was used without further purification. The properties of acetylacetone are presented in Table 3-1.

Table 3-1: Properties of acetylacetone used for vanadium and tantalum extraction experiments.

	Reagent	Form	Boiling point	Purity	Function
1	Acetylacetone (C ₅ H ₈ O ₂)	Colourless liquid	140.4 °C	≥99 %	Extractant

2. Metal source solids

Table 3-2 gives the details of the solids or metal sources used in the study. The vanadium spent catalyst was obtained from Foscort in Richards bay and is a sulphuric acid catalyst. The vanadium content of the spent vanadium catalyst was determined by acid digestion in aqua-regia and subsequent metal analysis by ICP-OES in the Department of Chemistry at the University of the Witwatersrand (WITS). For the tantalum experiments a synthetic ore was created using a mixture of silica sand and tantalum oxide.

Table 3-2: The metal source matrixes charged in the reaction column for extraction experiments.

Solid charge	Form	Metal content	Source
Spent Vanadium Catalyst	Yellowish-green solid	*49.03 (mg V/g-catalyst)	Foscort
Tantalum Oxide	White powder	99% Ta ₂ O ₅	Sigma-Aldrich
Silica sand	White solid granules	N/A	Sigma-Aldrich

* The concentration was determined using ICP-OES analysis

3.2 EXPERIMENTAL SETUP

The apparatus (Figure 3-1) used for the gas phase extraction process consists of four major components, a pre-heater, an evaporation unit, a column reactor, and a condenser. The auxiliary equipment includes two peristaltic pumps, one for feeding the ligand to the process and another for circulating heating oil to the pre-heater, a stirrer-heating plate for heating the silicone oil and, and a submersible pump for pumping cooling water to the condenser.

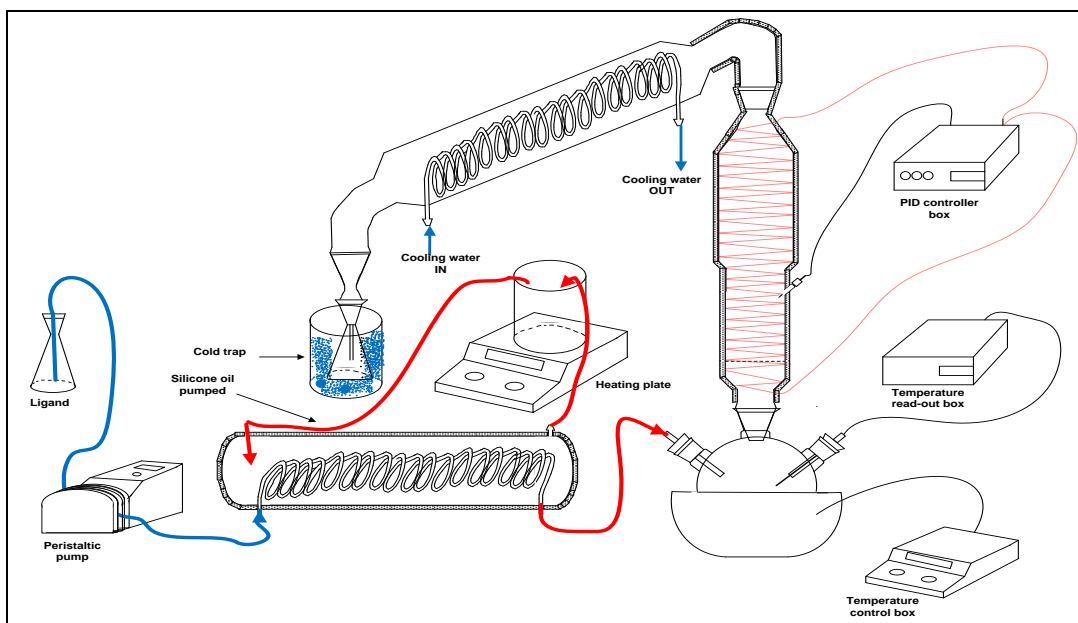


Figure 3-1: The gas phase extraction schematic diagram.

The ligand is fed through a pre-heater Figure 3-2 to heat up the extractant to 140 °C and assist the evaporation process before being fed to the evaporation flask. The evaporating flask is a three neck borosilicate glass round bottom flask of 500 mL capacity with standard female joints of 19/26, 24/29 and 19/26. The two 19/26 angled joints are for fitting the ligand feed and thermocouple adapters, and the non-angled 24/29 joint is for inserting the column reactor. The evaporating flask is heated by a ceramic heating mantle connected to a temperature controller and is used for heating the evaporating flask to the desired preset temperature. The portion of the flask surface not immersed in the heating mantle is insulated with 4 cm thick ceramic wool, to ensure that there is minimal heat loss. Figure 3-3 shows a schematic diagram of the evaporating flask unit.

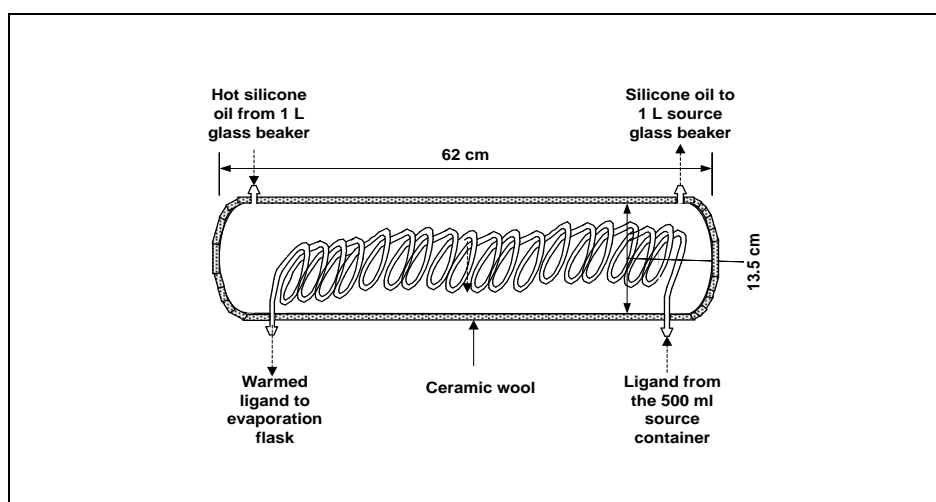


Figure 3-2: Extractant pre-heater.

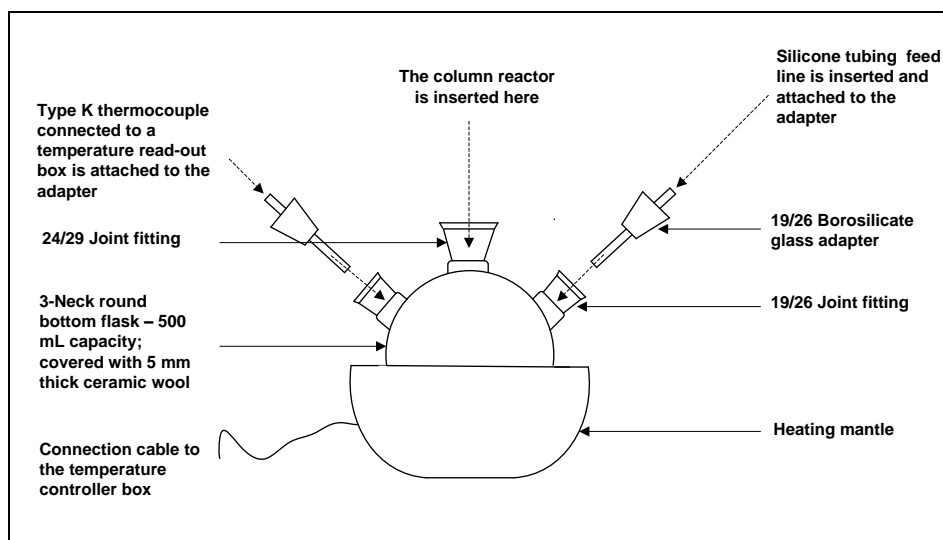


Figure 3-3: Evaporation unit consisting of heating mantle and evaporation flask.

The column reactor fits into the evaporator and is made from a cylindrical borosilicate glass, fitted with a perforated frit that serves as a gas distributor. The column is heated by heating wire (5 m long and 5 mm thick) wrapped along its length and insulated with ceramic wool covered with aluminium foil. The heating wire is connected to a PID controller. A 1.5 mm thick stainless steel type-K thermocouple with a probe length of 5.5 cm also connected to a PID controller and inserted midway along the length of the column reactor to measure the temperature inside the column. A schematic diagram of the column reactor is shown in Figure 3-4.

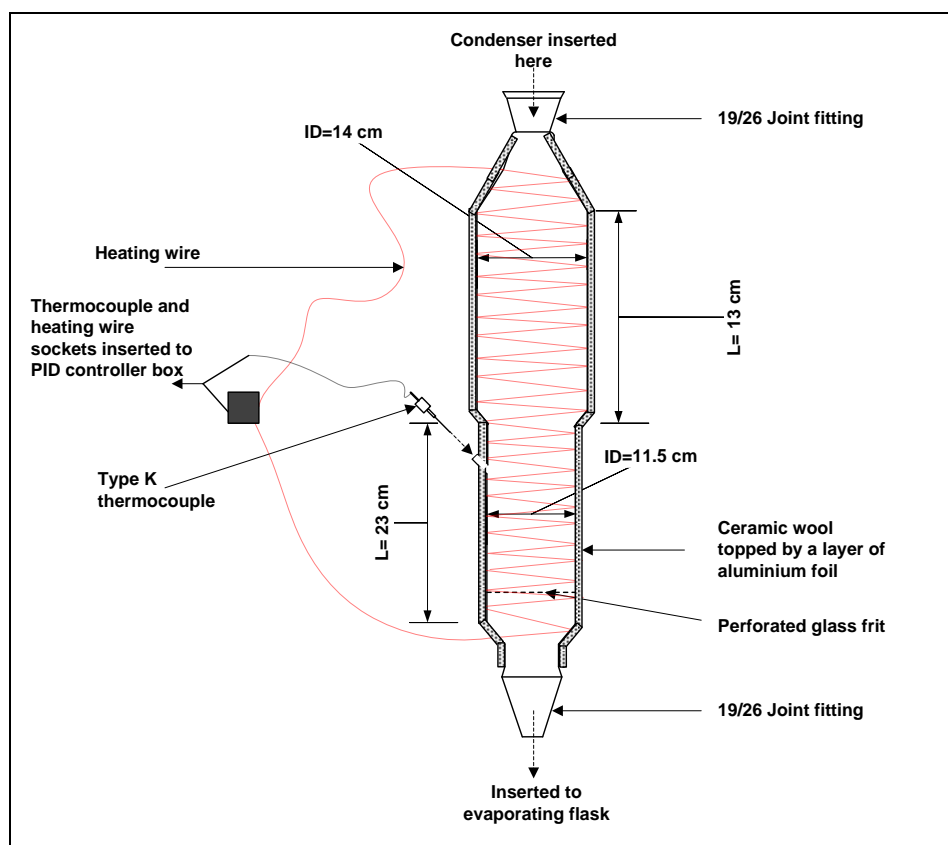


Figure 3-4: Column reactor used in the gas phase extraction process.

The gaseous products from the column reactor are condensed in a 400 mm long borosilicate glass condenser composed of an internal spiral glass tube for cooling water (24/29 standard joint fittings are used). A schematic diagram of the condenser is presented in Figure 3-5 and includes the dimensions and other detail.

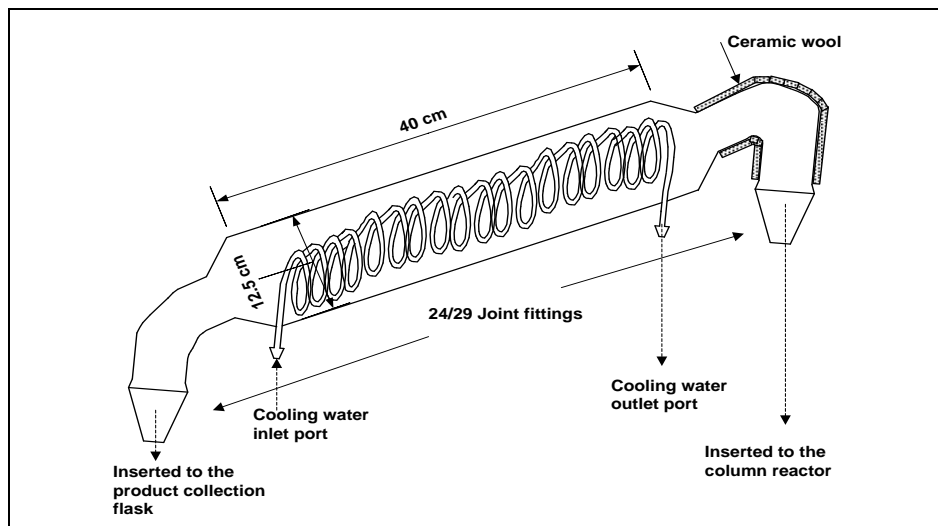


Figure 3-5: Condenser Column.

3.3 EXPERIMENTAL PROCEDURE

3.3.1 Sample preparation

As mentioned earlier, the vanadium extraction experiments were performed using an industrial spent vanadium catalyst obtained from Foskor in Richards Bay. The catalyst particles were ground in a mortar and pestle and sieved to attain particle size fractions ranges of [+2mm to -4mm] ,[+500 μ m to -1mm] and [+250 μ m to -500 μ m] for use in extraction studies, the [+1mm to -2mm] size fraction was not investigated as it was seen from other studies that higher extractions are achieved at much lower particle size range . For the tantalum experiments, tantalum oxide was mixed with silica sand (2 wt% and 10 wt%) to produce a synthetic ore mixture.

3.3.2 Process start-up and operation procedure

After the sample preparation step, a 5 -50 g charge of the prepared sample, either spent vanadium catalyst or tantalum oxide/silica sand mixture was loaded in the reactor column. Thereafter, 250 mL of acetylacetone was added to the conical flask, followed by the adjustment of the ligand peristaltic pump to the desired flowrate. Next, the desired reaction temperature was registered as a set-point temperature in the PID controller box; consequently, the process components were assembled as shown in Figure 3-1. The column reactor was then heated to the desired reaction temperature T_2 whereas the evaporation flask was heated to T_1 , which was regulated by the volatilization temperature of acetylacetone. Silicone oil (heating fluid), was heated and magnetically stirred for 20 min, and then circulated to the pre-heater

using a peristaltic pump revolving at 220 rpm. At the same time, the cooling water was also allowed to flow counter-current to the direction of the anticipated gaseous product through the condenser column. Once the temperature for each unit was stable at the set conditions, the peristaltic pump discharging the volatile ligand at the desired flowrate was switched on. The reaction was allowed to progress for a period of t_1 , and the product was collected at time intervals of 30 min to 1 h. The feed peristaltic pump was stopped for 5 min at each time interval of collecting the product, and this was to allow the entire gaseous product in the reactor to condense into the product collection flask.

3.3.3 Process shut-down procedure

At the end of the reaction period t_1 , the pump feeding the ligand to the system was switched off, and all other process units were allowed to continue running for an additional 5 min. This was to ensure that the entire gaseous product was collected in the collection flask. Subsequently, the reactor heating wire and the heating mantle were also switched off, 3 minutes later, following the latter step, the cooling water pump was stopped, and the liquid product sample was collected. The condenser was disconnected, followed by the reactor column and evaporating flask, to allow for the collection of the solid residue. The liquid samples of the extraction experiments (vanadium and tantalum) were analysed for its metal content using atomic absorption spectroscopy.

3.4 EXPERIMENTAL METHODS

Identification of significant process parameters in gas phase vanadium extraction

The 2^4 full factorial design method was used to design experiments. And the technique outlined by Montgomery et al. (1995) was used for designing these experiments. The interactions between the reaction temperature, acetylacetone flowrate, particle size and catalyst weight were investigated. The results of the experiments were used to identify and evaluate of significant process parameters that strongly affect the extraction extent of vanadium from the spent vanadium catalyst. The experimental conditions for each experimental run are shown in Table 3-3. The temperature of the evaporating flask was maintained at $T_1 = 140\text{ }^\circ\text{C}$ (boiling point of acetylacetone) for all the experiments. The reaction was allowed to proceed for 7 hours and within this period, 8 product samples were collected. The first two samples were collected 30 minutes apart and thereafter, all other samples were collected hourly.

Table 3-3: Factorial design experiments for vanadium extraction case study, using acetylacetone.

Experiment Number	Temperature (T_2)	Particle size	Q_{Hacac}	Catalyst weight	Runs
9	150 °C	+500 μ m -1mm	1 mL/min	5 g	1
13	200 °C	+500 μ m -1mm	1 mL/min	5 g	2
14	150 °C	+2mm -4mm	1 mL/min	5 g	3
10	200 °C	+2mm -4mm	1 mL/min	5 g	4
5	150 °C	+500 μ m -1mm	5 mL/min	5 g	5
6	200 °C	+500 μ m -1mm	5 mL/min	5 g	6
1	150 °C	+2mm -4mm	5 mL/min	5 g	7
2	200 °C	+2mm -4mm	5 mL/min	5 g	8
16	150 °C	+500 μ m -1mm	1 mL/min	15 g	9
11	200 °C	+500 μ m -1mm	1 mL/min	15 g	10
15	150 °C	+2mm -4mm	1 mL/min	15 g	11
12	200 °C	+2mm -4mm	1 mL/min	15 g	12
8	150 °C	+500 μ m -1mm	5 mL/min	15 g	13
7	200 °C	+500 μ m -1mm	5 mL/min	15 g	14
4	150 °C	+2mm -4mm	5 mL/min	15 g	15
3	200 °C	+2mm -4mm	5 mL/min	15 g	16

Additional experiments for vanadium extraction experiments

Similarly, a 2^3 full factorial design method was used to design the experiments in Table 3-4 with the anticipation of improving the extraction degree of vanadium. The operational temperature of the evaporating flask was kept at $T_1 = 140$ °C, and the reaction temperature of $T_1 = 200$ °C was maintained for all experimental runs. The reaction was allowed to proceed for 7 hours. And the results of the experiments were used to identify and evaluate of significant process parameters at the conditions presented in Table 3-4:

Table 3-4: Optimization experiments for vanadium extraction experiments.

Experiment Number	Particle size	Q_{Hacac}	Catalyst weight	Runs
2	+250 μ m -500 μ m	5 mL/min	15 g	1
8	+500 μ m -1mm	5 mL/min	15 g	2
4	+250 μ m -500 μ m	7 mL/min	15 g	3
6	+500 μ m -1mm	7 mL/min	15 g	4
1	+250 μ m -500 μ m	5 mL/min	50 g	5
5	+500 μ m -1mm	5 mL/min	50 g	6
3	+250 μ m -500 μ m	7 mL/min	50 g	7
7	+500 μ m -1mm	7 mL/min	50 g	8

Identification of significant process parameters in gas phase tantalum extraction

A similar approach for design of experiments was used, in order to identify and evaluate the important process parameters for tantalum extraction. The experimental conditions for each experimental run are shown in Table 3-5. The temperature of the evaporating flask was maintained at $T_1 = 140\text{ }^{\circ}\text{C}$ for all the experiments and each experimental run was allowed to occur for duration of 5 hours, instead of 7 hours due to the availability of acetylacetone. A total of 7 product samples were collected within the 5 hour duration, the first four product samples were collected after 30 minutes of reaction time, whereas the last three samples were collected in hourly reaction intervals.

Table 3-5: Factorial design experiments for vanadium extraction case study.

Experiment Number	Ta ₂ O ₅ wt%	Temperature (T ₂)	Flowrate	Catalyst weight	Runs
1	2 wt%	150 °C	1 mL/min	15 g	1
7	10 wt%	150 °C	1 mL/min	15 g	2
4	2 wt%	200 °C	1 mL/min	15 g	3
6	10 wt%	200 °C	1 mL/min	15 g	4
12	2 wt%	150 °C	5 mL/min	15 g	5
9	10 wt%	150 °C	5 mL/min	15 g	6
10	2 wt%	200 °C	5 mL/min	15 g	7
14	10 wt%	200 °C	5 mL/min	15 g	8
2	2 wt%	150 °C	1 mL/min	50 g	9
3	10 wt%	150 °C	1 mL/min	50 g	10
8	2 wt%	200 °C	1 mL/min	50 g	11
5	10 wt%	200 °C	1 mL/min	50 g	12
13	2 wt%	150 °C	5 mL/min	50 g	13
15	10 wt%	150 °C	5 mL/min	50 g	14
11	2 wt%	200 °C	5 mL/min	50 g	15
16	10 wt%	200 °C	5 mL/min	50 g	16

Kinetic analysis of the gas-solid reactions in the gas phase extraction process

Considering that the reaction column of the gas phase extraction process was insulated, and the possibility of flowrate and temperature influencing the extraction reaction, the shrinking unreacted core model incorporating both mass transfer and chemical reaction effects was applied for kinetic analysis. It was further assumed that since the catalyst particles or tantalum oxide-silica- sand particles were spherical in shape. Therefore, considering these, the shrinking unreacted core model described by equation (3) was simplified to equation (14), which is used to conduct the kinetic study of the extraction reactions of vanadium and tantalum extraction.

$$t^* = t/\tau = 1 - (1 - X)^{1/3} + \sigma_s^2 [1 - 3(1 - X)^{2/3} + 2(1 - X)] \quad (14)$$

The experimental data of the degree of extraction versus reaction time was fitted with the model described by equation (14). In order to fit the model, an initial estimate of σ_s^2 was required. A random initial value was ascribed to σ_s^2 . Thereafter, an objective function described by equation (15) was developed, so as to minimize the error between the experimental and model predicted extractions.

$$\text{Objective function} = \min(f(\sigma_s^2)) = \min \left(\sum_{i=1}^n (X^{exp} - X^{model})_i^2 \right) \quad (15)$$

Anon-linear regression method, using least squares error minimisation was executed using *Solver* in *Excel* to estimate σ_s^2 , and the restrictions imposed on the propagated least squares error were stiffened, such that it was always less than 3 % ($\zeta \leq 0.03$).

Estimation of the reaction rate constant (k) and effective diffusivity (D_{eA})

The determination of the kinetic rate constant (k) was dependent on the attained value of the shrinking core-reaction modulus (σ_s^2). The summary of the criterion used to attain an estimate of k is highlighted in Table 3-6.

Table 3-6: Criteria used to estimate k at different values of σ_s^2 (Szekely et al., 1976).

Shrinking core reaction modulus(σ_s^2).	Plots used to aid with estimating (k)
$\sigma_s^2 < 0.1$ (chemical controlled)	$1 - (1 - X)^{1/3}$ vs t
$0.1 < \sigma_s^2 < 10$ (mixed controlled)	$1 - (1 - X)^{1/3} + \sigma_s^2 [1 - 3(1 - X)^{2/3} + 2(1 - X)]$ vs t
$\sigma_s^2 > 10$ (diffusion controlled)	$1 - 3(1 - X)^{2/3} + 2(1 - X)$ vs t

A gradient of a straight line through the plots presented in Table 3-6, yielded the reaction rate constant (k) (Szekely et al., 1976). The associated coefficient of determination (R^2) indicates the degree of accuracy of fitting the data with a linear function, which in turn shows the precision of the attained k -value. Thus, if R^2 is very close to 1, it shows that the data is well fitted by a linear curve. Lastly, the attained (k) value was then used to determine the effective diffusivity of acetylacetone (D_{eA}), by applying equation (10).

4 RESULTS AND DISCUSSION OF RESULTS

The results of the experimental studies is presented and discussed in this section along with some modelling studies of the extraction of vanadium and tantalum. Before any experimental work commenced, the existing gas phase experimental setup was modified to improve its operation. An acetylacetone preheater was designed, fabricated and fitted to the system to improve ligand evaporation and the condenser was replaced. The new condenser has a larger heat transfer area and allowed for better condensation of the gaseous product. A description of the experimental equipment is provided in the experimental section.

4.1 VANADIUM EXTRACTION FROM SPENT VANADIUM CATALYST

The reaction (16) that governs the recovery process of vanadium from spent catalysts is shown below:



The by-products of this reaction are acetic anhydride ((CH₃CO)₂CO) and water (H₂O) (van Dyk et al., 2016)

4.1.1 Determination of significant experimental factors

An initial experimental study was conducted to determine the influence of the extraction variables, reaction temperature, acetylacetone flowrate, particle size and catalyst bed weight. This was later expanded to include a wider experimental parameter range based on the results that were obtained initially.

Initial experiments

A single replicate of the 2⁴ factorial design experiments was conducted in a gas phase extraction process, in order to study the process variable parameters thought to have significant influence on the extraction extent of vanadium from the spent vanadium catalyst. A summary of the results for vanadium extraction are presented in Table 4-1.

The extraction results show that the gas phase extraction process achieved the highest vanadium extraction (49.9%) when 15 g of fine catalyst particles (+500 µm to -1 mm) was contacted with 5 mL/min of acetylacetone for 7 hours at a reaction temperature of 200 °C. The lowest vanadium extraction (5.4%) was attained when low bed weight (5 g) of coarse catalyst particles (+2 mm to -4 mm), was subjected to 1 mL/min of acetylacetone at a reaction temperature of 150 °C for the same duration of time. Moreover, these results reveal that the lowest vanadium extractions were achieved at an acetylacetone flowrate of 1 mL/min. The highest vanadium extraction achieved at low flowrates of 1 mL/min was 16.2 %, whereas the lowest achieved at 5

mL/min was 22.8 %. It can therefore be seen that the acetylacetone flowrate might be one of the parameters that greatly influence the extraction of vanadium in this process. To confirm this, a significance test was performed (discussed later).

The extraction time curves of the 16 experimental runs are presented in Figure 4-1 to Figure 4-4. It shows how the extraction reaction proceeded with time at different reaction conditions. By examining Figure 4-3 to Figure 4-4 it can be seen that, extractions at the elevated temperature of 200 °C are generally higher than those attained at lower temperature of 150 °C, irrespective of the bed weight, acetylacetone flowrate or catalyst particle size

.

Table 4-1: Summary results of 2⁴ factorial design experiments for vanadium extraction.

Experimental variables					% Extraction
Runs	Temp. (A)	Particle size (B)	Flowrate (C)	Bed Load (D)	(Y)
1	150 °C	+0.5 mm -1mm	1 mL/min	5 g	10.7%
2	200 °C	+0.5 mm -1mm	5 mL/min	15 g	11.9%
3	150 °C	+2 mm - 4 mm	1 mL/min	5 g	5.4%
4	200 °C	+2 mm - 4 mm	5 mL/min	15 g	16.2%
5	150 °C	+0.5 mm -1mm	1 mL/min	5 g	29.1%
6	200 °C	+0.5 mm -1mm	5 mL/min	15 g	46.6%
7	150 °C	+2 mm - 4 mm	1 mL/min	5 g	35.3%
8	200 °C	+2 mm - 4 mm	5 mL/min	15 g	47.7%
9	150 °C	+0.5 mm -1mm	1 mL/min	5 g	6.9%
10	200 °C	+0.5 mm -1mm	5 mL/min	15 g	10.1%
11	150 °C	+2 mm - 4 mm	1 mL/min	5 g	8.7%
12	200 °C	+2 mm - 4 mm	5 mL/min	15 g	11.3%
13	150 °C	+0.5 mm -1mm	1 mL/min	5 g	48.1%
14	200 °C	+0.5 mm -1mm	5 mL/min	15 g	49.9%
15	150 °C	+2 mm - 4 mm	1 mL/min	5 g	22.8%
16	200 °C	+2 mm - 4 mm	5 mL/min	15 g	41.0%

Furthermore, it is seen that at high catalyst bed weight (15 g) and high acetylacetone flowrate (5 mL/min), the overall extraction is sensitive to temperature changes for coarse particles, compared with fine particles, which exhibit a small variation in extraction at different reaction temperatures. An evaluation of results presented in Figure 4-1 to Figure 4-4 suggests that flowrate and temperature might be significant process parameters in the extraction of vanadium from spent vanadium catalyst. The aforementioned assumptions were validated and the results are presented. In addition, it was of great importance to study the joint factor effects of these process variables.

A statistical method integrating the 15-factor effects (2⁴-1) of these experiments was applied to aid with the determination of the most significant process parameters that influence the extraction of vanadium in the gas phase extraction process. The four main effects are associated with temperature (A), particle size (B), acetylacetone flowrate (C) and spent catalyst loading (D), whereas 11 degrees of freedom are associated with interaction effects AB, AC, AD, BC, BD, CD, ABC, ABD, ACD, BCD and ABCD. The calculations of the factor effect estimates are shown in Appendix B.

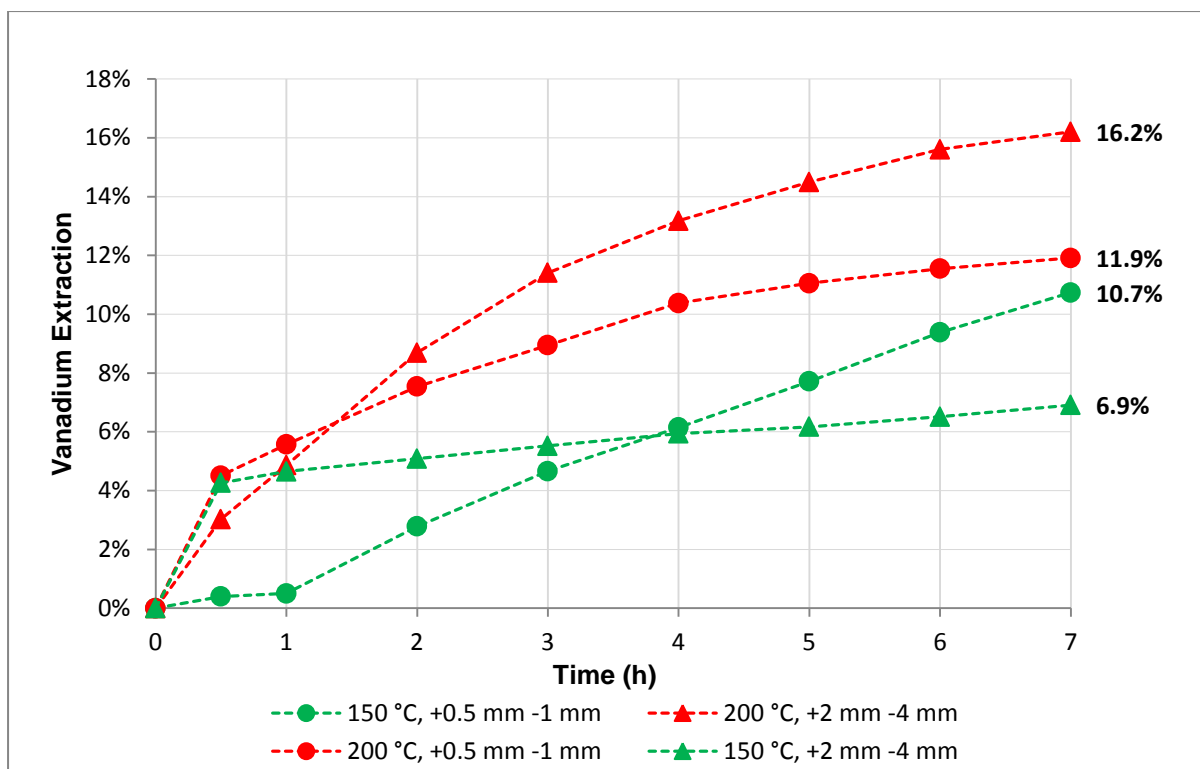


Figure 4-1: Vanadium extraction with time (5 g bed loading and acetylacetone flowrate of 1 mL/min).

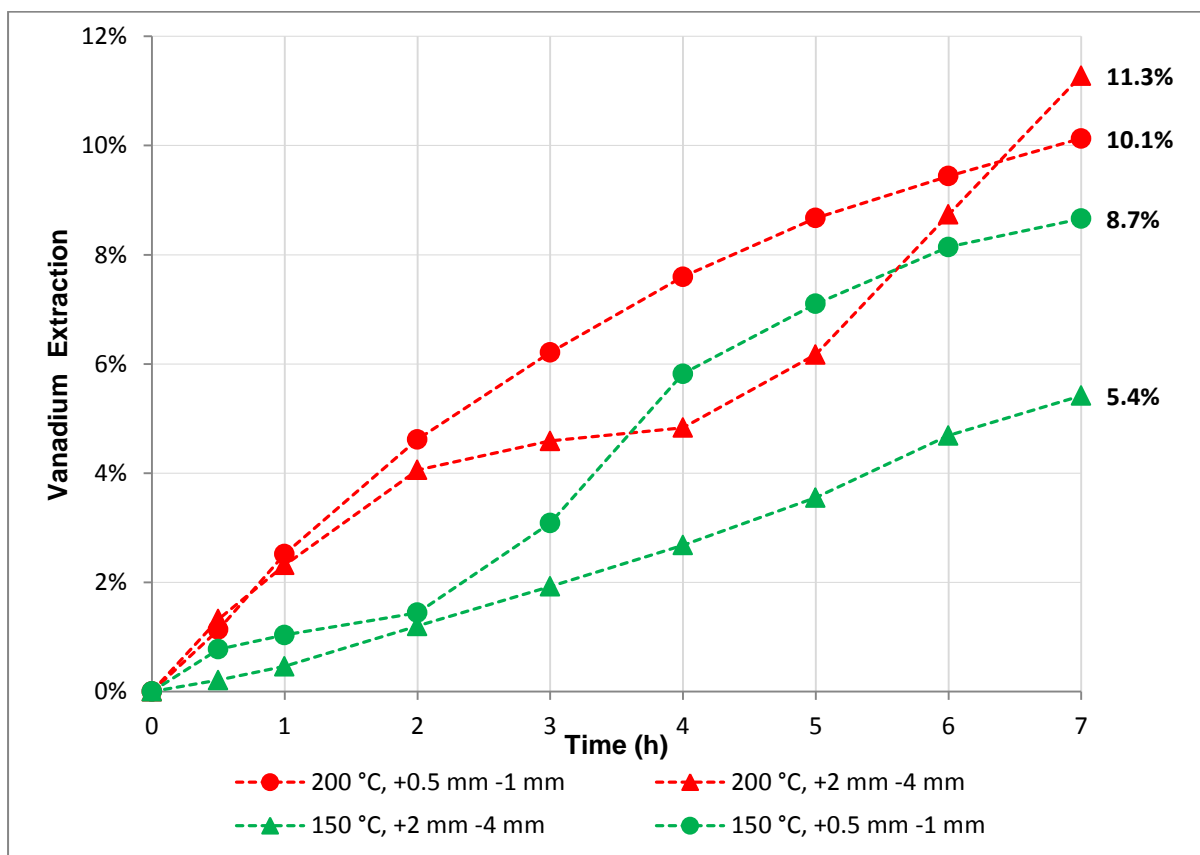


Figure 4-2: Vanadium extraction with time (15 g bed loading and acetylacetone flowrate of 1 mL/min).

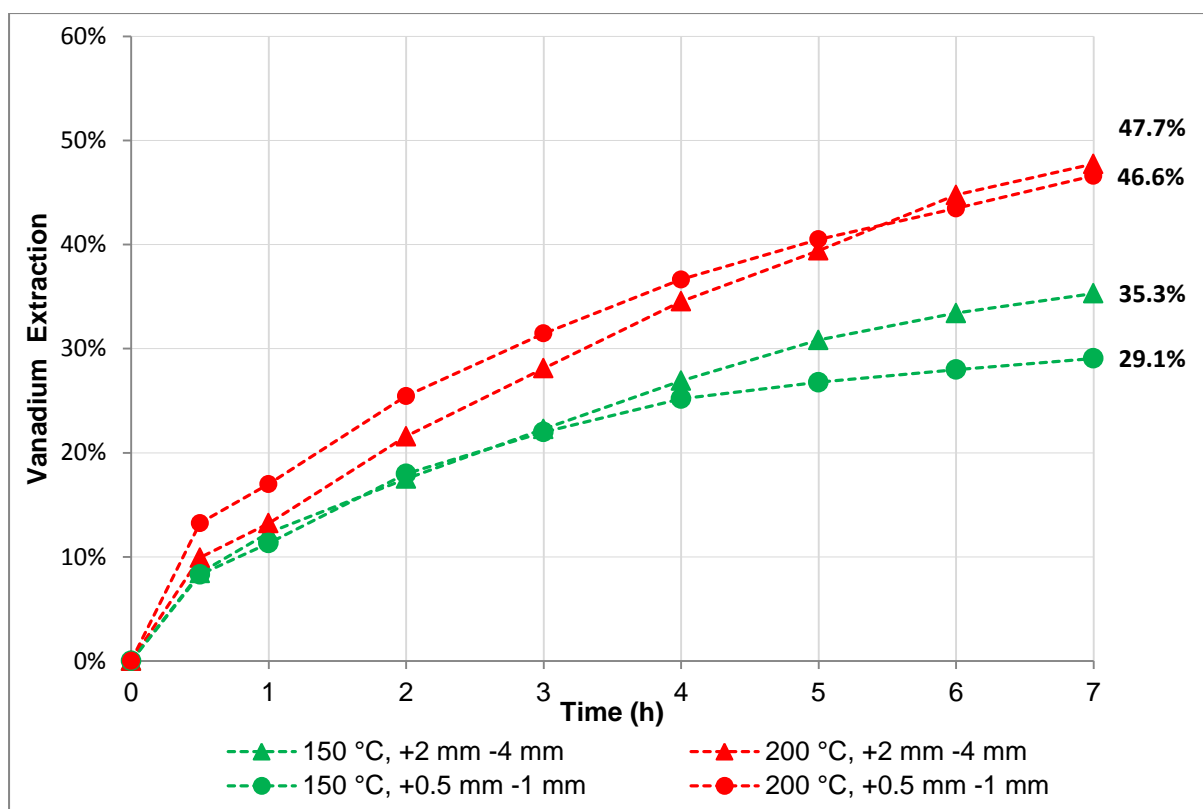


Figure 4-3: Vanadium extraction with time (5 g bed loading and acetylacetone flowrate of 5 mL/min).

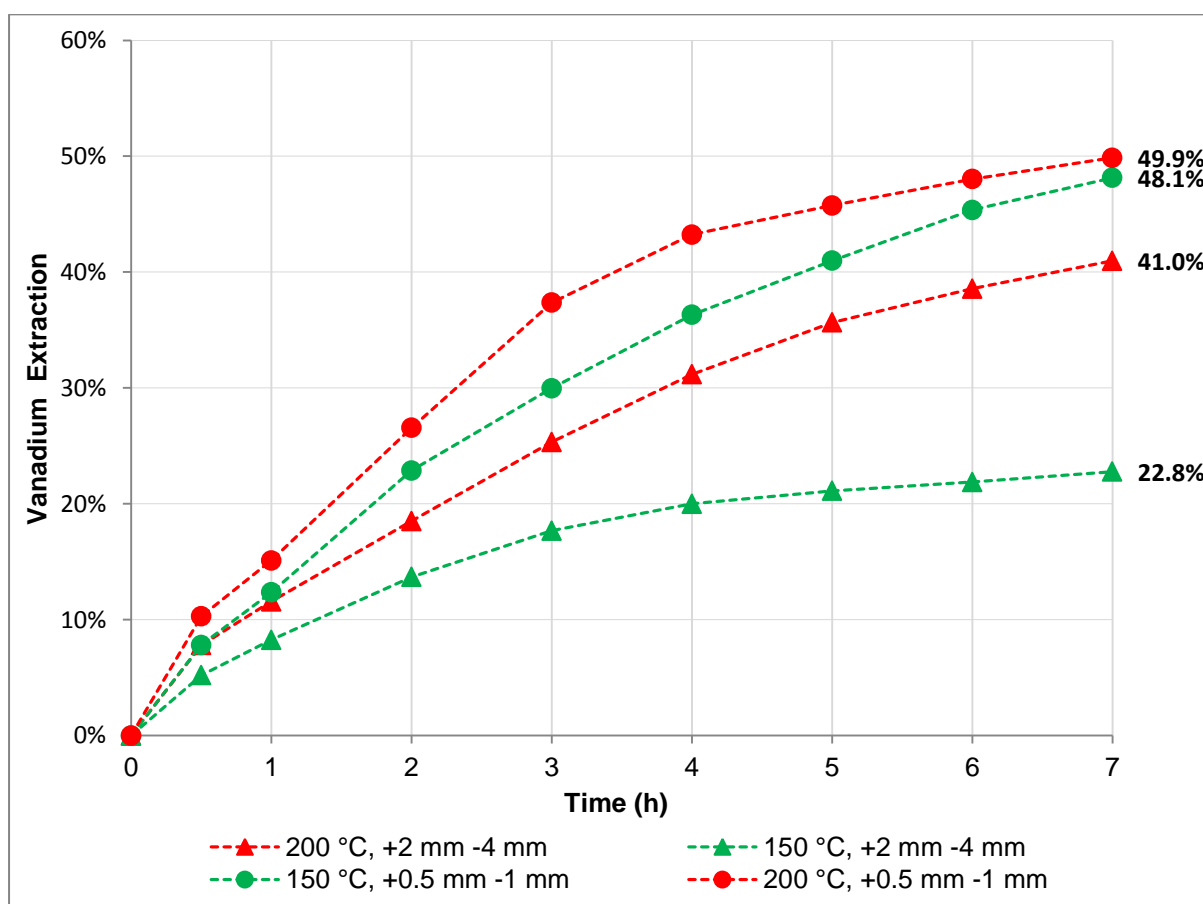


Figure 4-4: Vanadium extraction with time (15 g bed loading and acetylacetone flowrate of 5 mL/min).

The statistical analysis of results was initiated by constructing a normal probability plot, which helps with the preliminary determination of significant process parameters. Thereafter, the conclusions from examining the normal probability plot were either endorsed or rejected by performing the analysis of variance, which specify the statistical significance of the factors that emerged to have played a key role in the extraction process.

The normal probability plot of the effect estimates for the experiments is shown in Figure 4-5. All the effects that lie close or along the mean value line are considered insignificant, whereas the effects furthest away from the mean value line are significant. Temperature (*A*), particle size (*B*), acetylacetone flowrate (*C*) as well as *BD*, *AC* and *BCD* interaction effects, emerge as major contributing factor effects towards the overall extraction process.

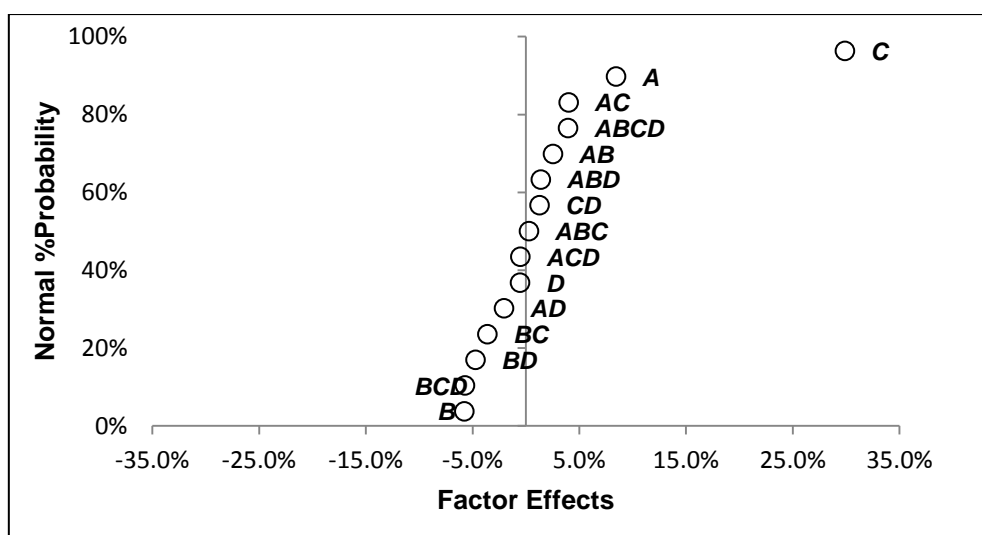


Figure 4-5: Normal probability plot of factor effects on vanadium extraction response.

Thus, the analysis of variance (Table 4-2) for the experimental design was used to confirm the magnitude of these effects, and based on the P-values ($P < 0.05$), it can be concluded that temperature (*A*), acetylacetone flowrate(*C*) and *BCD* interaction effects are statistically significant at 95% confidence level.

Table 4-2: Analysis of variance for vanadium extraction factorial design experiments.

Source of Variation	Sum of Squares	D.O.F	Mean Square	F_0	P-Value
C	0.3577	1	0.3577	149.9228	2.42E-07
A	0.0286	1	0.0286	12.0011	6.08E-03
B	0.0039	1	0.0039	1.6379	2.30E-01
BCD	0.0130	1	0.0130	5.4416	4.19E-02
BD	0.0089	1	0.01	3.7272	8.24E-02
Error	0.0239	10	0.0024		
Total	0.4360	15			

The main and interaction factor effect plots of the identified significant parameters were constructed. The reaction temperature (A), acetylacetone flowrate (C) and BCD interaction effect plots are presented in Figure 4-6 to Figure 4-8. These figures were constructed by plotting the average vanadium extraction against the identified significant main factor or interaction factor effect at low (-1) and high (+1) level setting.

Through examining the factor effect plots, it can be seen that acetylacetone flowrate has a greater influence on the extraction of vanadium as compared to reaction temperature, and this is validated by the slope of the main factor effect plots (Figure 4-6 and Figure 4-7). The change in flowrate from 1 mL/min to 5 mL/min led to an average increase of vanadium extraction of 25%, whereas the adjustment of reaction temperature from 150 °C to 200 °C yielded an average extraction difference of 8%. According to Habashi (1970), the overall reaction rate of a heterogeneous gas-solid reaction, is classified as being governed by diffusion if it is strongly affected by flowrate, and slightly influenced by temperature. Therefore, based on the average percentage change brought about by increasing the reaction temperature and acetylacetone flowrate, it might be concluded that the overall reaction process is governed by diffusion. However, the attained P-values (Table 4-2) suggested that both temperature and flowrate are significantly contributing towards the overall reaction process at 95% confidence level. Consequently, there is a possibility that diffusion and chemical reaction mechanisms may have comparable resistances in the overall extraction rate.

On the other hand, Figure 4-8 shows that the interaction effect between particle size and flowrate (BC) strongly influences the extraction rate of vanadium at high catalyst bed loading, effect whereas at small bed loads the BC interaction leads to minor variation in the extraction rate. The former and latter observations suggest that at high bed loading the overall reaction rate is possibly governed by mass transfer and by chemical reaction at small bed loads. But, the kinetic study puts clarity as to which mechanism governs in the extraction of vanadium for each experimental run. Furthermore, it is seen that the highest vanadium extraction is achieved when a high bed load ($D_+ = 15\text{ g}$) of fine catalyst particles is subjected to high acetylacetone flowrate ($B_{[+500\mu\text{m} - 1\text{ mm}]} \times C_{5\text{ ml/min}} = -1 \times 1 = -1$). This may be because an increase in the degree of fineness of the catalyst particles results in an increased reaction surface area of the catalyst, and the available reaction surface area is further enhanced upon loading large quantity of catalyst in the reaction column. Additionally, adjusting ligand flowrate to high level setting translates into an increase in molar flowrate of acetylacetone.

As a result, combination of the aforementioned set of conditions amplifies the contact frequency between the catalyst particles and acetylacetone molecules, provided the flowrate is such that acetylacetone is in excess, thus enhancing the reaction rate constant, and consequently converting large fraction of the vanadium

spent catalyst into product. Likewise, the rapid formation of product quickly off-sets the reaction zone from the outer surface of each catalyst particle into the inner solid,

leaving behind an ash layer, through which both the product and reactant has to diffuse through. Hence, since the diffusion barrier is enlarged, the mass transfer coefficient becomes more pronounced as compared to the reaction rate constant. Thus, explaining why it is more probable for mass transfer to govern the overall extraction rate at high bed loads.

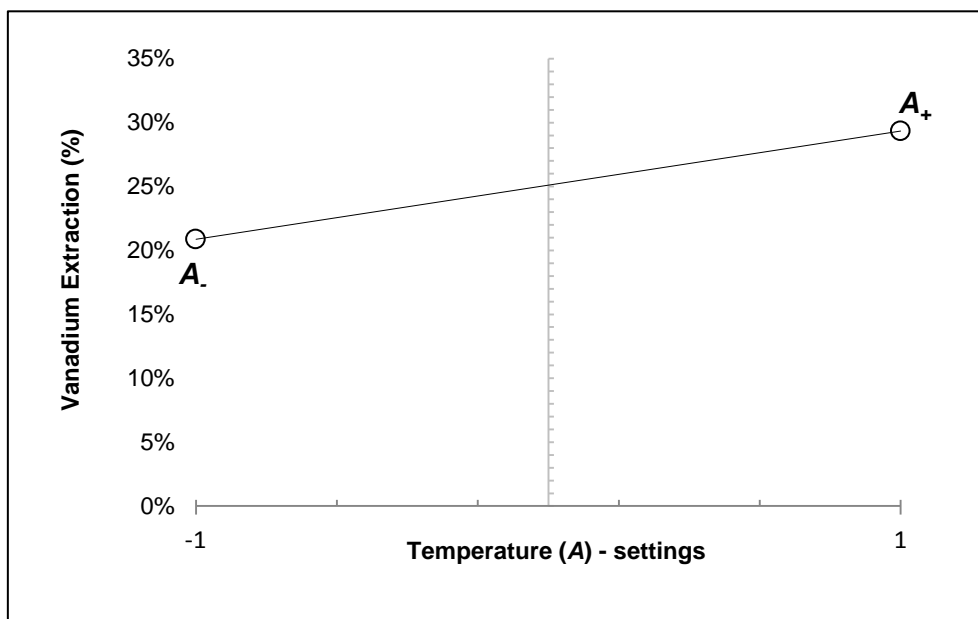


Figure 4-6: Effect of temperature on the extraction extent of vanadium from spent vanadium catalyst, using acetylacetone as a volatile ligand.

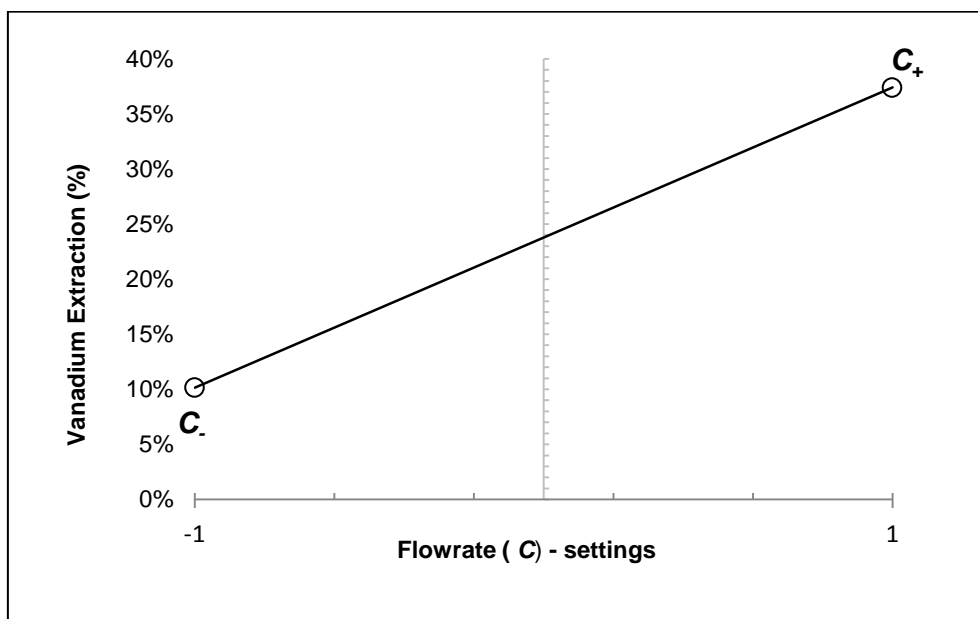


Figure 4-7: Effect of acetylacetone flowrate on the extraction extent of vanadium from spent vanadium catalyst.

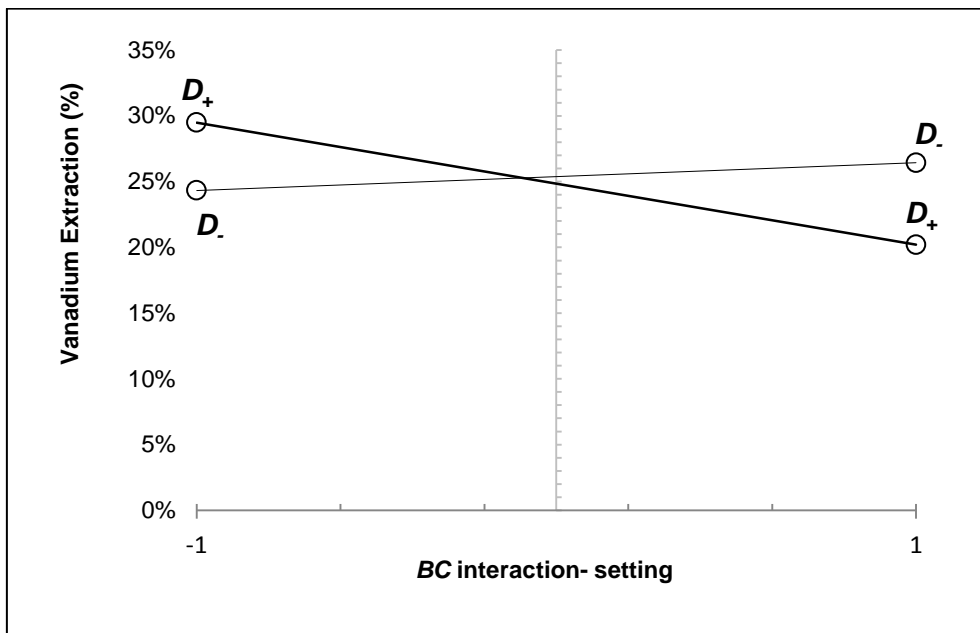


Figure 4-8: Influence of BCD interaction effect on the extraction extent of vanadium from spent vanadium catalyst, using acetylacetone as a volatile ligand.

Additional Vanadium Extraction Experiments

The highest vanadium extraction that could be achieved during the initial experiments were 49.9% at 200 °C, 5 mL/min Hacac flowrate from 15 g sample of +0.5 mm -1 mm particle size. Consequently, additional experiments were conducted to improve the degree of extraction of vanadium, by broadening the significant factor parameter limits. Therefore, taking into consideration the observations above, for this set of experiments, the reaction temperature was kept constant at 200 °C. In addition, previous thermogravimetric studies (Dilli & Patsalides, 1976) showed that $\text{VO}(\text{acac})_2$ decomposed at temperatures of 250 °C, thus the reaction temperature was kept far away from the decomposition temperature. Additionally, the catalyst particles were further reduced into smaller size fractions, while the acetylacetone flowrate was increased, along with a substantial adjustment of the catalyst bed weight. The maximum acetylacetone flowrate and smallest particle size of the catalyst particles were dictated by an elutriation phenomenon, whereas the bed load was limited by the available column reaction volume. Elutriation phenomenon of the catalyst particles to the product collection flask, was observed when the catalyst particles were ground to size fractions of (+106 μm -250 μm), even when acetylacetone was pumped at a rate of 5 mL/min. Hence, based on this observation, the finest catalyst size fraction was chosen to be (+250 μm -500 μm).

The acetylacetone flowrate was adjusted to a maximum of 7 mL/min, at this rate, the supplied heat from the heating mantle was still sufficient enough to vaporize the incoming mass flux of acetylacetone; it was observed that the acetylacetone vaporized instantly as it was fed to the evaporator. Furthermore, at this flowrate, elutriation phenomenon of catalyst particles to the product collection flask was not observed, and for these reasons, it was chosen as the maximum flowrate. The vanadium extraction results for this set of experiments are shown in Table 4-3.

These results show that the adjustments made to catalyst particle size, acetylacetone flowrate and catalyst bed weight led to an improvement in the extraction degree of vanadium, wherein the lowest extraction recorded was 31%, compared to 5.4% which was attained in the previous set of experiments. Additionally, in this instance, the highest vanadium extraction (55.1%) was achieved when 15 g of smallest catalyst particles (+0.25 mm -0.5 mm) was brought into contact with acetylacetone fed at 7 mL/min for 7 hours, at a reaction temperature of 200 °C. Furthermore, the results indicate that the highest extractions of vanadium were generally achieved at small bed loads (15 g). The latter observation is in contrast with the trend seen in the previous set of experiments, which fairly insinuated that, an increase in bed weight of fine catalyst particles subject to high ligand flowrate, results in an increased extraction extent.

The deviation might have surfaced as a result of drastic adjustment of catalyst weight which may exceed the bed weight threshold beyond which extraction does not increase. The adjustments could have been such that, the initial reaction rates are very rapid compared to the diffusion rate of product to the bulk gas, subsequently causing an increased diffusion barrier attributed to the both the ash layer and the gas film layer, thus contributing to the significant slowing of the reaction, resulting in low degrees of extractions.

Table 4-3: Summary results of 2³ factorial design experiments for vanadium extraction.

Experimental variables			% Extraction
Particle size (B)	Flowrate (C)	Bed loading (D)	(Y)
+0.25 mm -0.5 mm	5 mL/min	15 g	41.6%
+0.5 m -1 mm	5 mL/min	15 g	49.9%
+0.25 mm -0.5 mm	7 mL/min	15 g	55.1%
+0.5 m -1 mm	7 mL/min	15 g	44.3%
+0.25 mm -0.5 mm	5 mL/min	50 g	34.0%
+0.5 m -1 mm	5 mL/min	50 g	31.0%
+0.25 mm -0.5 mm	7 mL/min	50 g	33.1%
+0.5 m -1 mm	7 mL/min	50 g	35.3%

The extraction time curves of the 8 experimental runs are presented in Figure 4-9 to Figure 4-10. It shows how the extraction reaction proceeded with time at different reaction conditions. By the examining Figure 4-9 to Figure 4-10, it can be seen that the flowrate effect is more prominent at small bed weight, which might imply that at small bed weight mass transfer is the dominant mechanism dictating the reaction rate. At high bed weight, the change in flowrate slightly improved the extraction extent of vanadium, and it seems as though mass transfer and chemical reaction mechanisms interchanged its dominance for fine catalyst particles as time progressed, and this is seen by the coinciding extents of extractions at different flowrates for the first two hours, implying chemical reaction dominance, followed by variation in extraction between the second and sixth hour, meaning mass transfer was controlling, and further dominance by chemical reaction in the last hour of reaction. Likewise, to confirm this, a significance test and kinetic study was performed.

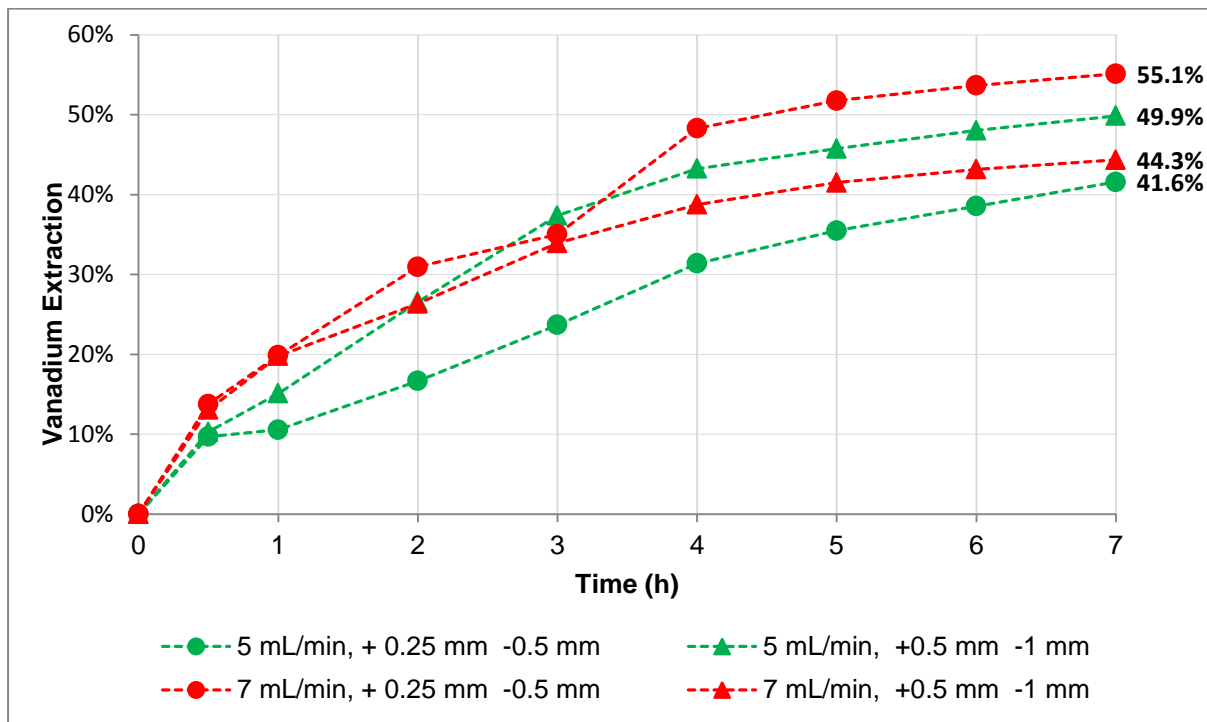


Figure 4-9: Vanadium extraction with time (15 g bed loading and reaction temperature of 200 °C).

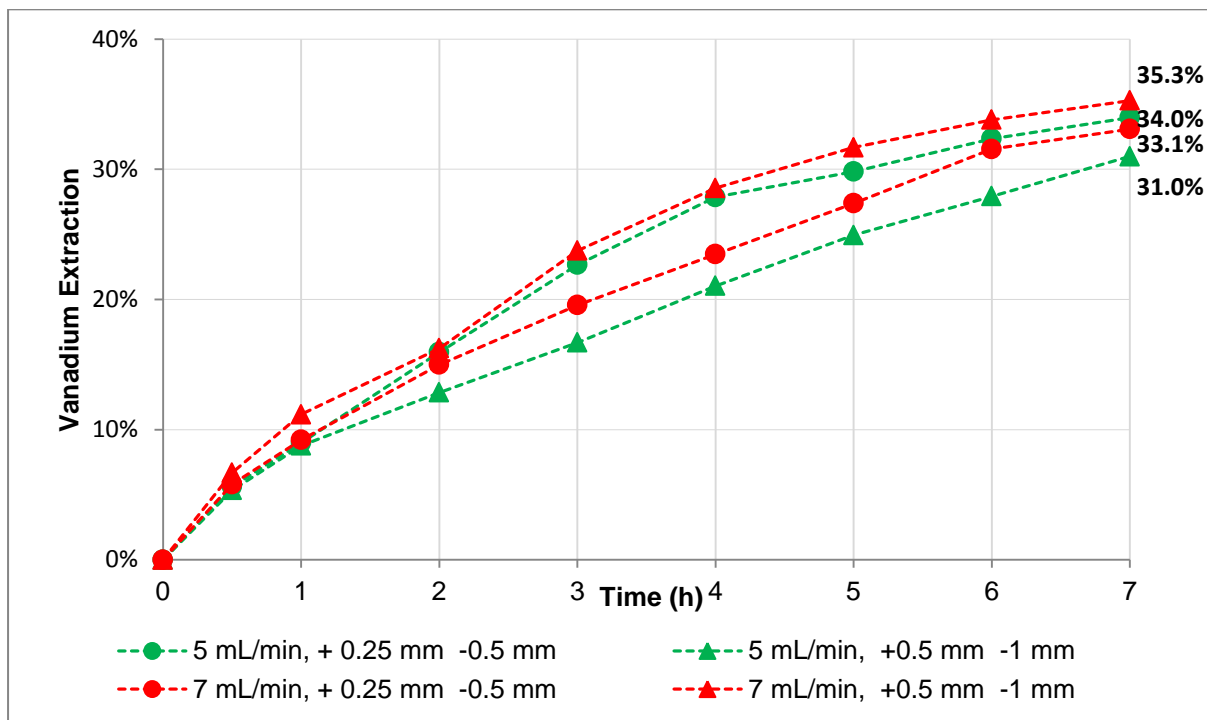


Figure 4-10: Vanadium extraction with time (50 g bed loading and reaction temperature of 200 °C).

The important factors emerging by examining Figure 4-11 can be seen as the catalyst bed loading (*D*), acetylacetone flowrate (*C*), *BC* and *BCD* interaction effects. The P-values obtained in Table 4-4 confirms that the aforesaid parameters are indeed significant at 95% confidence level ($P < 0.05$).

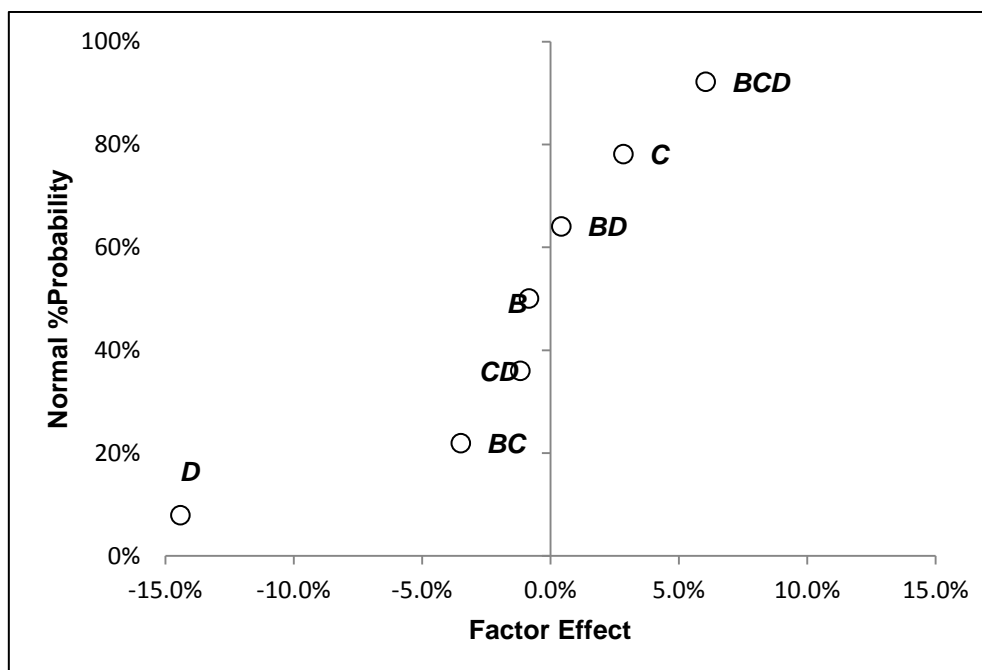


Figure 4-11: Normal probability plot of factor effects on the vanadium extraction response.

Table 4-4: Analysis of variance for the design.

Source of Variation	Sum of Squares	D.O.F	Mean Square	F ₀	P-Value
C	0.0016	1	0.0016	11.0691	1.26E-02
D	0.0415	1	0.0415	281.7538	6.52E-07
BC	0.0024	1	0.0024	16.4174	4.86E-03
BCD	0.0073	1	0.0073	49.8763	2.00E-04
Error	0.0004	3	0.00015		
Total	0.0534	7			

The significant main factor effect plots (Figure 4-12 and Figure 4-13) further highlight that, the change in flowrate led to an average increase of vanadium extraction by 3%, while the adjustment of bed weight caused an average decrease of 14%. In addition, Figure 4-14 shows that *BC* interaction brought about a considerable difference (10%) in extent of vanadium extraction at small bed loads, but a minute change at high bed loads (3%). Therefore, based on these observations, mass transfer might be controlling the extraction rate at small bed loads, particularly for fine catalyst particles (Figure 4-9), and at high bed loads the chemical reaction mechanism was governing the overall extraction rate of vanadium from the spent catalyst.

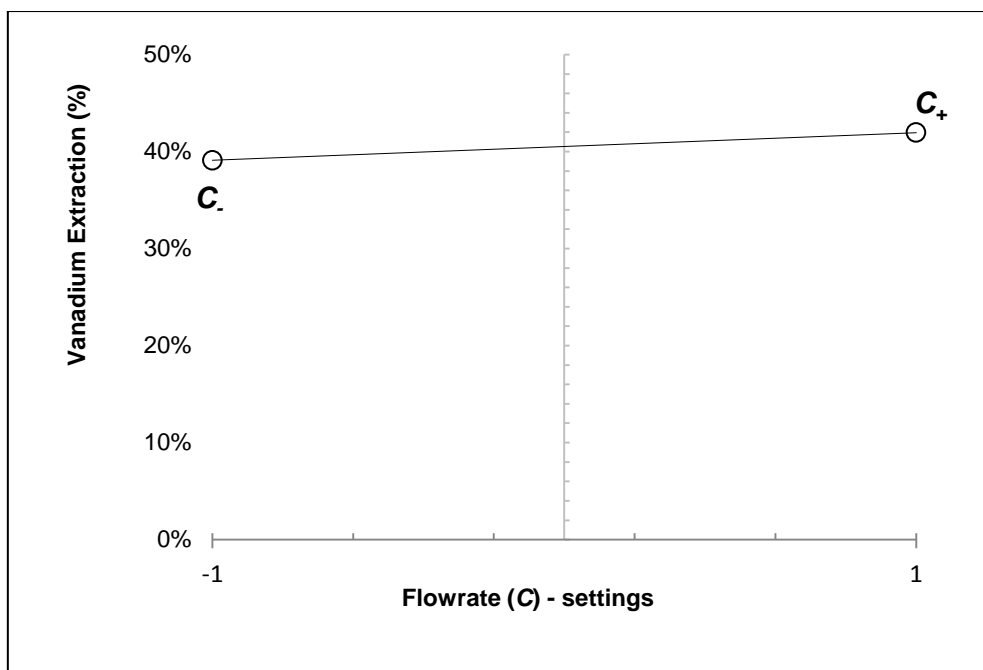


Figure 4-12: Effect of flowrate on the extraction extent of vanadium from spent vanadium catalyst.

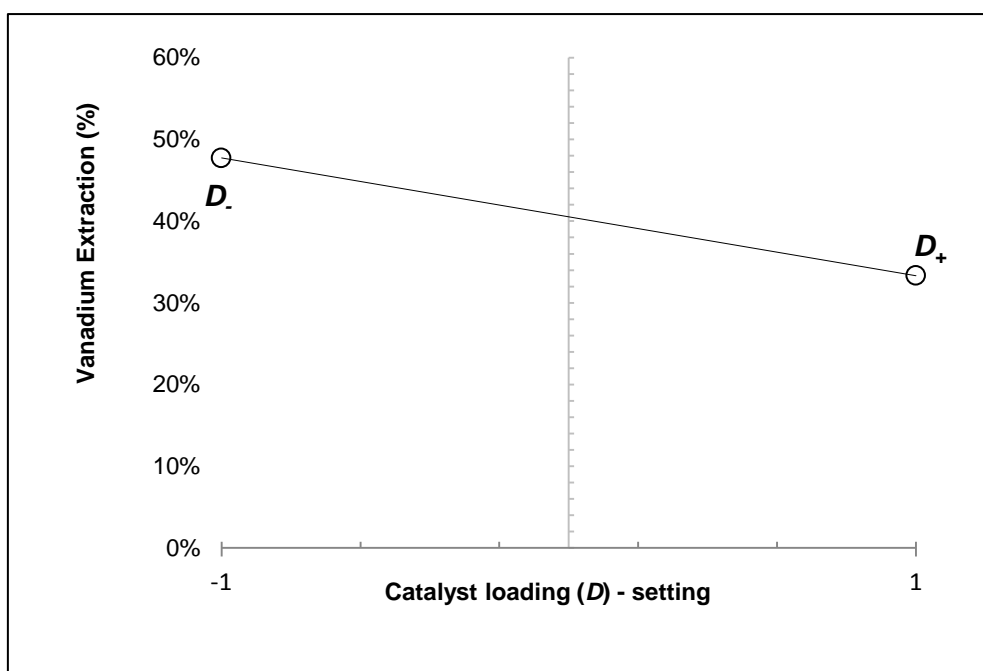


Figure 4-13: Effect of bed loading on the extraction extent of vanadium from spent vanadium catalyst

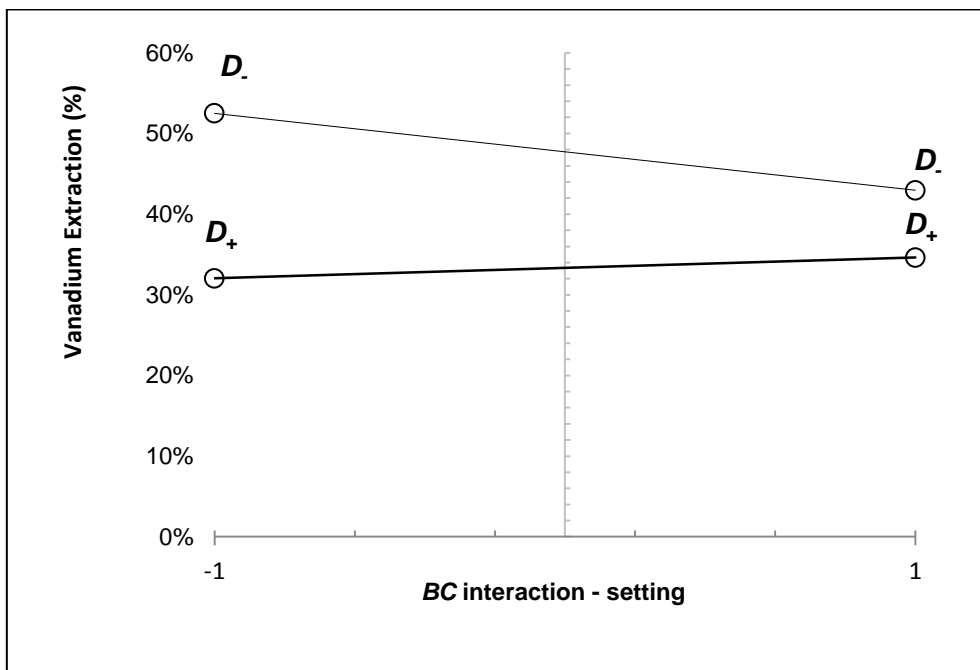


Figure 4-14: Influence of BCD interaction effect on the extraction extent of vanadium from spent vanadium catalyst

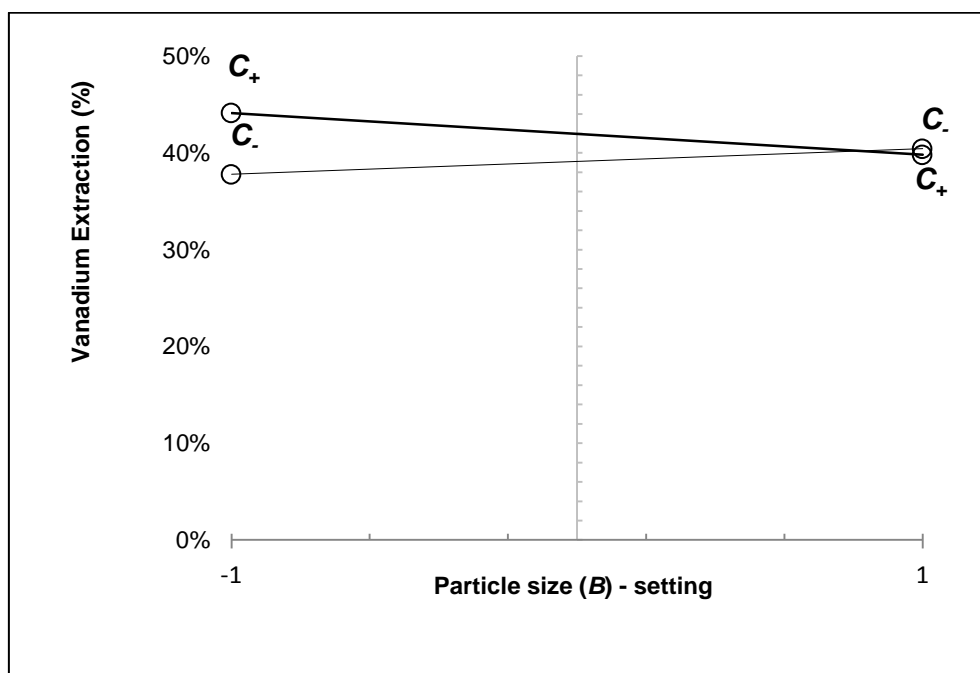


Figure 4-15: Influence of BC interaction effect on the extraction extent of vanadium from spent vanadium catalyst

4.1.2 Kinetic analysis of vanadium extraction experiments

By examining the results in Table 4-5 it can be seen that the values of the shrinking core-reaction modulus are consistently higher ($\sigma_s^2 > 10$) at low flowrates of acetylacetone (1 mL/min), implying that the overall extraction rate was governed by diffusion through the ash layer. Moreover, in light of conclusions arrived at, through examining Figure 4-14, it can be said with certainty that the interaction between particle size, flowrate and bed weight (BCD -interaction) impacts the reaction

parameters considerably, yielding differences in σ_s^2 . Lower values of σ_s^2 are observed at high bed loads, and this may result because the tortuosity (δ) of the reactant gas molecules is amplified at high bed loads, with probable reduction in porosity (ε) across the bed height, consequently decreasing the effective diffusivity of the reactant gas molecules ($D_{eA} = D_A \varepsilon / \delta$).

On a different note, by reverting to Figure 4-1 to Figure 4-4 and also in view of the conclusions implied by the values of σ^2 (>10) it can be said that the resulting product layer surrounding the catalyst particle(s) is possibly non-porous, and may be accountable for the decrease in the extraction rate. First thing to remember is that, the chelating reagent (acetylacetone) has to diffuse through the protective film around the catalyst particle(s) before reaching the reaction interface, and it follows that if the mass transport resistance increases over the reaction period, then this can only mean that the protective film is non-porous (Habashi, 1979). The most compelling evidence would be the considerable slowing of the extraction rate, which is in fact the case with vanadium extraction experiments, and the rate seems to slow substantially after 3 hours, with the exception being those which were conducted at elevated acetylacetone flowrates (Figure 4-3 and Figure 4-4) where the consequent phenomenon occurred after 4 hours.

For this reason, as the reaction proceeded, it was found that the pressure within the evaporating flask gradually increased, and this can only take place if the mass flux of the volatilized acetylacetone through the catalyst bed height was considerably minimized, resulting in the accumulation of acetylacetone in the evaporating flask. And thus, at this present time, this occurrence can be rationalized by the former conclusion, classifying the protective film of the ash layer as possibly being non-porous.

The kinetic rate constants are considerably small at lower acetylacetone flowrate (1 mL/min). Moreover, the effect of temperature can be seen to have caused an approximate twofold increase on the kinetic rate constant for most of the experiments. In addition, the flowrate adjustments (from 1 mL/min to 5 mL/min) led to a substantial hundredfold increase in the kinetic rate constant, and an approximate thousand fold decrease in the effective diffusivity of acetylacetone. Higher effective diffusivity values are observed at high acetylacetone flowrates, suggesting that the adjustments in flowrate from 1 mL/min to 5 mL/min caused a considerable dissipation of the gas film resistance due to increased turbulence.

Table 4-5: Kinetic rate constants and effective diffusivities of initial vanadium experiments.

Experiments with Hacac flowrate of 1 mL/ min and bed weight of 5 g					
<i>Temperature</i>	<i>Particle size</i>	σ_s^2	k	R^2	$D_{eA}(cm^2/min)$
150 °C	+0.5 mm -1 mm	32.08	2.52E-06	0.996	2.95E-09
200 °C	+0.5 mm -1 mm	17.55	1.16E-05	0.973	2.48E-08
150 °C	+2 mm -4 mm	20.38	1.03E-05	0.944	3.79E-08
200 °C	+2 mm -4 mm	12.59	2.48E-05	0.986	1.48E-07
Experiments with Hacac flowrate of 1 mL/ min and bed weight of 15 g					
<i>Temperature</i>	<i>Particle size</i>	σ_s^2	k	R^2	$D_{eA}(cm^2/min)$
150 °C	+0.5 mm -1 mm	24.48	7.36E-06	0.942	1.13E-08
200 °C	+0.5 mm -1 mm	21.31	9.45E-06	0.997	1.66E-08
150 °C	+2 mm -4 mm	41.34	2.51E-06	0.895	4.55E-09
200 °C	+2 mm -4 mm	19.87	9.52E-06	0.801	3.59E-08
Experiments with Hacac flowrate of 5 mL/ min and bed weight of 5 g					
<i>Temperature</i>	<i>Particle size</i>	σ_s^2	k	R^2	$D_{eA}(cm^2/min)$
150 °C	+0.5 mm -1 mm	6.38	7.19E-04	0.957	4.23E-06
200 °C	+0.5 mm -1 mm	3.58	1.30E-03	0.996	1.36E-05
150 °C	+2 mm -4 mm	5.14	9.30E-04	0.996	1.36E-05
200 °C	+2 mm -4 mm	3.45	9.95E-04	0.985	2.17E-05
Experiments with Hacac flowrate of 5 mL/ min and bed weight of 15 g					
<i>Temperature</i>	<i>Particle size</i>	σ_s^2	k	R^2	$D_{eA}(cm^2/min)$
150 °C	+0.5 mm -1 mm	3.37	1.33E-03	0.998	1.48E-06
200 °C	+0.5 mm -1 mm	3.08	1.35E-03	0.958	1.64E-05
150 °C	+2 mm -4 mm	8.45	5.78E-04	0.939	5.13E-05
200 °C	+2 mm -4 mm	4.21	1.13E-03	0.995	2.02E-05

In Figure 4-9 to Figure 4-10 to it was seen that the gas phase extraction process achieved lower extractions of vanadium at high bed loads (50 g), and in Table 4-6 it can be seen that it is at that condition in which high values of the shrinking core reaction modulus are recorded. Now, considering that temperature was kept this set of experiments (200 °C) the attained values of the kinetic rate constants are comparatively the same. Hence, according to equation (10), the differences in the values of the shrinking core reaction modulus are brought upon by differences in effective diffusivity of acetylacetone through diffusion barriers. The underlying key result from this outcome could be that due to the probable amplified interaction between the catalyst particles and acetylacetone at high bed loads, it follows that there is a rapid formation of the protective film surrounding the catalyst particles. For this reason, acetylacetone is inhibited from accessing certain portion(s) of the reacting particle(s), leading to slowing of the reaction rate due to reduced interactions between the gaseous extractant and reacting solid.

Table 4-6: Kinetic rate constants and effective diffusivities of initial vanadium experiments.

<i>Temperature</i>	<i>Particle size</i>	σ_s^2	k	$D_{eA}(cm^2/min)$
5 mL/min	+0.25 mm -0.5 mm	4.14	1.11E-03	5.02E-06
7 mL/min	+0.25 mm -0.5 mm	2.61	1.48E-03	1.06E-05
5 mL/min	+0.5 mm -1 mm	3.08	1.35E-03	1.64E-05
7 mL/min	+0.5 mm -1 mm	3.66	1.10E-03	1.13E-05
<i>Temperature</i>	<i>Particle size</i>	σ_s^2	k	$D_{eA}(cm^2/min)$
5 mL/min	+0.25 mm -0.5 mm	5.30	8.91E-04	3.15E-06
7 mL/min	+0.25 mm -0.5 mm	5.58	9.05E-04	3.04E-06
5 mL/min	+0.5 mm -1 mm	6.20	8.31E-04	5.03E-06
7 mL/min	+0.5 mm -1 mm	5.03	9.65E-03	7.19E-06

4.1.3 Optimization experiments

Therefore, the selection criteria of operational conditions for optimization considered the conclusions arrived from the statistical and kinetic analyses. Figure 4-16 shows the optimization results. Opt. 1 and Opt 2 experiments were carried out by solely relying on the statistical analysis results (Figure 4-12 to Figure 4-15) , which suggested that chemical reaction governs the extraction rate at bed loads of 50 g for for fine catalyst particles (+0.25 mm 0.5 mm), subjected to maximum acetylacetone of 7 mL/min. As a result the reaction temperature was adjusted to 210 °C. And since the maximum vanadium extraction (55.1%) was achieved at smallest particles size (+250 μ m -500 μ m) and high acetylacetone flowrate (7 mL/min) these conditions were unaltered. Opt. 1 and Opt. 2 were carried-out with the anticipation of also determining the transition point at which an increase in the mass of catalyst loading led to a decrease in the extraction degree of vanadium. However, due to limited number of experiments conducted, the latter could not be deduced. But as can be seen from Figure 4-16, with particular attention to Opt.1 and Opt. 2, it was observed that within the selected operating range, an increase in the mass of catalyst loading led to a further decrease in the extraction degree of vanadium.

The reason as to why this was observed could be attributed to the rapid formation of protective film surrounding the catalyst particles at high bed loads. Additionally, it was also established that the extraction rate at high catalyst bed loads were mixed controlled and not solely chemical controlled as stipulated by the outcome from the factor effect plots (Figure 4-14), implying that the optimization process needed to take an integrated account of both the statistical outcome from the factor effect plots and the kinetic analysis results.

Henceforth, an additional optimization experiment (Opt. 3) was carried-out, considering the integrated outcome of both the statistical and kinetic analysis results. The reaction temperature and bed load were lowered to 190 °C and 15 g so as to slightly lower the intrinsic extraction rate or the rate of metal extraction around each individual particle, and slow the formation of the protective film around the catalyst particles. And so, as seen from Figure 4-16, the optimization experiment (Opt. 3) enhanced the extraction degree to 60.4%.

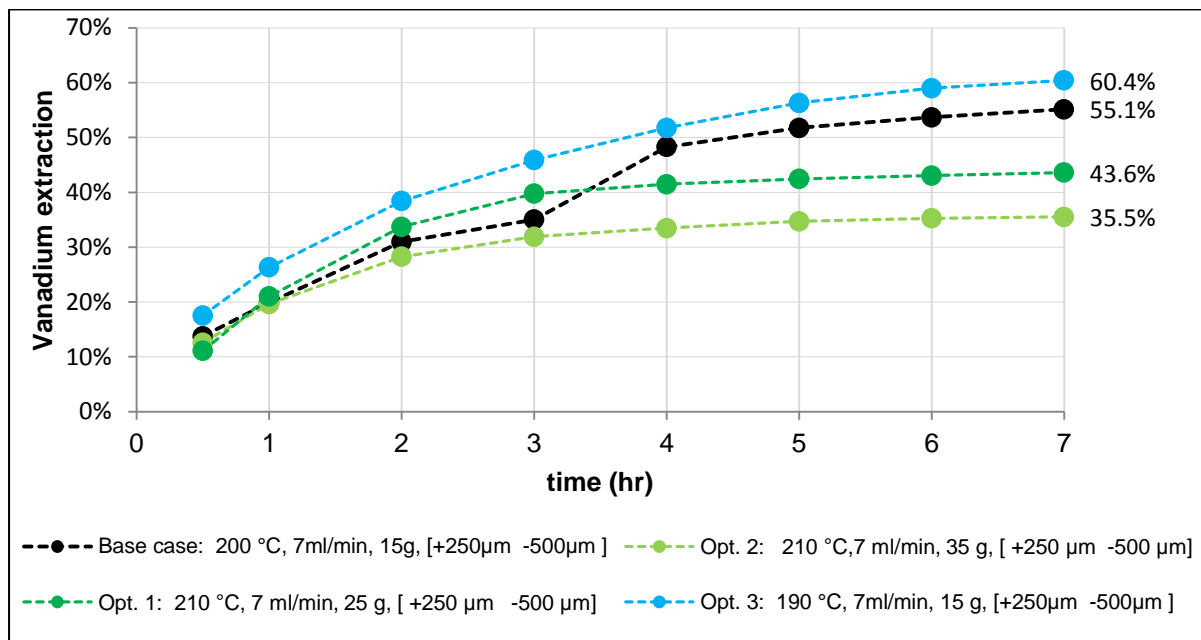


Figure 4-16: Optimization experiments for vanadium extraction from spent vanadium catalyst over the duration of 7 hours.

4.2 TANTALUM EXTRACTION FROM TANTALUM OXIDE -SILICA SAND MIXTURE

4.2.1 Determination of significant parameters

Similarly, a single replicate of the 2^4 factorial design experiments was conducted in a gas phase extraction process, in order to study the joint factor effects of the process variables. The summary of tantalum extraction results for the 16 experiments is presented in Table 4-7. The highest tantalum extraction (56.4%) was attained when low bed weight (15 g) of lean mixture (2 wt% Ta_2O_5) of tantalum oxide and silica sand, was subjected to 5 mL/min of acetylacetone at reaction temperature of 200 °C for 5 hours. The process achieved the lowest extractions (1.0%) when 50 g of synthetic tantalum bearing matrix containing (10 wt% Ta_2O_5) was contacted with 3 mL/min of acetylacetone at a reaction temperature of 150 °C for 5 hours.

Table 4-7: The design matrix and summary results for vanadium extraction experiments, using acetylacetone as extractant.

Runs	Experimental parameters				% Extraction
	Ta (A)	Temp. (B)	Flowrate (C)	Bed Load (D)	(Y)
1	2 wt%	150 °C	3 mL/min	15 g	13.7%
2	10 wt%	150 °C	3 mL/min	15 g	4.3%
3	2 wt%	200 °C	3 mL/min	15 g	22.8%
4	10 wt%	200 °C	3 mL/min	15 g	6.7%
5	2 wt%	150 °C	5 mL/min	15 g	56.4%
6	10 wt%	150 °C	5 mL/min	15 g	6.5%
7	2 wt%	200 °C	5 mL/min	15 g	51.2%
8	10 wt%	200 °C	5 mL/min	15 g	5.3%
9	2 wt%	150 °C	3 mL/min	50 g	5.0%
10	10 wt%	150 °C	3 mL/min	50 g	1.0%
11	2 wt%	200 °C	3 mL/min	50 g	5.0%
12	10 wt%	200 °C	3 mL/min	50 g	2.5%
13	2 wt%	150 °C	5 mL/min	50 g	17.2%
14	10 wt%	150 °C	5 mL/min	50 g	1.3%
15	2 wt%	200 °C	5 mL/min	50 g	12.0%
16	10 wt%	200 °C	5 mL/min	50 g	1.1%

The extraction time curves of the 16 tantalum extraction experiments are presented in Figure 4-17 to Figure 4-20. The figures show how the extraction reaction proceeded with time at different reaction conditions. By examining Figure 4-17 to Figure 4-20 it can be seen that, higher degrees of tantalum extraction were consistently achieved at small bed loads (15 g) of synthetic tantalum bearing mixture containing 2 wt% Ta₂O₅, irrespective of reaction temperature, acetylacetone flowrate. In addition, an increase in acetylacetone flowrate seemed to have a greater influence on the extraction degree of tantalum. Furthermore, the observations are in agreement with the studies conducted by Tshofu (2015) and Van Dyk et al. (2011), which showed that an increase in acetylacetone flowrate and a decrease in concentration of the of metal of interest in the metal oxide mixture led to an increase in extraction degree, in a gas phase extraction process. The dependence of tantalum extraction rate on acetylacetone flowrate suggests that the extraction reactions are diffusion controlled (Habashi, 1970). The statistical method was applied to aid with the determination of the most significant process parameters that influence the extraction of tantalum in the gas phase extraction process.

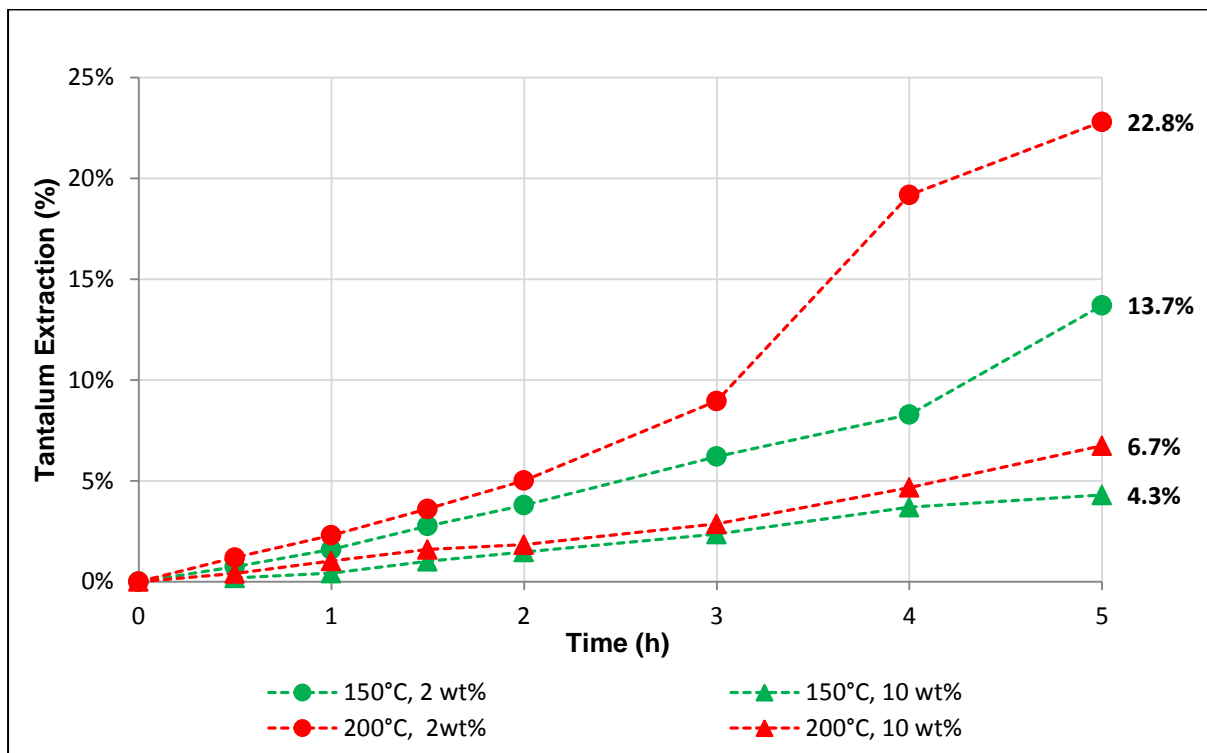


Figure 4-17: Tantalum extraction with time (15 g bed loading and acetylacetone flowrate of 5 mL/min).

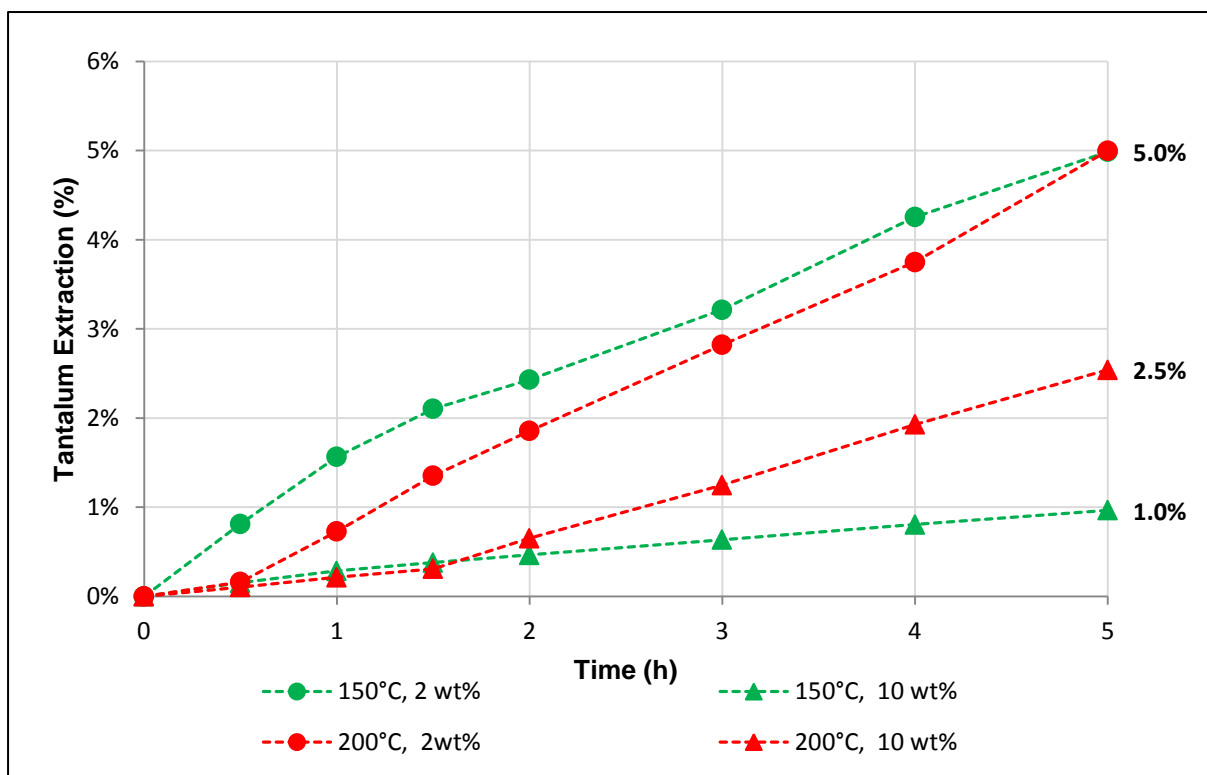


Figure 4-18: Tantalum extraction with time (50 g bed loading and acetylacetone flowrate of 5 mL/min).

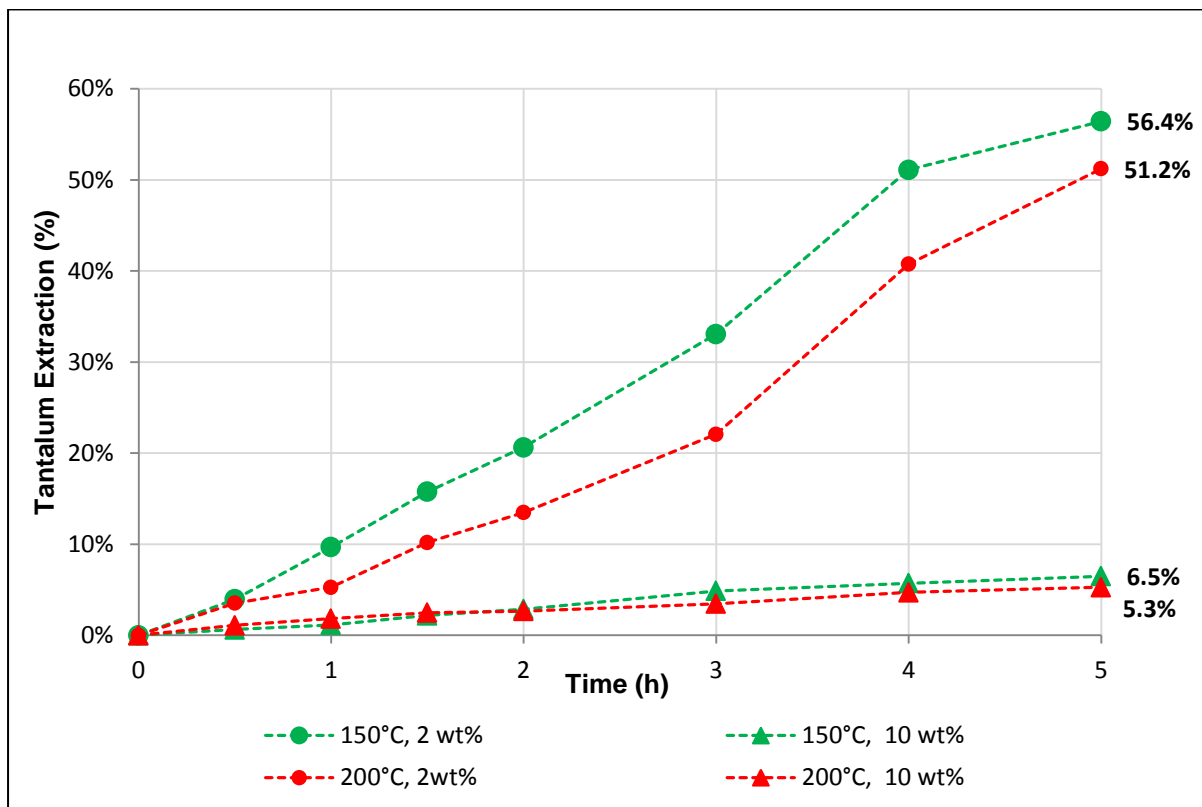


Figure 4-19: Tantalum extraction with time (15 g bed loading and acetylacetone flowrate of 7 mL/min).

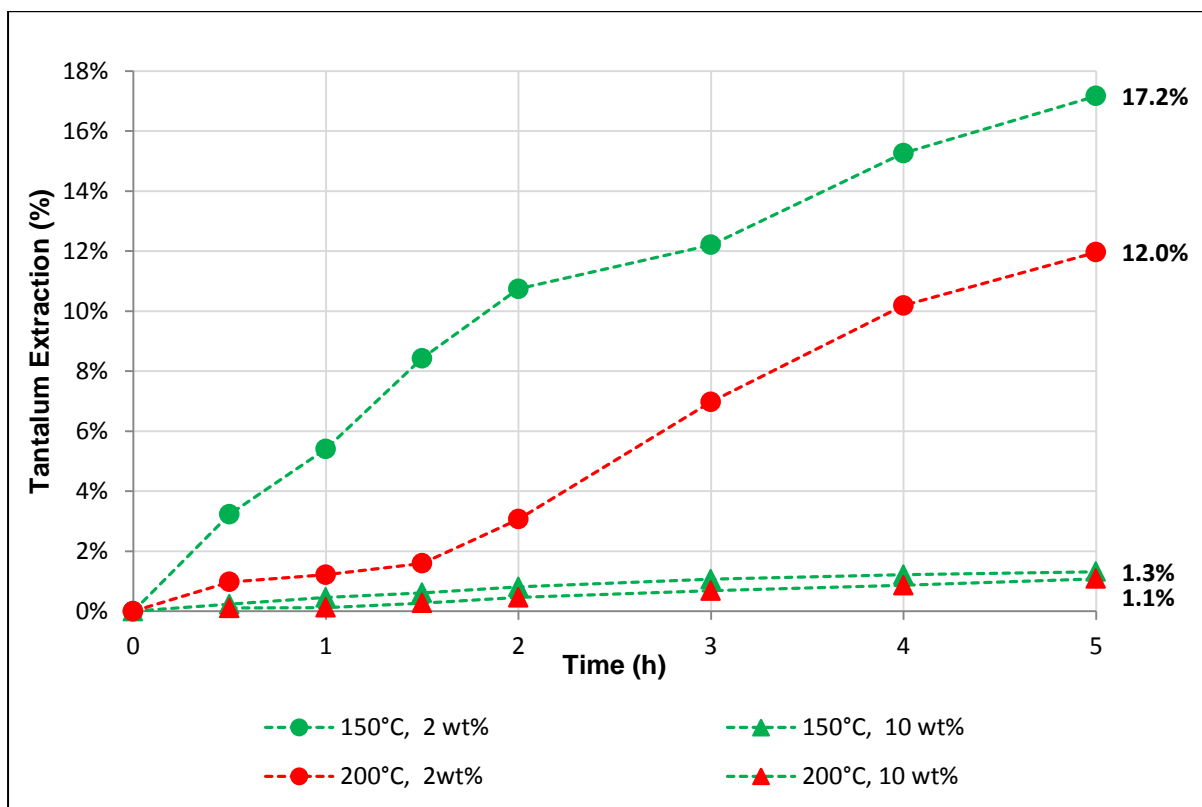


Figure 4-20: Tantalum extraction with time (50 g bed loading and acetylacetone flowrate of 7 mL/min).

The important factors emerging from the normal probability plot presented in Figure 4-21 are identified as being tantalum oxide concentration (*A*), acetylacetone flowrate (*C*), bed loading (*D*), *AC*, *AD* and *ACD* interaction effects.

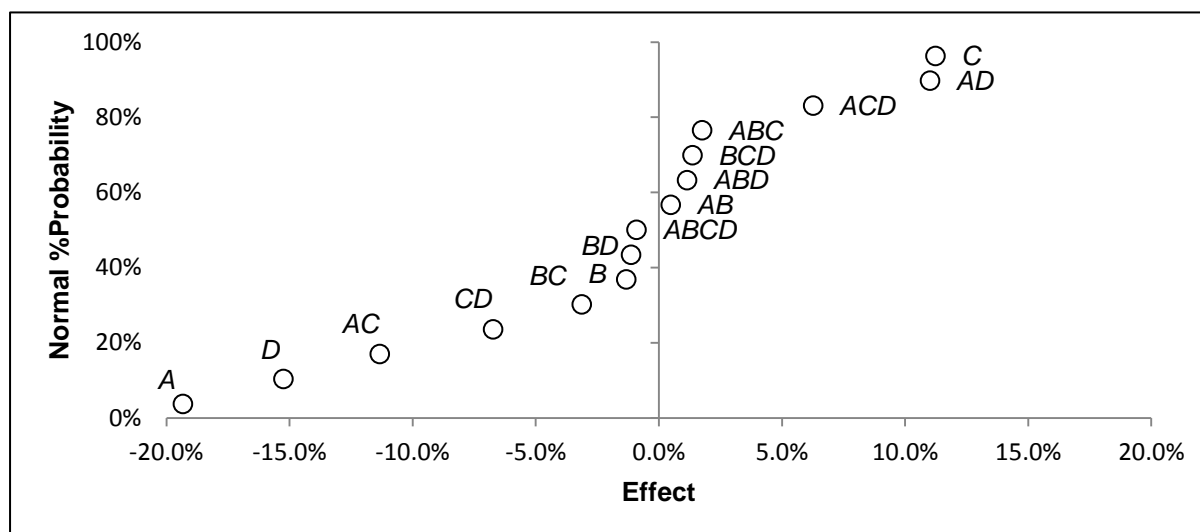


Figure 4-21: Normal probability plot of factor effects on tantalum extraction results.

Furthermore, the attained P-values in Table 4-8 validate the significance of these factors ($P < 0.05$), which have been accepted to have emerged as being important, at 95% confidence level. The factor effect plots for all the factors listed in Table 4-8 are presented in Figure 4-22 to Figure 4-28 to aid with the interpretation of the experimental observations.

Table 4-8: Analysis of variance for tantalum extraction results.

Source of Variation	Sum of Squares	D.O.F	Mean Square	F_0	P-Value
A	14.94%	1	14.94%	162.62	1.35E-06
C	5.05%	1	5.05%	55.02	7.49E-05
D	9.29%	1	9.29%	101.15	8.13E-06
AC	5.14%	1	5.14%	55.95	7.06E-05
AD	4.86%	1	4.86%	52.91	8.61E-05
CD	1.81%	1	1.81%	19.72	2.17E-03
ACD	1.57%	1	1.57%	17.14	3.25E-03
Error	0.735%	8	0.09%		
Total	43.41%	15			

The main factor effect plots (Figure 4-22 to Figure 4-24) indicate that, an increase in the concentration of tantalum oxide (*A*) contained in the synthetic tantalum bearing matrix, led to a 19% average decrease of tantalum extraction, whereas the adjustment to high acetylacetone flowrate and low bed weight of the synthetic low grade ore matrix set about an average increase of tantalum extraction by 10% and 15% respectively. The dependency of the extraction rate on these factors suggests that the reactions are rather diffusion controlled (Habashi, 1970 and Szekely et al., 1976).

However, Figure 4-24 and Figure 4-25 shows that the extraction rate of tantalum is more sensitive to variations in Ta_2O_5 concentration (*A*) at elevated acetylacetone

flowrates (C) and low bed weights (D), where 30% average increase in extraction was attained by decreasing A, as compared to a mere 8% increase, which was achieved though similar adjustments of A at low flowrates and high bed loads. Thus, the reactions carried out at elevated acetylacetone flowrates and low bed loads are governed by diffusion, shedding to light as to why the extraction extent is higher at low reaction temperatures in Figure 4-19 and Figure 4-20 (Szekely (1976)). According to Szekely (1976), mass transfer effects are minimized when the reaction system is operated at lower temperatures for a mixed controlled or diffusion controlled gas-solid reaction. Therefore, as in this case, for lean tantalum source matrix, it is seen that the lowering of temperature improved the extraction rate of tantalum, affirming the minimization of mass transfer effects of tantalum extraction reactions. It could be argued that the reactions are chemical controlled at low acetylacetone flowrates and high bed load, due to minor dependence of extraction rate on reactant concentration (Figure 4-25 and Figure 4-26 and Habashi, 1976), but since the extraction rate is less sensitive to temperature variation, more especially for low grade Ta matrix containing lower concentrations of tantalum oxide (Figure 4-18), it becomes more ambiguous as to which mechanism dominates, yet it could suggest that the extraction rate is mixed controlled. But the kinetic analysis below clarifies this observation.

Additionally, Figure 4-27 and Figure 4-28 further highlights that the interaction effect between tantalum oxide concentration (A) and acetylacetone flowrates (C) is more pronounced at small bed loads and this is because at low bed loads the average change instigated by AC interaction amounts to 17%, as opposed to a minute 3% variation at high bed loads. And so, these observations imply that mass transfer is more dominant at small bed loads as compared to that in high bed loads.

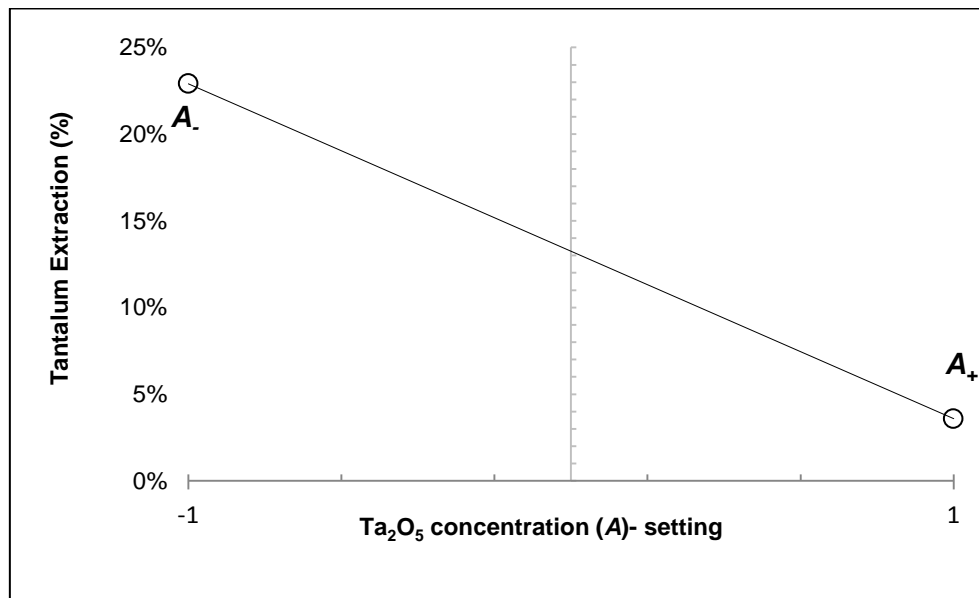


Figure 4-22: Effect of tantalum oxide concentration on the extraction extent.

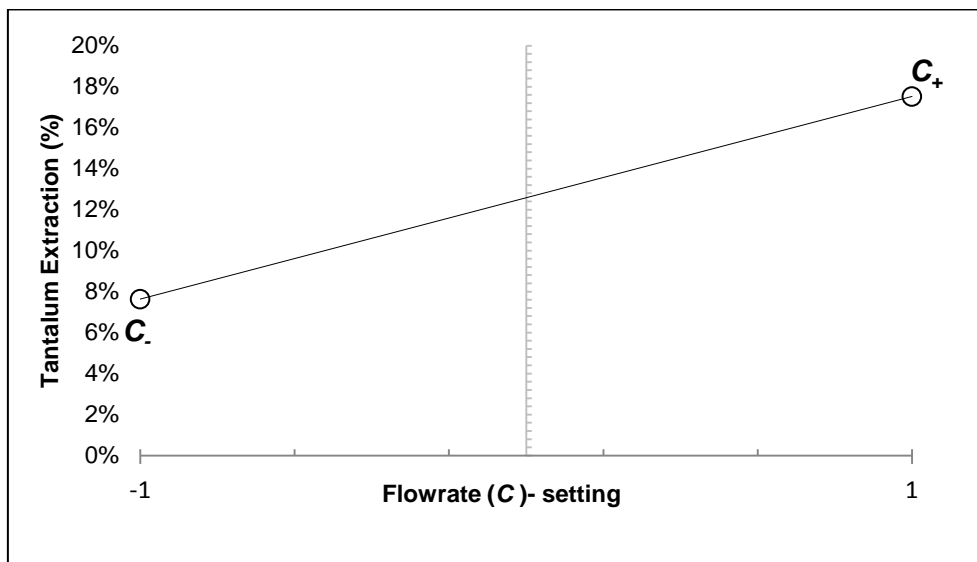


Figure 4-23: Effect of acetylacetone flowrate on the extraction extent of tantalum from tantalum oxide/silica mixture.

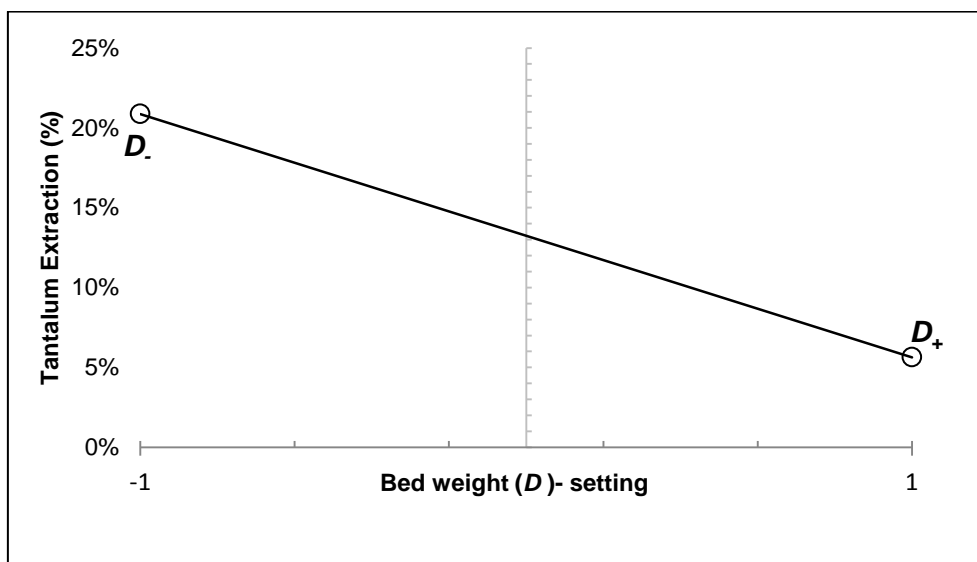


Figure 4-24: Influence of bed load on the extraction extent of tantalum from tantalum oxide/silica mixture.

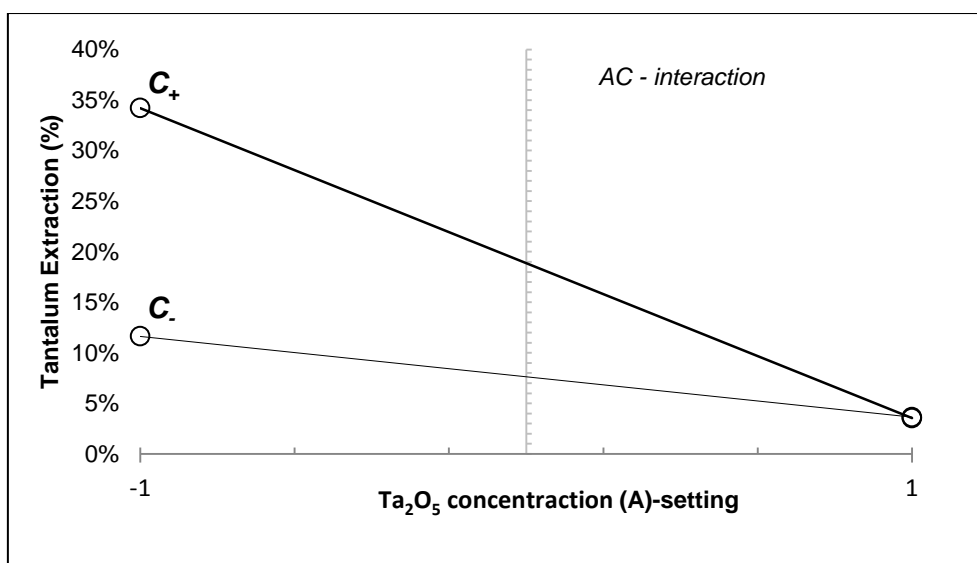


Figure 4-25: Influence of AC interaction effect on the extraction extent of tantalum from tantalum oxide/silica mixture.

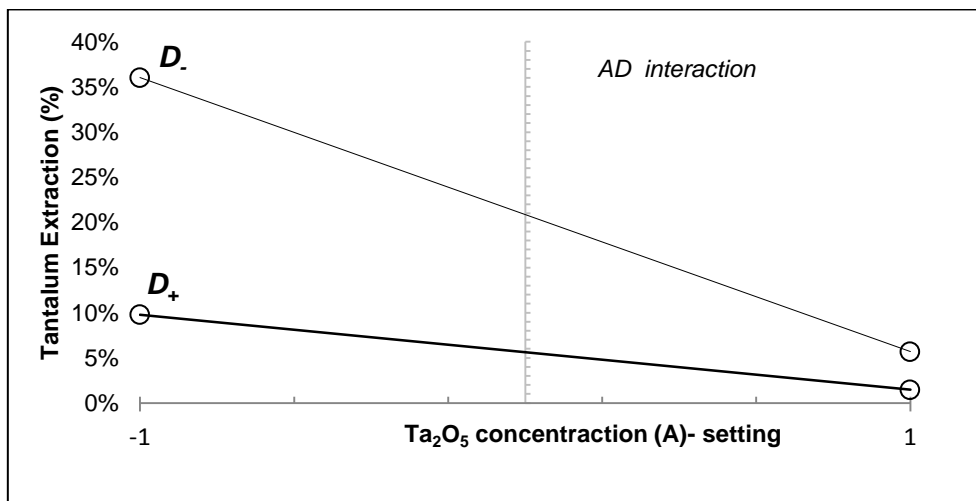


Figure 4-26: Influence of AD interaction effect on the extraction extent of tantalum from tantalum oxide/silica mixture, using acetylacetone as a volatile ligand.

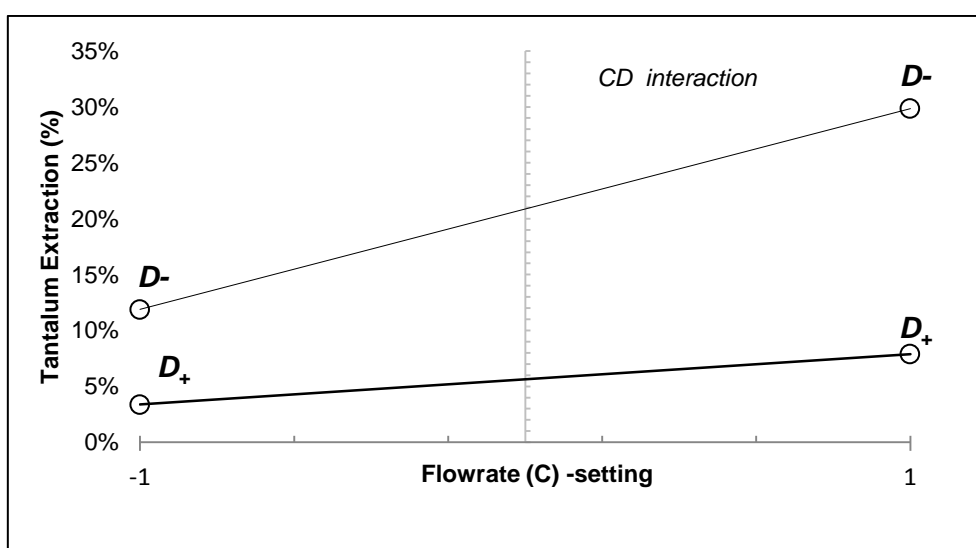


Figure 4-27: Influence of CD interaction effect on the extraction extent of tantalum from tantalum oxide/silica mixture, using acetylacetone as a volatile ligand.

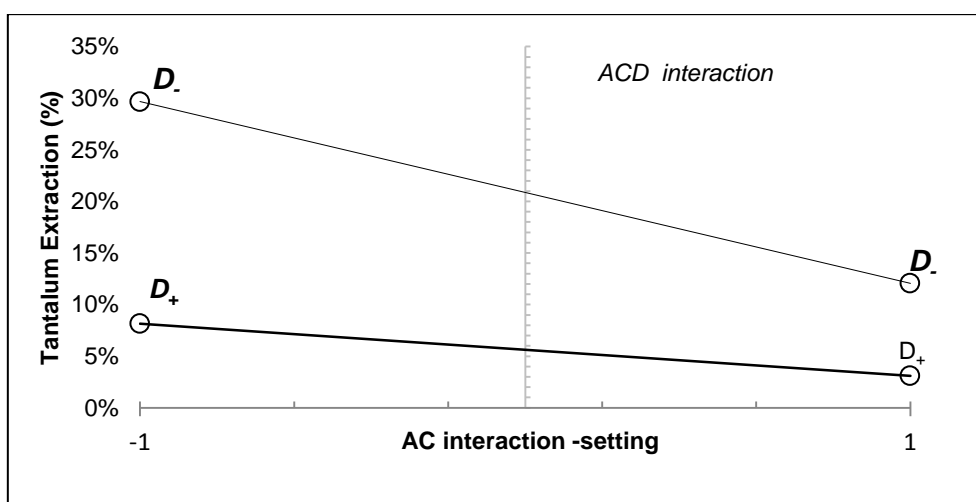


Figure 4-28: Influence of ACD interaction effect on the extraction extent of tantalum from tantalum oxide/silica mixture, using acetylacetone as a volatile ligand.

4.2.2 Kinetic analysis of tantalum extraction experiments

The tantalum extraction experimental results were fitted with the shrinking core unreacted core model described by equation (14) to determine the value σ^2 . The extraction reaction is classified as being mass transfer controlled if $\sigma^2 > 10$, at $0.1 < \sigma^2 < 10$ both chemical and mass transfer reaction mechanisms have comparable resistances, and the reaction can be said to be mixed controlled. For $\sigma^2 > 10$ the reaction can be regarded as being chemical controlled (Szekely et al., 1976).

The kinetic analysis results presented in Table 4-5 suggest that for the most part, the reactions were diffusion controlled ($\sigma^2 > 10$). In addition, at high concentration (10 wt%) of Ta_2O_5 and this suggests that the mass transfer resistance was higher at high concentrations. Consequently, it can be seen from that the lowest values of the kinetic rate constants were attained when the process was operated at low acetylacetone flowrates and high bed loads of the synthetic tantalum oxide mixture, most especially for that which constitutes 10 wt% tantalum oxide. On the contrary, highest kinetic rate constants are observed at elevated flowrates of acetylacetone and small bed loads of synthetic mixture bearing tantalum.

Therefore, the former and latter observations suggest that the adjustments on these parameters, led to a considerable reduction of mass transfer resistance, which could arguably be attributed to dissipation of gas boundary layer. In addition, for the same adjustments mentioned above, particularly bringing attention onto the synthetic mixtures containing 2 wt% tantalum oxide, it is seen that, the reaction regimes changed from diffusion to mixed controlled, marking that the latter conditions are such that mass transport strongly depends on the extent of reaction (Habashi, 1970).

Table 4-9: Summary of the attained shrinking core-reaction modulus and kinetic rate constants for tantalum extraction experiments.

Experiments with Hacac flowrate of 3 mL/min and bed weight of 15 g				
<i>Temperature (°C)</i>	<i>Ta₂O₅ (wt%)</i>	<i>σ_s^2</i>	<i>k</i>	<i>R²</i>
150	2	15.24	2.10E-05	0.797
200	2	8.29	9.17E-04	0.890
150	10	50.93	1.79E-04	0.961
200	10	32.44	2.48E-04	0.886
Experiments with Hacac flowrate of 3 mL/min and bed weight of 50g				
<i>Temperature (°C)</i>	<i>Ta₂O₅ (wt%)</i>	<i>σ_s^2</i>	<i>k</i>	<i>R²</i>
150,	2	45.77	3.05E-06	0.974
200	2	45.16	3.04E-06	0.926
150	10	41.34	1.12E-07	0.976
200	10	87.64	7.95E-07	0.892
Experiments with Hacac flowrate of 5 mL/min and bed weight of 15 g				
<i>Temperature (°C)</i>	<i>Ta₂O₅ (wt%)</i>	<i>σ_s^2</i>	<i>k</i>	<i>R²</i>
150	2	2.52	5.81E-04	0.923
200	2	2.96	4.21E-04	0.855
150	10	33.72	2.72E-04	0.986
200	10	42.97	1.99E-04	0.982
Experiments with Hacac flowrate of 5 mL/min and bed weight of 50 g				
<i>Temperature (°C)</i>	<i>Ta₂O₅ (wt%)</i>	<i>σ_s^2</i>	<i>k</i>	<i>R²</i>
150	2	12.32	3.85E-05	0.991
200	2	17.36	1.98E-05	0.926
150	10	172.03	4.14E-05	0.991
200	10	211.94	4.40E-05	0.979

4.2.3 Additional Experiments

The tantalum extraction additional experiment was conducted having factored the conclusions reached through the statistical analysis and kinetic analysis of the extraction process. Since it was established that for the most part, the reactions were mass transfer controlled within the operation range of the experiments, the flowrate was adjusted from 5 mL/min to 7 mL/min and temperature was kept at 150 °C. Additionally, from the previous set of experiments, the maximum extraction of tantalum was coherently attained at low bed loads (15 g) of synthetic tantalum oxide mixture, for low weight percentage (2 wt% Ta₂O₅). For that reason, 15 g of synthetic mixture containing 2 wt% Ta₂O₅ was used to enhance the extraction degree of tantalum. Therefore, as seen from Figure 4-29 the adjustments based on tantalum

extraction process was successfully enhanced, and achieved the extraction degree of 93.4%.

Since tantalum has been found at very low concentrations in an oxide form in tailings dams in Africa , recovery using conventional mechanical techniques can possibly be uneconomical. (Ukaegbu & Ugodulunwa, 2008). the gas phase extraction process could be the potential recovery process for the extraction of tantalum from tantalum tailings.

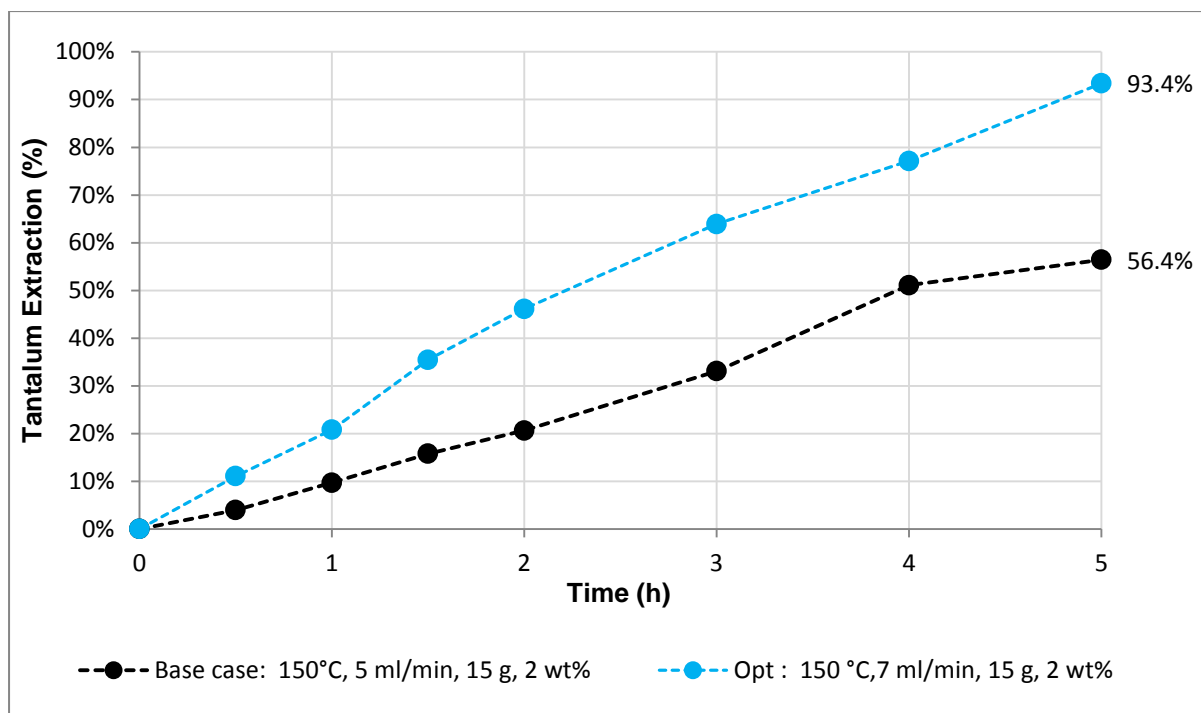


Figure 4-29: Additional experiments for tantalum extraction from synthetic tantalum containing mixture.

5 CONCLUSIONS

The research explored the possibility of using the gas phase extraction process to extract vanadium from spent sulphuric acid catalyst and tantalum from a synthetic tantalum oxide-silica sand mixture. An initial literature review was conducted to identify suitable volatile extractants to be used in the processes. Acetylacetone and its fluorinated derivatives, trifluoro-acetylacetone and hexafluoroacetylacetone were identified as suitable candidates, but due to safety considerations associated with fluoro-compounds it was decided to use acetylacetone only. Previous studies by Potgieter and co-workers (2006) on pure vanadium oxide systems showed that acetylacetone can be readily used as an effective extractant. In addition, some improvements were also made to the experimental setup to facilitate good evaporation of the volatile organic and complete condensation of the reaction products and unreacted reagents. To this effect an acetylacetone pre-heater was designed and fabricated and the condenser, located after the reaction column, was replaced.

In terms of the other objectives, the following main conclusions could be drawn from the experimental studies.

The extractions of vanadium from the spent catalyst with acetylacetone were investigated. The gas phase extraction process was able to achieve a maximum vanadium extraction of 60.3% after contacting 15 g of spent catalyst of particle size fraction range of (+250 μm -500 μm) to 7 mL/min of acetylacetone, at a reaction temperature of 190 °C for 7 hours. It was also found that the reaction temperature, acetylacetone flowrate and the joint interaction effect of particle size, acetylacetone flowrate and catalyst bed load had a significant influence on the vanadium extraction process at 95% confidence level. In addition, the kinetic study showed that the vanadium extraction reactions were mixed controlled or governed by diffusion.

The gas phase extraction process was also applied for the first time on a tantalum oxide-silica sand mixture for the extraction of tantalum. The highest tantalum extraction of 93.4% was attained from 15 g synthetic tantalum oxide mixture (2 wt% Ta_2O_5) at acetylacetone flowrate of 7 mL/min at a reaction temperature of 150 °C after 5 hours. The tantalum extraction gas phase reactions were significantly influenced by the joint interaction effect of tantalum oxide concentration, acetylacetone flowrate and bed weight of the synthetic mixture at 95% confidence level, and the highest extractions were generally achieved at low concentrations of tantalum oxide. These preliminary results imply that it might be possible to use the gas phase extraction process for tantalum extraction from low grade tantalum tailings/ ores. Furthermore, the kinetic study showed that the gas phase extraction reaction of tantalum was governed by diffusion.

6 RECOMMENDATIONS

Based on the attained results the following recommendations are made for future research:

- i. In order to further improve the extraction extent of vanadium from the spent vanadium catalyst, a nitrogen gas stream has to be incorporated in the process with the anticipation of inhibiting the growth of a passivation layer as the reaction proceeds.
- ii. As the research on tantalum extraction was only preliminary and conducted on a synthetic ore, it is proposed to apply the gas phase process on real ore systems such as tantalum tailings and electronic waste using acetylacetone and other suitable extractants.
- iii. With regards to the experimental setup, it is recommended to increase the size of the liquid evaporation surface area to allow for operating the system at much higher ligand flowrates. The experimental setup also needs to be adapted for the use of possible solid extractants as this will allow for the use of other chelating agents usually found in solid form at room temperature.

7 REFERENCES

- Akcil, A. & Gahan, C.S. 2015. Application of Industrial Waste in Biohydrometallurgy: A Review on Its Use as Neutralising Agent and Potential Source for Metal Recovery. In *Microbiology for Minerals, Metals, Materials and the Environment*. CRC Press. 185-208.
- Aliyu, H.N. & Mustapha, A. 2009. Synthesis and characterization of oxovanadium (iv) β -diketonate complexes. *Afr.Sci.* 10:124-126.
- Allimann-Lecourt, C., Bailey, T.H. & Cox, M. 2002. Purification of combustion fly ashes using the SERVO process. *Journal of Chemical Technology and Biotechnology.* 77(3):260-266.
- Allimann-Lecourt, C. 2004. Extraction of metals from contaminated land and industrial solid waste using a novel technology (servo process).
- Bartholomew, C.H. 2001. Mechanisms of catalyst deactivation. *Applied Catalysis A: General.* 212(1–2):17-60. DOI:[http://dx.doi.org/10.1016/S0926-860X\(00\)00843-7](http://dx.doi.org/10.1016/S0926-860X(00)00843-7).
- Belcher, R. 1973. The application of chelate compounds in analytical chemistry. *Pure and Applied Chemistry.* 34(1):13-28.
- Blaustein, B.D., Hauck, J.T., Olson, G.J. & Baltrus, J.P. 1993. Bioleaching of molybdenum from coal liquefaction catalyst residues. *Fuel.* 72(12):1613-1618.
- Brierley, C.L. & Brierley, J.A. 2013. Progress in bioleaching: part B: applications of microbial processes by the minerals industries. *Applied Microbiology and Biotechnology.* 97(17):7543-7552.
- Charry, I.D., González, L.M. & Montes de Correa, C. 2011. Characterization by temperature programmed techniques of spent and acid treated vanadium catalysts. *Revista Facultad De Ingeniería Universidad De Antioquia.* (57):31-37.
- Chen, Y., Mariba, E., Van Dyk, L. & Potgieter, J. 2011. A review of non-conventional metals extracting technologies from ore and waste. *International Journal of Mineral Processing.* 98(1):1-7.
- Chen, Y., Feng, Q., Shao, Y., Zhang, G., Ou, L. & Lu, Y. 2006. Research on the recycling of valuable metals in spent Al₂O₃-based catalyst. *Minerals Engineering.* 19(1):94-97. DOI:<http://dx.doi.org/10.1016/j.mineng.2005.06.008>.
- Cox, M., Gray, M.J. & Duke, P.W. 1985. *Winning Metal from Ore*.
- Cox, M., Nugteren, H. & Janssen-Jurkovičová, M. 2008. *Combustion residues: current, novel and renewable applications*. John Wiley & Sons.

- Crompton, T. 1987. Organometallic Compounds in the Environment. In *Comprehensive Organometallic Analysis*. Springer. 632-785.
- Cunningham, L.D. 2003. *Tantalum recycling in the United States in 1998*. US Department of the Interior, US Geological Survey.
- Davies, H.O., Leedham, T.J., Jones, A.C., O'Brien, P., White, A.J. & Williams, D.J. 1999. Some tantalum (V) β -diketonate and tantalum (V) aminoalcoholate derivatives potentially important in the deposition of tantalum-containing materials. *Polyhedron*. 18(24):3165-3172.
- De Lasa, H., Dogu, G., Dogu, G. & Ravella, A. 1992. *Chemical reactor technology for environmentally safe reactors and products*. Springer Science & Business Media.
- Delmon, B., Grange, P. & Froment, G. 1997. *Hydrotreatment and hydrocracking of oil fractions*. Elsevier.
- Dilli, S. & Patsalides, E. Volatility studies of metal chelates. II. Gas chromatographic properties of vanadium β -diketonates. *Australian Journal of Chemistry*. 29(11):2381-2388.
- Dilli, S. & Patsalides, E. 1976. Volatility studies of metal chelates. I. Thermal studies of vanadium β -diketonates. *Australian Journal of Chemistry*. 29(11):2369-2379.
- Dilli, S. & Patsalides, E. 1981. Volatility studies of metal chelates. V. Stability and volatility of transition metal chelates of tetradentate Schiff bases. *Australian Journal of Chemistry*. 34(8):1579-1591.
- Dufresne, P. 2007. Hydroprocessing catalysts regeneration and recycling. *Applied Catalysis A: General*. 322:67-75.
- El-Fatah, S.A., Goto, M., Kodama, A. & Hirose, T. 2004. Supercritical fluid extraction of hazardous metals from CCA wood. *The Journal of Supercritical Fluids*. 28(1):21-27.
- Espinoza, L.A.T. 2012. Case study: Tantalum in the world economy: History, uses and demand.
- Falak, O.A. Engineering & Technology Journal, 2008. Vanadium Oxide Recovery from Spent Catalysts by Chemical Leaching. 26(2).
- Fornalczyk, A. 2012. Industrial catalysts as a source of valuable metals. *J.Achievements Mater.Manuf.Eng.* 55(2):864.
- Forzatti, P. & Lietti, L. 1999. Catalyst deactivation. *Catalysis Today*. 52(2):165-181.
- Ghosh, A. & Ray, H.S. 1991. *Principles of extractive metallurgy*. New Age International.

- Goonan, T.G. 2011. *Vanadium recycling in the United States in 2004*. US Department of the Interior, US Geological Survey.
- Gupta, C.K. 2006. *Chemical metallurgy: principles and practice*. John Wiley & Sons.
- Habashi, F., (1969). *Principles of Extractive Metallurgy*. Gordon and Breach Science Publishers, Inc. vol. 2. pp. 142-149.
- Ho, E., Kyle, J., Lallenc, S., Muir, D. & Parker, A. 1994. Recovery of vanadium from spent catalysts and alumina residues. In *Hydrometallurgy'94*. Springer. 1105-1121.
- Jadhav, U. & Hocheng, H. 2012. A review of recovery of metals from industrial waste. *Journal of Achievements in Materials and Manufacturing Engineering*. 54(2):159.
- Kaka, A., Mahomedy, N., Wessels, M., van Dyk, L. 2016 Novel methods for the recovery of vanadium from spent catalyst., Hydrometallurgy Conference 2016 Symposium Series S89, SAIMM, pp. 383-392
- Kapoor, P. & Mehrotra, R. 1965. Organic compounds of niobium and tantalum IV. Reactions of niobium and tantalum pentaethoxides with β -diketones. *Journal of the Less Common Metals*. 8(5):339-346.
- Kepert, D. & Trigwell, K. 1976. Complexes of niobium, tantalum and tungsten pentahalides with fluorinated ditertiary arsines. *Australian Journal of Chemistry*. 29(2):433-436.
- Khorfan, S., Wahoud, A. & Reda, Y. 2003. Recovery of vanadium pentoxide from spent catalyst used in the manufacture of sulphuric acid. *Chemical Engineering*. 45(2):131-137.
- Khuhawar, M. & Soomro, A.I. 1993. Gas and liquid chromatographic studies of copper (II), nickel (II), palladium (II) and oxovanadium (IV) chelates of some fluorinated ketoamine Schiff bases. *Journal of Chromatography A*. 639(2):371-374.
- Ksibi, M., Elaloui, E., Houas, A. & Moussa, N. 2003. Diagnosis of deactivation sources for vanadium catalysts used in SO₂ oxidation reaction and optimization of vanadium extraction from deactivated catalysts. *Applied Surface Science*. 220(1):105-112.
- Laintz, K., Wai, C., Yonker, C. & Smith, R. 1992. Extraction of metal ions from liquid and solid materials by supercritical carbon dioxide. *Analytical Chemistry*. 64(22):2875-2878.
- Larsson, A. 2007. Study of Catalyst Deactivation in Three Different Industrial Processes.

- Lazenby, H. 2012. High-tech uses for vanadium to drive demand, prices higher. *Creamer Media's Mining Weekly*. DOI: <http://www.miningweekly.com/article/high-tech-uses-for-vanadium-to-drive-demand-prices-up-2012-08-23>.
- Leib, T.M. & Pereira, C.J. 2008. *Reaction Kinetics*. McGraw-Hill.
- Leofanti, G., Tozzola, G., Padovan, M., Petrini, G., Bordiga, S. & Zecchina, A. 1997. Catalyst characterization: applications. *Catalysis Today*. 34(3):329-352.
- Levenspiel, O. & Levenspiel, C. 1972. *Chemical reaction engineering*. Wiley New York etc.
- Lin, Y., Brauer, R., Laintz, K. & Wai, C. 1993. Supercritical fluid extraction of lanthanides and actinides from solid materials with a fluorinated. beta.-diketone. *Analytical Chemistry*. 65(18):2549-2551.
- Lloyd, L. 2011. *Handbook of industrial catalysts*. Springer Science & Business Media.
- Lopez, L.P.H. 2006. *Organometallic Complexes of Tungsten and Tantalum: Synthesis, Structure and Reactivity*.
- Lozano, L.J. & Juan, D. 2001. Solvent extraction of polyvanadates from sulphate solutions by Primene 81R. Its application to the recovery of vanadium from spent sulphuric acid catalysts leaching solutions. *Solvent Extraction and Ion Exchange*. 19(4):659-676.
- Lucid, M. 1973. *Vanadium Extraction using Mixture of Alkyl Phosphine Oxides and Fluorinated Beta Diketones*.
- Lucid, M.F. 1972. *Mixture of Alcohols and Fluorinated Beta-Diketones Useful as Extractant in Recovery of Vanadium*.
- MacKay, K.D. & Sudderth, R.B. 1977. *Use of Fluorinated β -Diketones in the Solvent Extraction of Zinc*.
- Marafi, M. & Stanislaus, A. 2008. Spent hydroprocessing catalyst management: A review: Part II. Advances in metal recovery and safe disposal methods. *Resources, Conservation and Recycling*. 53(1):1-26.
- Marafi, M. & Stanislaus, A. 2003. Options and processes for spent catalyst handling and utilization. *Journal of Hazardous Materials*. 101(2):123-132. DOI: [http://dx.doi.org/10.1016/S0304-3894\(03\)00145-6](http://dx.doi.org/10.1016/S0304-3894(03)00145-6).
- Marafi, M. & Stanislaus, A. 2008. Spent catalyst waste management: A review: Part I—Developments in hydroprocessing catalyst waste reduction and use. *Resources, Conservation and Recycling*. 52(6):859-873. DOI: <http://dx.doi.org/10.1016/j.resconrec.2008.02.004>.

- Matsuoka, R., Mineta, K. & Okabe, T.H. 2004. Recycling Process for Tantalum and some other metal scraps.
- Mazurek, K. 2013. Recovery of vanadium, potassium and iron from a spent vanadium catalyst by oxalic acid solution leaching, precipitation and ion exchange processes. *Hydrometallurgy*. 134:26-31.
- Mazurek, K., Białowicz, K. & Trypuć, M. 2010. Recovery of vanadium, potassium and iron from a spent catalyst using urea solution. *Hydrometallurgy*. 103(1):19-24.
- Mineta, K. & Okabe, T.H. 2005. Development of a recycling process for tantalum from capacitor scraps. *Journal of Physics and Chemistry of Solids*. 66(2):318-321.
- Mishra, D. & Rhee, Y. 2010. Current research trends of microbiological leaching for metal recovery from industrial wastes. *Curr Res Technol Educ Topics Appl Microbiol Microb Biotechnol*. 2:1289-1292.
- Mohanty, J., Rath, P., Bhattacharya, I. & Paramguru, R. 2011. The recovery of vanadium from spent catalyst: a case study. *Mineral Processing and Extractive Metallurgy*. 120(1):56-60.
- Montgomery, D.C. & Myers, R.H. 1995. Response surface methodology: process and product optimization using designed experiments. *Raymond H. Meyers and Douglas C. Montgomery. A Wiley-Interscience Publications*.
- Moskalyk, R. & Alfantazi, A. 2003. Processing of vanadium: a review. *Minerals Engineering*. 16(9):793-805.
- Mousa, K.M. & Kouba, S.K. Iraqi Journal of Chemical and Petroleum Engineering: 2010 . Study on Vanadium Recovery from Spent Catalyst Used in the Manufacture of Sulfuric Acid. 11(2):49-54.
- Narula, A., Singh, B., Kapoor, P. & Kapoor, R. 1983. Preparation and Characterisation of Tantalum (V) β -Diketonates (Part II). *Synthesis and Reactivity in Inorganic and Metal-Organic Chemistry*. 13(7):887-898.
- Natarajan, K. 2013. Developments in Biotechnology for Environmentally Benign Iron Ore Beneficiation. *Transactions of the Indian Institute of Metals*. 66(5-6):457-465.
- Occelli, M.L. 1996. *Hydrotreating technology for pollution control: catalysts, catalysis, and processes*. CRC Press.
- Ognyanova, A., Ferella, F., De Michelis, I., Taglieri, G. & Vegliò, F. 2009. Using of industrial wastes as secondary resources for metal recovery. *Chemical Engineering Transactions*. 17:1425-1430.

- Ognyanova, A., Ozturk, A., De Michelis, I., Ferella, F., Taglieri, G., Akcil, A. & Vegliò, F. 2009. Metal extraction from spent sulfuric acid catalyst through alkaline and acidic leaching. *Hydrometallurgy*. 100(1):20-28.
- Özel, M.Z., Burford, M.D., Clifford, A.A., Bartle, K.D., Shadrin, A., Smart, N.G. & Tinker, N.D. 1997. Supercritical fluid extraction of cobalt with fluorinated and non-fluorinated β -diketones. *Analytica Chimica Acta*. 346(1):73-80.
- Painuly, A.S. 2015. Separation and recovery of vanadium from spent vanadium pentaoxide catalyst by Cyanex 272. *Environmental Systems Research*. 4(1):1-7.
- Pandey, B. 2015. Microbial Extraction of Uranium from Ores.
- Pandey, B. & Natarajan, K. 2015. *Microbiology for Minerals, Metals, Materials and the Environment*. CRC Press.
- Polinares Consortium, 2012. Fact Sheet: Tantalum. Accessed June 24, 2015, at http://www.polinares.eu/docs/d21/polinares_wp2_annex2_factsheet2_v1_10.pdf
- Potgieter, J., Kabemba, M., Teodorovic, A., Potgieter-Vermaak, S. & Augustyn, W. 2006. An investigation into the feasibility of recovering valuable metals from solid oxide compounds by gas phase extraction in a fluidised bed. *Minerals Engineering*. 19(2):140-146.
- Raja, B. 2007. Vanadium market in the world. *Steelworld*. 13(2):19-22.
- Sahu, K., Agrawal, A. & Mishra, D. 2013. Hazardous waste to materials: Recovery of molybdenum and vanadium from acidic leach liquor of spent hydroprocessing catalyst using alamine 308. *Journal of Environmental Management*. 125:68-73.
- Seetharaman, S. 2005. *Fundamentals of metallurgy*. Elsevier.
- Shao, Y., Feng, Q., Chen, Y., Ou, L., Zhang, G. & Lu, Y. 2009. Studies on recovery of vanadium from desilication residue obtained from processing of a spent catalyst. *Hydrometallurgy*. 96(1):166-170.
- Sharma, B. 2000. *Industrial Chemistry (including Chemical Engineering)*. GOEL Publishing House.
- Shemi, A., Mpana, R., Ndlovu, S., Van Dyk, L., Sibanda, V. & Seepe, L. 2012. Alternative techniques for extracting alumina from coal fly ash. *Minerals Engineering*. 34:30-37.
- Sievers, R.E., Ponder, B., Morris, M.L. & Moshier, R.W. 1963. Gas phase chromatography of metal chelates of acetylacetone, trifluoroacetylacetone, and hexafluoroacetylacetone. *Inorganic Chemistry*. 2(4):693-698.
- Szekely, J. 1976. *Gas-solid reactions*. Elsevier.

- Takeshita, Y., Sato, Y. & Nishi, S. 2000. Study of extraction of metals from CCA-treated wood with supercritical CO₂ containing acetylacetone: extraction of Cu by continuous addition of acetylacetone. *Industrial & Engineering Chemistry Research*. 39(12):4496-4499.
- Trimm, D.L. 2001. The regeneration or disposal of deactivated heterogeneous catalysts. *Applied Catalysis A: General*. 212(1–2):153-160.
DOI:[http://dx.doi.org/10.1016/S0926-860X\(00\)00852-8](http://dx.doi.org/10.1016/S0926-860X(00)00852-8).
- Tshofu, G.S. 2015. *Green Extraction Technology for the Extraction of Iron from Iron Ore Fines*.
- Van der Put, Paul J 1998. *The inorganic chemistry of materials: how to make things out of elements*. Springer Science & Business Media.
- Van Dyk, L., Mariba, E., Chen, Y. & Potgieter, J.H. 2010. Gas phase extraction of iron from its oxide in a fluidized bed reactor. *Minerals Engineering*. 23(1):58-60.
- van Dyk, L., Mariba, E., Chen, Y., Johnson, A. & Potgieter, J. 2012. Gas-phase extraction of lead and iron from their oxides in a fluidized-bed reactor. *Journal of the Southern African Institute of Mining and Metallurgy*. 112(6):461-465.
- Wahoud, A., Alouche, A. & Abdalbake, M. 2011. Sulfuric acid baking and leaching of spent sulfuric acid catalyst. *Chemical Engineering*. 55(1):31-34.
- Willner, J., Kadukova, J., Fornalczyk, A. & Saturnus, M. 2015. Biohydrometallurgical methods for metals recovery from waste materials. *Metallurgija*. 54(1):255-258.
- Winkler, C.D. 2009. MECS catalyst products and technical services update. *Proceedings of the Sulphur and Sulphuric Acid Conference, Sun City, Republic of South Africa*. 117.
- Yahaya, A.S., Yee, C.S., RamLi, N.A. & Ahmad, F. 2012. Determination of the best probability plotting position for predicting parameters of the Weibull distribution. *International Journal of Applied Science and Technology*.
- Zeng, L. & Cheng, C.Y. 2009. A literature review of the recovery of molybdenum and vanadium from spent hydrodesulphurisation catalysts: Part I: Metallurgical processes. *Hydrometallurgy*. 98(1):1-9.
- Zeng, L. & Cheng, C.Y. 2009. A literature review of the recovery of molybdenum and vanadium from spent hydrodesulphurisation catalysts: Part II: Separation and purification. *Hydrometallurgy*. 98(1):10-20.

- Zeng, L. & Cheng, C.Y. 2010. Recovery of molybdenum and vanadium from synthetic sulphuric acid leach solutions of spent hydrodesulphurisation catalysts using solvent extraction. *Hydrometallurgy*. 101(3):141-147.
- Zhu, Z. & Cheng, C.Y. 2011. Solvent extraction technology for the separation and purification of niobium and tantalum: A review. *Hydrometallurgy*. 107(1):1-12.

APPENDIX A: EXPERIMENTAL DATA OF EXTRACTION EXPERIMENTS

Calculations of percentage metal extraction

The method used to attain the percentage extraction extent is as follows:

The concentration of vanadium in the collected sample was determined from the AAS analysis results, and as highlighted in previous sections, the vanadium content in the spent catalyst was determined to be 49.03 mg/g with the aid of ICP-OES analysis.

- To calculate the percentage extraction of vanadium from the catalyst, the following equation was applied:

$$\%Extraction = \frac{\text{amount of vanadium in collected sample}}{\text{amount of vanadium contained in spent catalyst}}$$

$$\%Extraction = \frac{\text{concentration of V in sample} \times \text{volume of collected product}}{\text{mass of catalyst} \times \text{fraction of vanadium in catalyst}}$$

$$\%Extraction = \frac{(c_{\text{vanadium}})_{\text{from AAS reading}} \times V_p \times 0.001}{m_{\text{cat}} \times 49.03} = \frac{m_{\text{vanadium}}}{m_{\text{cat}} \times 49.03}$$

- The cumulative extraction of vanadium was calculated as follows:

$$\%E(t_i) = \%E(t_{i-1}) + \left(\frac{m_{\text{vanadium}}}{m_{\text{cat}} \times 49.03} \right)_{t_i}$$

For tantalum Extraction

$$\%Extraction = \frac{(c_{\text{tantalum}})_{\text{from AAS reading}} \times V_p \times 0.001}{m_{\text{tantalum in tantalum oxide-silica sand mixture}}}$$

$$\%E(t_i) = \%E(t_{i-1}) + \left(\frac{m_{\text{tantalum}}}{m_{\text{antalum in tantalum oxide-silica sand mixture}}} \right)_{t_i}$$

Initial Vanadium Extraction Experiments

Experimental Design

This section serves to present raw data of all vanadium extraction experiments, wherein acetylacetone was applied as a leaching agent. And so, as seen below, Table A-1 and TableA-2 presents the legend table of parameters that were varied during the course of the experiments (Table A-1), followed by the experimental design matrix for the experiments (TableA-2). The randomization of experimental runs can be seen clearly in the far right column of TableA-2. Furthermore, the results raw data is presented in Table A-3 through to Table A-10.

Table A-1: Legend for variable experimental parameters at 2-level conditions.

Factor	Name	Low (-)	High (+)
A	Temperature	150 °C	200°C
B	Particle size	[+500µm -1 mm]	[+2 mm -4 mm]
C	Ligand flowrate (mL/min)	1 mL/min	5 mL/min
D	Bed loading (g)	5	15

TableA-2: Experimental design matrix for vanadium extraction experiments.

Runs	Experimental Factors				Exp. No
	Temp. (A)	Particle size (B)	Flowrate (C)	Bed Load (D)	
1	-	-	-	-	9
2	+	-	-	-	13
3	-	+	-	-	14
4	+	+	-	-	10
5	-	-	+	-	5
6	+	-	+	-	6
7	-	+	+	-	1
8	+	+	+	-	2
9	-	-	-	+	16
10	+	-	-	+	11
11	-	+	-	+	15
12	+	+	-	+	12
13	-	-	+	+	8
14	+	-	+	+	7
15	-	+	+	+	4
16	+	+	+	+	3

Experimental Raw Data of Experimental Results

Table A-3: Raw data for vanadium extraction experiments: Experimental design experiment 1-4.

Experiment	150 °C, 5mL/min, 5 g, +2mm -4mm [1]				200 °C, 5mL/min, 5 g, +2mm -4mm [2]			
t _{cumulative} (h)	V _p (mL)	c _{vanadium} (mg/L)	m _{vanadium} (mg)	%Extraction	V _p (mL)	c _{vanadium} (mg/L)	m _{vanadium} (mg)	%Extraction
0.5	120	172.45	20.69	8.4%	104	233.95	24.33	9.9%
1	110	86.33	9.50	12.3%	100	81.05	8.11	13.2%
2	230	55.25	12.71	17.5%	206	99.40	20.48	21.6%
3	212	55.28	11.72	22.3%	184	87.05	16.02	28.1%
4	234	48.48	11.34	26.9%	212	74.30	15.75	34.5%
5	204	47.26	9.64	30.8%	184	65.20	12.00	39.4%
6	238	26.58	6.33	33.4%	216	60.45	13.06	44.8%
7	212	21.91	4.64	35.3%	206	35.53	7.32	47.7%
Experiment	150 °C, 5mL/min, 15 g, +2mm -4mm [3]				200 °C, 5mL/min, 15 g, +2mm -4mm [4]			
t _{cumulative} (h)	V _p (mL)	c _{vanadium} (mg/L)	m _{vanadium} (mg)	%Extraction	V _p (mL)	c _{vanadium} (mg/L)	m _{vanadium} (mg)	%Extraction
0.5	104	552.40	57.45	7.8%	106	361.16	38.28	5.2%
1	84	329.16	27.65	11.6%	124	181.55	22.51	8.3%
2	210	243.09	51.05	18.5%	218	183.16	39.93	13.7%
3	228	220.05	50.17	25.3%	188	155.81	29.29	17.7%
4	232	185.28	42.98	31.2%	158	108.50	17.14	20.0%
5	210	156.87	32.94	35.7%	172	47.65	8.20	21.1%
6	230	92.88	21.36	38.6%	174	32.05	5.58	21.9%
7	214	82.67	17.69	41.0%	204	32.15	6.56	22.8%

Table A-4: Raw data for vanadium extraction experiments: Experimental design experiment 5-8.

Experiment	150 °C, 5mL/min, 5 g, +500µm -1mm [5]				200 °C, 5mL/min, 5 g, +500µm -1mm [6]			
t _{cumulative} (h)	V _p (mL)	c _{vanadium} (mg/L)	m _{vanadium} (mg)	%Extraction	V _p (mL)	c _{vanadium} (mg/L)	m _{vanadium} (mg)	%Extraction
0.5	84	242.50	20.37	8.3%	122	266.00	32.45	13.2%
1	104	71.04	7.39	11.3%	86	107.21	9.22	17.0%
2	224	72.86	16.32	18.0%	218	95.00	20.71	25.4%
3	244	40.28	9.83	22.0%	196	75.31	14.76	31.5%
4	238	32.96	7.84	25.2%	228	55.65	12.69	36.6%
5	222	17.54	3.89	26.8%	224	42.35	9.49	40.5%
6	222	13.30	2.95	28.0%	232	31.34	7.27	43.5%
7	214	12.47	2.67	29.1%	228	33.62	7.67	46.6%
Experiment	150 °C, 5mL/min, 15 g, +500µm -1mm [7]				200 °C, 5mL/min, 15 g, +500µm -1mm [8]			
t _{cumulative} (h)	V _p (mL)	c _{vanadium} (mg/L)	m _{vanadium} (mg)	%Extraction	V _p (mL)	c _{vanadium} (mg/L)	m _{vanadium} (mg)	%Extraction
0.5	110	522.96	57.53	7.8%	138	548.25	75.66	10.3%
1	104	321.12	33.40	12.4%	108	328.42	35.47	15.1%
2	232	333.25	77.31	22.9%	222	379.67	84.29	26.6%
3	232	225.17	52.24	30.0%	226	351.49	79.44	37.4%
4	236	197.68	46.65	36.3%	238	181.45	43.19	43.2%
5	228	150.46	34.30	41.0%	218	84.64	18.45	45.8%
6	244	132.00	32.21	45.4%	228	73.50	16.76	48.0%
7	214	95.32	20.40	48.1%	226	59.68	13.49	49.9%

Table A-5: Raw data for vanadium extraction experiments: Experimental design experiment 9-12.

Experiment	150 °C, 1mL/min, 15 g, +500µm -1mm [9]				200 °C, 1mL/min, 15 g, +2mm -4mm [10]			
t _{cumulative} (h)	V _p (mL)	c _{vanadium} (mg/L)	m _{vanadium} (mg)	%Extraction	V _p (mL)	c _{vanadium} (mg/L)	m _{vanadium} (mg)	%Extraction
0.5	36	27.03	0.97	0.4%	24	309.31	7.42	3.0%
1	11	22.84	0.25	0.5%	19	236.74	4.50	4.9%
2	48	116.48	5.59	2.8%	45	208.45	9.38	8.7%
3	48	96.01	4.61	4.7%	45	148.06	6.66	11.4%
4	44	82.83	3.64	6.1%	46	94.44	4.34	13.2%
5	46	83.62	3.85	7.7%	43	74.96	3.22	14.5%
6	48	85.01	4.08	9.4%	49	55.66	2.73	15.6%
7	43	77.44	3.33	10.7%	43	34.01	1.46	16.2%
Experiment	200 °C, 1mL/min, 15 g, +500µm -1mm [11]				200 °C, 1mL/min, 15 g, +2mm -4mm [12]			
t _{cumulative} (h)	V _p (mL)	c _{vanadium} (mg/L)	m _{vanadium} (mg)	%Extraction	V _p (mL)	c _{vanadium} (mg/L)	m _{vanadium} (mg)	%Extraction
0.5	23	362.50	8.34	1.1%	25	390.24	9.76	1.3%
1	20	510.10	10.20	2.5%	22	331.52	7.29	2.3%
2	41	376.50	15.44	4.6%	47	272.56	12.81	4.1%
3	41	285.31	11.70	6.2%	48	81.18	3.90	4.6%
4	40	254.88	10.20	7.6%	45	39.76	1.79	4.8%
5	46	171.87	7.91	8.7%	42	234.64	9.85	6.2%
6	40	141.32	5.65	9.4%	46	409.82	18.85	8.7%
7	40	126.93	5.08	10.1%	47	397.92	18.70	11.3%

Table A-6: Raw data for vanadium extraction experiments: Experimental design experiment 13-16.

Experiment	200 °C, 1mL/min, 5 g, +500µm -1mm [13]				150 °C, 1mL/min, 5 g, +2mm -4mm [14]			
t _{cumulative} (h)	V _p (mL)	C _{vanadium} (mg/L)	m _{vanadium} (mg)	%recovery	V _p (mL)	C _{vanadium} (mg/L)	m _{vanadium} (mg)	%recovery
0.5	22	502.68	11.06	4.5%	30	348.38	10.45	4.3%
1	19	410.52	7.80	5.6%	19	150.41	2.86	4.7%
2	42	345.38	14.51	7.5%	36	89.00	3.20	5.1%
3	41	251.22	10.30	8.9%	39	81.63	3.18	5.5%
4	62	169.97	10.54	10.4%	43	71.47	3.07	5.9%
5	45	110.56	4.98	11.1%	32	53.60	1.72	6.2%
6	43	84.86	3.65	11.6%	43	57.99	2.49	6.5%
7	40	66.72	2.67	11.9%	48	61.31	2.94	6.9%
Experiment	150 °C, 1mL/min,15 g, +2m -4mm [15]				150 °C, 1mL/min, 15 g, +500µm -1mm [16]			
t _{cumulative} (h)	V _p (mL)	C _{vanadium} (mg/L)	m _{vanadium} (mg)	%recovery	V _p (mL)	C _{vanadium} (mg/L)	m _{vanadium} (mg)	%recovery
0.5	15	102.17	1.53	0.2%	22	258.86	5.69	0.8%
1	19	97.73	1.86	0.5%	22	87.33	1.92	1.0%
2	36	150.92	5.43	1.2%	35	86.04	3.01	1.4%
3	41	130.04	5.33	1.9%	45	267.98	12.06	3.1%
4	42	132.30	5.56	2.7%	54	372.72	20.13	5.8%
5	46	139.30	6.41	3.6%	52	181.14	9.42	7.1%
6	55	152.12	8.37	4.7%	49	155.96	7.64	8.1%
7	35	153.53	5.37	5.4%	48	79.71	3.83	8.7%

Additional Vanadium Extraction Experiments

Experimental Design

Table A-7: Legend for variable experimental parameters at 2-level conditions: additional vanadium experiments.

Factor	Name	Low (-)	High (+)
A	Temperature	200 °C	200 °C
B	Particle size	[+250µm -500µm]	[+500µm -1 mm]
C	Ligand flowrate (mL/min)	5 mL/min	7 mL/min
D	Bed loading (g)	15	50

TableA-8: Experimental design matrix for additional vanadium extraction experiments.

Runs	Experimental Factors			Experiment #
	Particle size (B)	Flowrate (C)	Bed Load (D)	
1	-	-	-	2
2	+	-	-	8
3	-	+	-	4
4	+	+	-	6
5	-	-	+	1
6	+	-	+	5
7	-	+	+	3
8	+	+	+	7

Experimental raw data of vanadium extraction experiments

Table A-9: Raw data for vanadium extraction experiments: Experimental design experiment 1-4.

Experiment	200 °C, 5mL/min, 50 g, +250µm -500µm [1]				200 °C, 5mL/min, 15g, +250µm -500µm [2]			
t _{cumulative} (h)	V _p (mL)	c _{vanadium} (mg/L)	m _{vanadium} (mg)	%recovery	V _p (mL)	c _{vanadium} (mg/L)	m _{vanadium} (mg)	%recovery
0.5	100	1377.76	137.78	5.6%	150	475.53	71.33	9.7%
1	104	792.36	82.41	9.0%	118	53.88	6.36	10.6%
2	240	711.79	170.83	16.0%	208	216.21	44.97	16.7%
3	240	685.35	164.49	22.7%	252	204.19	51.46	23.7%
4	226	563.72	127.40	27.9%	222	255.44	56.71	31.4%
5	236	202.93	47.89	29.8%	218	138.47	30.19	35.5%
6	222	280.67	62.31	32.4%	206	109.36	22.53	38.6%
7	194	203.95	39.57	34.0%	204	109.32	22.30	41.6%
Experiment	200 °C, 7mL/min, 50 g, +250µm -500µm [3]				200 °C, 7mL/min, 15 g, +250µm -500µm [4]			
t _{cumulative} (h)	V _p (mL)	c _{vanadium} (mg/L)	m _{vanadium} (mg)	%recovery	V _p (mL)	c _{vanadium} (mg/L)	m _{vanadium} (mg)	%recovery
0.5	178	799.66	142.34	5.8%	130	778.26	101.17	13.8%
1	154	541.73	83.43	9.2%	142	316.68	44.97	19.9%
2	334	423.79	141.55	15.0%	254	321.31	81.61	31.0%
3	328	341.67	112.07	19.6%	120	248.26	29.79	35.0%
4	308	311.33	95.89	23.5%	376	259.57	97.60	48.3%
5	322	297.70	95.86	27.4%	204	125.16	25.53	51.8%
6	326	313.94	102.34	31.6%	276	50.79	14.02	53.7%
7	112	334.75	37.49	33.1%	300	36.03	10.81	55.1%

Table A-10: Raw data for vanadium extraction experiments: Experimental design experiment 5-8.

Experiment	200 °C, 5mL/min, 50 g, +500µm -1mm [5]				200 °C, 7mL/min, 15 g, +500µm -1mm [6]			
t _{cumulative} (h)	V _p (mL)	c _{vanadium} (mg/L)	m _{vanadium} (mg)	%recovery	V _p (mL)	c _{vanadium} (mg/L)	m _{vanadium} (mg)	%recovery
0.5	114	1149.14	131.00	5.3%	150	640.03	96.01	13.1%
1	130	644.82	83.83	8.8%	172	288.43	49.61	19.8%
2	230	435.92	100.26	12.9%	190	253.45	48.16	26.3%
3	222	422.48	93.79	16.7%	350	159.14	55.70	33.9%
4	230	464.03	106.73	21.0%	372	95.74	35.62	38.8%
5	230	416.38	95.77	24.9%	318	63.43	20.17	41.5%
6	226	323.93	73.21	27.9%	340	35.66	12.12	43.2%
7	240	312.49	75.00	31.0%	316	27.55	8.71	44.3%
Experiment	200 °C, 7mL/min, 50 g, +500µm -1mm [7]				200 °C, 5mL/min, 15 g, +500µm -1mm [8]			
t _{cumulative} (h)	V _p (mL)	c _{vanadium} (mg/L)	m _{vanadium} (mg)	%recovery	V _p (mL)	c _{vanadium} (mg/L)	m _{vanadium} (mg)	%recovery
0.5	152	1079.14	164.03	6.7%	138	548.25	75.66	10.3%
1	176	622.41	109.54	11.2%	108	328.42	35.47	15.1%
2	342	363.92	124.46	16.2%	222	379.67	84.29	26.6%
3	334	550.37	183.82	23.7%	226	351.49	79.44	37.4%
4	308	382.88	117.93	28.5%	238	181.45	43.19	43.2%
5	324	236.70	76.69	31.7%	218	84.64	18.45	45.8%
6	330	157.89	52.10	33.8%	228	73.50	16.76	48.0%
7	294	122.42	35.99	35.3%	226	59.68	13.49	49.9%

Table A-11: Vanadium extraction optimisation experiments.

Experiment	Base case: 200 °C, 7mL/min, 15g, +250µm -500 µm				Opt 2: 210 °C, 7mL/min, 35g, +250µm -500 µm			
t _{cumulative} (h)	V _p (ml)	%Extraction	m _{vanadium} (mg)	%recovery	V _p (ml)	c _{vanadium} (mg/L)	m _{vanadium} (mg)	%Extraction
0.5	130	778	101.17	13.8%	212	1017	215.57	12.6%
1	142	317	44.97	19.9%	160	759	121.43	19.6%
1.5	254	321	81.61	31.0%	302	490	147.87	28.3%
2	120	248	29.79	35.0%	294	214	62.82	31.9%
2.5	376	260	97.60	48.3%	234	114	26.62	33.5%
3	204	125	25.53	51.8%	212	99	21.00	34.7%
4	276	51	14.02	53.7%	170	57	9.72	35.3%
5	300	36	10.81	55.1%	58	80	4.64	35.5%
Experiment	Opt 1: 210 °C, 7mL/min, 25g, +250µm -500 µm				Opt 3: 190 °C, 7mL/min, 15g, +250µm -500 µm			
t _{cumulative} (h)	V _p (ml)	c _{vanadium} (mg/L)	m _{vanadium} (mg)	%Extraction	V _p (ml)	c _{vanadium} (mg/L)	%Extraction	
0.5	162	838	135.73	11.1%	182	709	129.01	17.5%
1	170	717	121.89	21.0%	180	359	64.58	26.3%
1.5	338	461	155.70	33.7%	352	253	88.93	38.4%
2	336	220	73.99	39.8%	346	159	54.89	45.9%
2.5	284	74	21.07	41.5%	324	133	43.17	51.7%
3	352	34	11.86	42.4%	338	99	33.56	56.3%
4	244	31	7.51	43.1%	200	98	19.64	59.0%
5	304	23	6.95	43.6%	154	69	10.56	60.4%

Table A-12: Additional vanadium extraction experiment.

Experiment	Base case: 150 °C, 5 mL/min, 15g, 2 wt%				Opt: 150 °C, 7 mL/min, 15g, 2 wt%			
t _{cumulative} (h)	V _p (ml)	c _{vanadium} (mg/L)	m _{vanadium} (mg)	%Extraction	V _p (ml)	c _{vanadium} (mg/L)	m _{vanadium} (mg)	%Extraction
0.5	130	91	11.83	3.9%	192	173	33.22	11.1%
1	122	141	17.20	9.7%	146	200	29.20	20.8%
1.5	96	190	18.24	15.8%	220	200	44.00	35.5%
2	128	114	14.59	20.6%	140	228	31.92	46.1%
3	210	178	37.38	33.1%	246	217	53.38	63.9%
4	208	260	54.08	51.1%	190	209	39.71	77.1%
5	216	74	15.98	56.4%	230	212	48.76	93.4%

Tantalum Extraction Experiments with Acetylacetone

Experimental Design

Likewise, this section presents the experimental raw data of tantalum extraction experiments in which acetylacetone was used as a leaching agent. Table A-13 and Table A-14 show the legend of the experimental variables at 2-level settings and the experimental design matrix for the experiments respectively. In addition, the raw data of each experimental run is presented in Table A-15 through to Table A-18.

Table A-13: Legend for variable experimental parameters at 2-level conditions.

Factor	Name	Low (-)	High (+)
A	Tantalum wt%	2%	10%
B	Temperature	150 °C	200 °C
C	Ligand flowrate (mL/min)	3 mL/min	5 mL/min
D	Bed loading (g)	15	50

Table A-14: Experimental design matrix for tantalum extraction experiments.

Runs	Experimental parameters				Experiment #
	Tantalum wt% (A)	Temp. (B)	Flowrate (C)	Bed Load (D)	
1	-	-	-	-	1
2	+	-	-	-	7
3	-	+	-	-	4
4	+	+	-	-	6
5	-	-	+	-	12
6	+	-	+	-	9
7	-	+	+	-	10
8	+	+	+	-	14
9	-	-	-	+	2
10	+	-	-	+	3
11	-	+	-	+	8
12	+	+	-	+	5
13	-	-	+	+	13
14	+	-	+	+	15
15	-	+	+	+	11
16	+	+	+	+	16

Experimental raw data of tantalum extraction experiments

Table A-15: Raw data for tantalum extraction experiments: Experimental design experiment 1-4.

Experiment	150 °C, 3 mL/min, 15g, 2 wt% [1]				150 °C, 3 mL/min, 50g, 2 wt% [2]			
t _{cumulative} (h)	V _p (mL)	c _{tantalum} (mg/L)	m _{tantalum} (mg)	%Extraction	V _p (mL)	c _{tantalum} (mg/L)	m _{tantalum} (mg)	%Extraction
0.5	90	25.00	2.25	0.75%	108	113.00	12.20	0.81%
1	94	27.00	2.54	1.60%	98	115.00	11.27	1.56%
1.5	92	38.00	3.50	2.76%	80	101.00	8.08	2.10%
2	86	36.00	3.10	3.79%	102	48.00	4.90	2.43%
3	186	39.00	7.25	6.21%	190	62.00	11.78	3.22%
4	160	39.00	6.24	8.29%	188	83.00	15.60	4.26%
5	198	82.00	16.24	13.70%	180	61.00	10.98	4.99%
Experiment	150 °C, 3 mL/min, 15g, 10 wt% [3]				200 °C, 3 mL/min, 15g, 2 wt% [4]			
t _{cumulative} (h)	V _p (mL)	c _{tantalum} (mg/L)	m _{tantalum} (mg)	%Extraction	V _p (mL)	c _{tantalum} (mg/L)	m _{tantalum} (mg)	%Extraction
0.5	134	57.00	7.64	0.15%	90	40.00	3.60	1.20%
1	102	65.00	6.63	0.29%	92	36.00	3.31	2.30%
1.5	90	52.00	4.68	0.38%	82	48.00	3.94	3.62%
2	84	51.00	4.28	0.46%	100	42.00	4.20	5.02%
3	178	48.00	8.54	0.64%	188	63.00	11.84	8.96%
4	202	42.00	8.48	0.81%	188	163.00	30.64	19.18%
5	148	54.00	7.99	0.97%	170	64.00	10.88	22.81%

Table A-16: Raw data for tantalum extraction experiments: Experimental design experiment 5-6.

Experiment	200 °C, 3 mL/min, 50g, 10 wt% [5]				200 °C, 3 mL/min, 15g, 10 wt% [6]			
t _{cumulative} (min)	V _p (mL)	c _{tantalum} (mg/L)	m _{tantalum} (mg)	%Extraction	V _p (mL)	c _{tantalum} (mg/L)	m _{tantalum} (mg)	%Extraction
0.5	104	50.00	5.20	0.10%	64	96.00	6.14	0.41%
1	88	62.00	5.46	0.21%	86	108.00	9.29	1.03%
1.5	92	52.00	4.78	0.31%	90	95.00	8.55	1.60%
2	84	204.00	17.14	0.65%	92	39.00	3.59	1.84%
3	196	152.00	29.79	1.25%	186	83.00	15.44	2.87%
4	182	187.00	34.03	1.93%	192	141.00	27.07	4.67%
5	196	156.00	30.58	2.54%	190	163.00	30.97	6.74%
Experiment	150 °C, 3 mL/min, 15g, 10 wt% [7]				200 °C, 3 mL/min, 50g, 2 wt% [8]			
t _{cumulative} (min)	V _p (mL)	c _{tantalum} (mg/L)	m _{tantalum} (mg)	%Extraction	V _p (mL)	c _{tantalum} (mg/L)	m _{tantalum} (mg)	%Extraction
0.5	104	26.00	2.70	0.18%	90	18.00	1.62	0.16%
1	92	39.00	3.59	0.42%	90	63.00	5.67	0.73%
1.5	92	96.00	8.83	1.01%	130	48.00	6.24	1.35%
2	92	75.00	6.90	1.47%	90	56.00	5.04	1.86%
3	186	72.00	13.39	2.36%	182	53.00	9.65	2.82%
4	182	110.00	20.02	3.70%	172	54.00	9.29	3.75%
5	176	51.00	8.98	4.29%	198	63.00	12.47	5.00%

Table A-17: Raw data for tantalum extraction experiments: Experimental design experiment 9-12.

Experiment	150 °C, 5 mL/min, 15g, 10 wt% [9]				200 °C, 5 mL/min, 15g, 10 wt% [10]			
t _{cumulative} (hr)	V _p (mL)	c _{tantalum} (mg/L)	m _{tantalum} (mg)	%Extraction	V _p (mL)	c _{tantalum} (mg/L)	m _{tantalum} (mg)	%Extraction
0.5	143	66.00	9.44	0.63%	98	108.00	10.58	3.53%
1	122	62.00	7.56	1.13%	84	62.00	5.21	5.26%
1.5	130	120.00	15.60	2.17%	120	123.00	14.76	10.18%
2	134	76.00	10.18	2.85%	130	76.00	9.88	13.48%
3	228	132.00	30.10	4.86%	224	115.00	25.76	22.06%
4	220	58.00	12.76	5.71%	226	248.00	56.05	40.75%
5	200	58.00	11.60	6.48%	214	147.00	31.46	51.23%
Experiment	200 °C, 5 mL/min, 50g, 2 wt% [11]				200 °C, 5 mL/min, 50g, 2 wt% [12]			
t _{cumulative} (min)	V _p (mL)	c _{tantalum} (mg/L)	m _{tantalum} (mg)	%Extraction	V _p (mL)	c _{tantalum} (mg/L)	m _{tantalum} (mg)	%Extraction
0.5	138	71.00	9.80	0.98%	130	91.00	11.83	3.94%
1	100	24.00	2.40	1.22%	122	141.00	17.20	9.68%
1.5	130	29.00	3.77	1.60%	96	190.00	18.24	15.76%
2	130	113.00	14.69	3.07%	128	114.00	14.59	20.62%
3	208	188.00	39.10	6.98%	210	178.00	37.38	33.08%
4	190	169.00	32.11	10.19%	208	260.00	54.08	51.11%
5	202	88.00	17.78	11.96%	216	74.00	15.98	56.44%

Table A-18: Raw data for tantalum extraction experiments: Experimental design experiment 13-16.

Experiment	150 °C, 5 mL/min, 50g, 2 wt% [13]				200 °C, 5 mL/min, 15g, 10 wt% [14]			
t _{cumulative} (min)	V _p (mL)	c _{tantalum} (mg/L)	m _{tantalum} (mg)	%recovery	V _p (mL)	c _{tantalum} (mg/L)	m _{tantalum} (mg)	%recovery
0.50	140	231.00	32.34	3.23%	112	146.00	16.35	1.09%
1.00	112	194.00	21.73	5.41%	128	85.00	10.88	1.82%
2.00	128	236.00	30.21	8.43%	94	104.00	9.78	2.47%
3.00	120	193.00	23.16	10.74%	80	33.00	2.64	2.64%
4.00	206	71.00	14.63	12.21%	146	84.00	12.26	3.46%
5.00	190	161.00	30.59	15.27%	142	131.00	18.60	4.70%
6.00	178	107.00	19.05	17.17%	140	61.00	8.54	5.27%
	150 °C, 5 mL/min, 50g, 10 wt% [15]				200 °C, 5 mL/min, 50g, 10 wt% [16]			
t _{cumulative} (min)	V _p (mL)	c _{tantalum} (mg/L)	m _{tantalum} (mg)	%recovery	V _p (mL)	c _{tantalum} (mg/L)	m _{tantalum} (mg)	%recovery
0.50	138	85.00	11.73	0.23%	134	41.00	5.49	0.11%
1.00	126	89.00	11.21	0.46%	130	6.00	0.78	0.13%
2.00	146	53.00	7.74	0.61%	126	58.00	7.31	0.27%
3.00	112	89.00	9.97	0.81%	134	71.00	9.51	0.46%
4.00	218	58.00	12.64	1.07%	212	52.00	11.02	0.68%
5.00	212	36.00	7.63	1.22%	206	45.00	9.27	0.87%
6.00	200	25.00	5.00	1.32%	210	52.00	10.92	1.09%

APPENDIX B: STATISTICAL ANALYSIS CALCULATIONS

The algebraic signs table and equations used to calculate the interaction effects of experimental parameters

The algebraic signs tables integrated with the attained extraction degrees, effect estimates and sum of squares, are presented in Table B-1 through to Table B-3. The equations for determining the factor effect estimates were developed with the aid of the algebraic signs table and the resulting equations are presented in below. The equations were adapted from Myers et al. (2009).

Table B-1: Algebraic signs for calculating the factor effects in the 2^4 design: Vanadium extraction experiments

% Extraction	Main Effects				Interaction Effects										
	A	B	C	D	AB	AC	AD	BC	BD	CD	ABC	ABD	ACD	BCD	ABCD
(-1) = 10.7%	-1	-1	-1	-1	1	1	1	1	1	1	-1	-1	-1	-1	1
a = 11.9%	1	-1	-1	-1	-1	-1	-1	1	1	1	1	1	1	-1	-1
b = 5.4%	-1	1	-1	-1	-1	1	1	-1	-1	1	1	1	-1	1	-1
ab = 16.2%	1	1	-1	-1	1	-1	-1	-1	-1	1	-1	-1	1	1	1
c = 29.1%	-1	-1	1	-1	1	-1	1	-1	1	-1	1	-1	1	1	-1
ac = 46.6%	1	-1	1	-1	-1	1	-1	-1	1	-1	-1	1	-1	1	1
bc = 35.3%	-1	1	1	-1	-1	-1	1	1	-1	-1	-1	1	1	-1	1
abc = 47.7%	1	1	1	-1	1	1	-1	1	-1	-1	1	-1	-1	-1	-1
d = 6.9%	-1	-1	-1	1	1	1	-1	1	-1	-1	-1	1	1	1	-1
ad = 10.1%	1	-1	-1	1	-1	-1	1	1	-1	-1	1	-1	-1	1	1
bd = 8.7%	-1	1	-1	1	-1	1	-1	-1	1	-1	1	-1	1	-1	1
abd = 11.3%	1	1	-1	1	1	-1	1	-1	1	-1	-1	1	-1	-1	-1
cd = 48.1%	-1	-1	1	1	1	-1	-1	-1	-1	1	1	1	-1	-1	1
acd = 49.9%	1	-1	1	1	-1	1	1	-1	-1	1	-1	-1	1	-1	-1
bcd = 22.8%	-1	1	1	1	-1	-1	-1	1	1	1	-1	-1	-1	1	-1
abcd = 41.0%	1	1	1	1	1	1	1	1	1	1	1	1	1	1	1
Effects Estimates	8.46%	-5.74%	29.90%	-0.54%	2.55%	4.01%	-2.02%	-3.59%	-4.72%	1.29%	0.29%	1.42%	-0.49%	-5.70%	3.97%
Sum of Squares	2.86%	0.39%	35.77%	0.01%	0.26%	0.64%	0.16%	0.52%	0.89%	0.07%	0.00%	0.08%	0.01%	1.30%	0.63%

Table B-2: Algebraic signs for calculating the factor effects in the 2³ design: Additional vanadium extraction experiments

% Extraction	Main Effects			Interaction Effects			
	B	C	D	BC	BD	CD	BCD
(-1) = 41.6%	-1	-1	-1	1	1	1	-1
b = 49.9%	1	-1	-1	-1	-1	1	1
c = 55.1%	-1	1	-1	-1	1	-1	1
bc = 44.3%	1	1	-1	1	-1	-1	-1
d = 34.0%	-1	-1	1	1	-1	-1	1
bd = 31.0%	1	-1	1	-1	1	-1	-1
cd = 33.1%	-1	1	1	-1	-1	1	-1
bcd = 35.3%	1	1	1	1	1	1	1
Effects Estimate	-0.83%	2.86%	-14.41%	-3.48%	0.43%	-1.16%	6.06%
Sum of Squares	0.01%	0.16%	4.15%	0.24%	0.00%	0.03%	0.73%

Table B-3: Algebraic signs for calculating the factor effects in the 2⁴ design: Tantalum extraction experiments

% Extraction	Main Effects				Interaction Effects										
	A	B	C	D	AB	AC	AD	BC	BD	CD	ABC	ABD	ACD	BCD	ABCD
(-1) = 13.7%	-1	-1	-1	-1	1	1	1	1	1	1	-1	-1	-1	-1	1
a = 4.3%	1	-1	-1	-1	-1	-1	-1	1	1	1	1	1	1	-1	-1
b = 22.8%	-1	1	-1	-1	-1	1	1	-1	-1	1	1	1	-1	1	-1
ab = 6.7%	1	1	-1	-1	1	-1	-1	-1	-1	1	-1	-1	1	1	1
c = 56.4%	-1	-1	1	-1	1	-1	1	-1	1	-1	1	-1	1	1	-1
ac = 6.5%	1	-1	1	-1	-1	1	-1	-1	1	-1	-1	1	-1	1	1
bc = 51.2%	-1	1	1	-1	-1	-1	1	1	-1	-1	-1	1	1	-1	1
abc = 5.3%	1	1	1	-1	1	1	-1	1	-1	-1	1	-1	-1	-1	-1
d = 5.0%	-1	-1	-1	1	1	1	-1	1	-1	-1	-1	1	1	1	-1
ad = 1.0%	1	-1	-1	1	-1	-1	1	1	-1	-1	1	-1	-1	1	1
bd = 5.0%	-1	1	-1	1	-1	1	-1	-1	1	-1	1	-1	1	-1	1
abc = 2.5%	1	1	-1	1	1	-1	1	-1	1	-1	-1	1	-1	-1	-1
cd = 17.2%	-1	-1	1	1	1	-1	-1	-1	-1	1	1	1	-1	-1	1
acd = 1.3%	1	-1	1	1	-1	1	1	-1	-1	1	-1	-1	1	-1	-1
bcd = 12.0%	-1	1	1	1	-1	-1	-1	1	1	1	-1	-1	-1	1	-1
abcd = 1.1%	1	1	1	1	1	1	1	1	1	1	1	1	1	1	1
Effects Estimates	-19.3%	-1.3%	11.2%	-15.2%	0.5%	-11.3%	11.0%	-3.1%	-1.1%	-6.7%	1.8%	1.2%	6.3%	1.4%	-0.9%
Sum of Squares	14.9%	0.0%	5.1%	9.3%	0.0%	5.1%	4.9%	0.4%	0.1%	1.8%	0.1%	0.1%	1.6%	0.1%	0.0%

The following equations were applied to determine the magnitude of the interaction effects for a 2⁴ factorial design experiments.

Main factor effects:

$$A = \frac{1}{8n} [a + ab + ac + abc + ad + abd + acd + abcd - (1) - b - c - bc - d - bd - cd - bcd]$$

$$B = \frac{1}{8n} [b + ab + bc + abc + bd + abd + bcd + abcd - (1) - a - c - ac - d - ad - cd - acd]$$

$$C = \frac{1}{8n} [c + ac + bc + abc + cd + acd + bcd + abcd - (1) - a - b - ab - d - ad - bd - abd]$$

$$D = \frac{1}{8n} [d + ad + bd + abd + cd + acd + bcd + abcd - (1) - a - b - ab - c - ac - bc - abc]$$

Two-factor interactions:

$$AB = \frac{1}{8n} [ab - b + abc - bc + abd - bd + abcd - bcd - a + (1) - ac + c - ad + d - acd + cd]$$

$$AC = \frac{1}{8n} [ac - c + abc - bc + acd - cd + abcd + bcd - a + (1) - c + ab - ad + d - abd + bd]$$

$$AD = \frac{1}{8n} [ad - d + abd - bd + acd - cd + abcd - bcd - a + (1) - c + ab - bc + ac + abc - bc]$$

$$BC = \frac{1}{8n} [bc - c + abc - ac + bcd - cd + abcd - acd - b + (1) - c + ab - bd + d + abd - ad]$$

$$BD = \frac{1}{8n} [bd - d + abd - ad + bcd - cd + abcd - acd - b + (1) - c + ab - bc + c - abc + ac]$$

$$CD = \frac{1}{8n} [cd - d + acd - ad + bcd - bd + abcd - abd - c + (1) - ac + a - bc + b - abc + ab]$$

Three-factor interactions and four-factor interaction:

$$ABC = \frac{1}{8n} [c - ac + abc - bc + cd - acd + abcd - bcd - (1) + a - ab + b - d + ad - abd - bd]$$

$$ABD = \frac{1}{8n} [d - ad + abd - bd + cd - acd + abcd - bcd - (1) + a - ab + b - c + ac - abc - bc]$$

$$ACD = \frac{1}{8n} [ac - c + abc - bc + acd - cd + abcd - bcd - (1) + a - b + ab - d + ad - bd - abd]$$

$$BCD = \frac{1}{8n} [d - bd + ad - abd + bcd - cd + abcd - acd - (1) + b - a + ab - bc + c - abc - ac]$$

$$ABCD = \frac{1}{8n} [ad - d + bd - abd + cd - acd + abcd - bcd - a + (1) - b + ab - c + ac - abc - ac]$$

The following equations were applied to determine the magnitude of the interaction effects in a 2^3 factorial design experiments.

Main factor effects:

$$B = \frac{1}{4n} [b + bc + bd + bcd - (-1) - c - d - cd]$$

$$C = \frac{1}{4n} [c + bc + cd + bcd - (-1) - b - d - bd]$$

$$D = \frac{1}{4n} [d + bd + cd + bcd - (-1) - b - c - bc]$$

Two-factor interaction

$$BC = \frac{1}{4n} [bc - c + bcd - cd - (-1) + b - d + bd]$$

$$BD = \frac{1}{4n} [bd - d + bcd - cd - (-1) + b - bc + c]$$

$$CD = \frac{1}{4n} [bcd - bd + cd - d - (-1) + c - b + bc]$$

Three-factor interactions

$$BCD = \frac{1}{4n} [bcd - cd + d - bd - b + (-1) - c + bc]$$

Sum of Squares and mean square calculations

The equation used to calculate the sum of squares for 2^4 factorial design experiments is displayed below:

$$SS_i = \frac{(contrast)^2}{16n}$$

But for 2^3 factorial experiments, the equation applied was as shown below:

$$SS_i = \frac{(contrast)^2}{8n}$$

The mean square was determined through applying the following equation

$$MS_i = \frac{SS_i}{degree\ of\ freedom}$$

Normal Probability Plotting

The Gringorten probability plotting position was used in the construction of the normal probability plot, and this is because it was found to be the best for all sample sizes (Yahaya et al., 2012). The formula defining the Gringorten positioning is as follows:

$$\text{Gringorten positioning} = (i - 0.44)/(n + 0.12)$$

Therefore, the probability plots were computed by applying the aforesaid positioning method, and the calculated factor effect estimate. Table B-4 through to Table B-6 present the normal probability tables attained for all the experiments.

Table B-4: Normal probability table for vanadium extraction experiments.

Effect	Estimate	i	(i-0.44)/(n+0.12)
B	-0.0574	1	4%
BCD	-0.0570	2	10%
BD	-0.0472	3	17%
BC	-0.0359	4	24%
AD	-0.0202	5	30%
D	-0.0054	6	37%
ACD	-0.0049	7	43%
ABC	0.0029	8	50%
CD	0.0129	9	57%
ABD	0.0142	10	63%
AB	0.0255	11	70%
ABCD	0.0397	12	76%
AC	0.0401	13	83%
A	0.0846	14	90%
C	0.2990	15	96%
n		15	

Table B-5: Normal probability table for additional vanadium extraction experiments.

Effect	Estimate	i	(i-0.44)/(n+0.12)
D	-0.1441	1	8%
BC	-0.0348	2	22%
CD	-0.0116	3	36%
B	-0.0083	4	50%
BD	0.0043	5	64%
C	0.0286	6	78%
BCD	0.0606	7	92%
n		7	

Table B-6: Normal probability table for vanadium extraction experiments.

Effect	Estimate	i	(i-0.44)/(n+0.12)
A	-0.1933	1	4%
D	-0.1524	2	10%
AC	-0.1134	3	17%
CD	-0.0673	4	24%
BC	-0.0312	5	30%
B	-0.0132	6	37%
BD	-0.0112	7	43%
ABCD	-0.0091	8	50%
AB	0.0048	9	57%
ABD	0.0115	10	63%
BCD	0.0137	11	70%
ABC	0.0176	12	76%
ACD	0.0627	13	83%
AD	0.1102	14	90%
C	0.1124	15	96%
	n	15	

APPENDIX C: KINETIC ANALYSIS - VANADIUM EXTRACTION EXPERIMENTS

Model Fitting Results of Vanadium Extraction Experiments

Table C-1: Regression results of kinetic model fitting for vanadium response curves 5 g and 1 mL/min.

150 °C, 1 mL/min, 5 g, [+500 µm -1 mm] σ^2 32.08						150 °C, 1 mL/min, 5 g, [+2 mm -4 mm] σ^2 20.38					
t (min)	%Extraction	$g_{Fp}(X_i)$	$P_{Fp}(X_i)$	t/ τ	Error	t (min)	%Extraction	$g_{Fp}(X_i)$	$P_{Fp}(X_i)$	t/ τ	Error
30.0	4.26%	0.0144	6.18E-04	3.42%	7.06E-05	30.0	0.40%	0.0013	5.26E-06	0.0014	6.44E-06
60.0	4.65%	0.0158	7.37E-04	3.94%	5.09E-05	60.0	0.50%	0.0017	8.33E-06	0.0018	9.97E-06
120.0	5.09%	0.0173	8.83E-04	4.56%	2.81E-05	120.0	2.78%	0.0094	2.61E-04	0.0147	1.72E-04
180.0	5.52%	0.0188	1.04E-03	5.22%	9.25E-06	180.0	4.66%	0.0158	7.39E-04	0.0308	2.48E-04
240.0	5.94%	0.0202	1.21E-03	5.89%	1.99E-07	240.0	6.15%	0.0209	1.30E-03	0.0473	2.00E-04
300.0	6.17%	0.0210	1.31E-03	6.29%	1.39E-06	300.0	7.72%	0.0264	2.06E-03	0.0683	7.84E-05
360.0	6.51%	0.0222	1.46E-03	6.89%	1.42E-05	360.0	9.38%	0.0323	3.06E-03	0.0947	8.18E-07
420.0	6.91%	0.0236	1.64E-03	7.63%	5.16E-05	420.0	10.74%	0.0372	4.04E-03	0.1195	1.46E-04
					0.02%						0.09%

200 °C, 1 mL/min, 5 g, [+500 µm -1 mm] σ^2 17.55						200 °C, 1 mL/min, 5 g, [+2 mm -4mm] σ^2 12.59					
t (min)	%Extraction	$g_{Fp}(X_i)$	$P_{Fp}(X_i)$	t/ τ	Error	t (min)	%Extraction	$g_{Fp}(X_i)$	$P_{Fp}(X_i)$	t/ τ	Error
30.0	4.51%	0.0153	6.92E-04	2.74%	3.13E-04	30.0	3.03%	0.0102	3.10E-04	1.41%	2.62E-04
60.0	5.57%	0.0189	1.06E-03	3.76%	3.30E-04	60.0	4.86%	0.0165	8.06E-04	2.66%	4.84E-04
120.0	7.54%	0.0258	1.96E-03	6.03%	2.30E-04	120.0	8.69%	0.0298	2.62E-03	6.28%	5.79E-04
180.0	8.94%	0.0308	2.78E-03	7.95%	9.84E-05	180.0	11.41%	0.0396	4.57E-03	9.71%	2.87E-04
240.0	10.38%	0.0359	3.77E-03	10.20%	3.26E-06	240.0	13.18%	0.0460	6.16E-03	12.35%	6.81E-05
300.0	11.05%	0.0383	4.29E-03	11.35%	9.04E-06	300.0	14.49%	0.0509	7.50E-03	14.52%	8.30E-08
360.0	11.55%	0.0401	4.69E-03	12.24%	4.82E-05	360.0	15.61%	0.0550	8.74E-03	16.50%	8.01E-05
420.0	11.91%	0.0414	5.00E-03	12.92%	1.01E-04	420.0	16.20%	0.0572	9.45E-03	17.62%	2.00E-04
					0.11%						0.20%

Table C-2: Regression results of kinetic model fitting for vanadium response curves 15 g and 1 mL/min.

150 °C, 1 mL/min, 15 g, [+500 μ m -1 mm] σ^2 24.48						150 °C, 1 mL/min, 15 g, [+2 mm -4 mm] σ^2 41.34					
t (min)	%Extraction	$g_{Fp}(X_i)$	$P_{Fp}(X_i)$	t/ τ	Error	t (min)	%Extraction	$g_{Fp}(X_i)$	$P_{Fp}(X_i)$	t/ τ	Error
30.0	0.77%	0.0026	2.01E-05	0.31%	2.18E-05	30.0	0.21%	0.0007	1.45E-06	0.08%	1.77E-06
60.0	1.04%	0.0035	3.59E-05	0.43%	3.62E-05	60.0	0.46%	0.0015	7.09E-06	0.18%	7.71E-06
120.0	1.45%	0.0048	7.01E-05	0.66%	6.23E-05	120.0	1.20%	0.0040	4.82E-05	0.60%	3.59E-05
180.0	3.08%	0.0104	3.22E-04	1.83%	1.58E-04	180.0	1.92%	0.0065	1.25E-04	1.16%	5.84E-05
240.0	5.82%	0.0198	1.16E-03	4.82%	1.00E-04	240.0	2.68%	0.0090	2.42E-04	1.90%	6.04E-05
300.0	7.10%	0.0243	1.74E-03	6.68%	1.80E-05	300.0	3.55%	0.0120	4.27E-04	2.96%	3.45E-05
360.0	8.14%	0.0279	2.29E-03	8.41%	7.02E-06	360.0	4.69%	0.0159	7.49E-04	4.68%	4.27E-09
420.0	8.66%	0.0297	2.60E-03	9.35%	4.69E-05	420.0	5.42%	0.0184	1.00E-03	5.99%	3.23E-05
					0.05%						0.02%

200 °C, 1 mL/min, 15 g, [+500 μ m -1 mm] σ^2 21.31						200 °C, 1 mL/min, 15 g, [+2 mm -4 mm] σ^2 19.87					
t (min)	%Extraction	$g_{Fp}(X_i)$	$P_{Fp}(X_i)$	t/ τ	Error	t (min)	%Extraction	$g_{Fp}(X_i)$	$P_{Fp}(X_i)$	t/ τ	Error
30.0	1.13%	0.0038	4.31E-05	0.47%	4.39E-05	30.0	1.33%	0.0044	5.90E-05	0.56%	5.85E-05
60.0	2.52%	0.0085	2.14E-04	1.30%	1.48E-04	60.0	2.32%	0.0078	1.81E-04	1.14%	1.39E-04
120.0	4.62%	0.0156	7.26E-04	3.11%	2.27E-04	120.0	4.06%	0.0137	5.60E-04	2.48%	2.48E-04
180.0	6.21%	0.0211	1.32E-03	4.93%	1.63E-04	180.0	4.59%	0.0155	7.17E-04	2.98%	2.60E-04
240.0	7.60%	0.0260	1.99E-03	6.84%	5.67E-05	240.0	4.83%	0.0164	7.96E-04	3.22%	2.60E-04
300.0	8.67%	0.0298	2.61E-03	8.54%	1.80E-06	300.0	6.17%	0.0210	1.31E-03	4.70%	2.18E-04
360.0	9.44%	0.0325	3.10E-03	9.86%	1.79E-05	360.0	8.74%	0.0300	2.65E-03	8.26%	2.23E-05
420.0	10.13%	0.0350	3.58E-03	11.14%	1.01E-04	420.0	11.28%	0.0391	4.47E-03	12.79%	2.29E-04
					0.08%						0.14%

Table C-3: Regression results of kinetic model fitting for vanadium response curves 5 g and 5 mL/min.

150 °C, 5 mL/min, 5 g, [+500 μ m -1 mm] σ^2 6.38						150 °C, 5 mL/min, 5 g, [+2 mm -4 mm] σ^2 5.14					
t (min)	%Extraction	$g_{Fp}(X_i)$	$P_{Fp}(X_i)$	t/ τ	Error	t (min)	%Extraction	$g_{Fp}(X_i)$	$P_{Fp}(X_i)$	t/ τ	Error
30.0	8.31%	0.0285	0.0024	4.38%	1.55E-03	30.0	8.44%	0.0290	0.0025	4.17%	1.83E-03
60.0	11.32%	0.0393	0.0045	6.80%	2.05E-03	60.0	12.32%	0.0429	0.0054	7.04%	2.79E-03
120.0	17.98%	0.0639	0.0117	13.88%	1.68E-03	120.0	17.50%	0.0621	0.0111	11.91%	3.13E-03
180.0	21.99%	0.0794	0.0179	19.38%	6.80E-04	180.0	22.28%	0.0806	0.0184	17.53%	2.26E-03
240.0	25.19%	0.0922	0.0239	24.49%	4.91E-05	240.0	26.91%	0.0992	0.0276	24.08%	7.98E-04
300.0	26.78%	0.0987	0.0273	27.27%	2.46E-05	300.0	30.84%	0.1157	0.0370	30.59%	6.34E-06
360.0	27.98%	0.1036	0.0300	29.50%	2.30E-04	360.0	33.42%	0.1268	0.0442	35.36%	3.76E-04
420.0	29.07%	0.1082	0.0326	31.60%	6.39E-04	420.0	35.32%	0.1352	0.0499	39.13%	1.45E-03
					0.69%						1.26%

200 °C, 5 mL/min, 5 g, [+500 μ m -1 mm] σ^2 3.58						200 °C, 5 mL/min, 5 g, [+2 mm -4mm] σ^2 3.45					
t (min)	%Extraction	$g_{Fp}(X_i)$	$P_{Fp}(X_i)$	t/ τ	Error	t (min)	%Extraction	$g_{Fp}(X_i)$	$P_{Fp}(X_i)$	t/ τ	Error
30.0	13.24%	0.0462	0.0062	6.85%	4.09E-03	30.0	9.93%	0.0342	0.0034	4.61%	2.83E-03
60.0	17.00%	0.0602	0.0104	9.76%	5.24E-03	60.0	13.23%	0.0462	0.0062	6.76%	4.19E-03
120.0	25.45%	0.0932	0.0245	18.08%	5.43E-03	120.0	21.58%	0.0779	0.0172	13.72%	6.18E-03
180.0	31.47%	0.1183	0.0387	25.68%	3.35E-03	180.0	28.12%	0.1042	0.0303	20.87%	5.26E-03
240.0	36.64%	0.1411	0.0541	33.48%	1.00E-03	240.0	34.54%	0.1317	0.0475	29.54%	2.51E-03
300.0	40.51%	0.1590	0.0678	40.15%	1.33E-05	300.0	39.44%	0.1539	0.0638	37.38%	4.25E-04
360.0	43.48%	0.1732	0.0796	45.80%	5.37E-04	360.0	44.76%	0.1795	0.0851	47.27%	6.30E-04
420.0	46.61%	0.1887	0.0934	52.29%	3.23E-03	420.0	47.75%	0.1946	0.0988	53.51%	3.32E-03
					2.29%						2.53%

Table C-4: Regression results of kinetic model fitting for vanadium response curves at 15 g and 5 mL/min.

150°C, 5mL/min,15g,[+500µm -1mm]						150°C, 5mL/min,15g,[+2mm -4mm]					
σ^2 3.37						σ^2 8.45					
t (min)	%Extraction	$g_{Fp}(X_i)$	$P_{Fp}(X_i)$	t/ τ	Error	t (min)	%Extraction	$g_{Fp}(X_i)$	$P_{Fp}(X_i)$	t/ τ	Error
30.0	7.82%	0.0268	0.0021	3.39%	0.20%	30.0	5.21%	0.0177	0.0009	2.55%	7.06E-04
60.0	12.36%	0.0430	0.0054	6.12%	0.39%	60.0	8.27%	0.0284	0.0024	4.83%	1.18E-03
120.0	22.88%	0.0829	0.0195	14.87%	0.64%	120.0	13.70%	0.0479	0.0067	10.42%	1.07E-03
180.0	29.98%	0.1120	0.0348	22.95%	0.49%	180.0	17.68%	0.0628	0.0113	15.85%	3.33E-04
240.0	36.32%	0.1397	0.0531	31.88%	0.20%	240.0	20.01%	0.0717	0.0147	19.59%	1.79E-05
300.0	40.99%	0.1612	0.0696	39.61%	0.02%	300.0	21.12%	0.0761	0.0165	21.52%	1.59E-05
360.0	45.37%	0.1825	0.0878	47.87%	0.06%	360.0	21.88%	0.0790	0.0177	22.90%	1.03E-04
420.0	48.14%	0.1966	0.1007	53.66%	0.30%	420.0	22.77%	0.0825	0.0193	24.57%	3.23E-04
2.30%						0.37%					

200°C, 5mL/min,15g,[+500µm -1mm]						200°C, 5mL/min,15g,[+2mm -4mm]					
σ^2 3.08						σ^2 4.21					
t (min)	%Extraction	$g_{Fp}(X_i)$	$P_{Fp}(X_i)$	t/ τ	Error	t (min)	%Extraction	$g_{Fp}(X_i)$	$P_{Fp}(X_i)$	t/ τ	Error
30.0	10.29%	0.0355	0.0037	4.69%	3.13E-03	30.0	7.81%	0.0267	0.0021	3.56%	1.81E-03
60.0	15.11%	0.0531	0.0082	7.83%	5.29E-03	60.0	11.57%	0.0402	0.0047	6.00%	3.11E-03
120.0	26.57%	0.0978	0.0268	18.06%	7.24E-03	120.0	18.51%	0.0660	0.0125	11.85%	4.45E-03
180.0	37.37%	0.1444	0.0566	31.88%	3.01E-03	180.0	25.33%	0.0928	0.0242	19.47%	3.44E-03
240.0	43.24%	0.1721	0.0786	41.45%	3.21E-04	240.0	31.18%	0.1171	0.0379	27.66%	1.24E-03
300.0	45.75%	0.1844	0.0895	46.05%	8.58E-06	300.0	35.66%	0.1367	0.0509	35.10%	3.15E-05
360.0	48.03%	0.1960	0.1002	50.51%	6.12E-04	360.0	38.56%	0.1499	0.0607	40.50%	3.76E-04
420.0	49.87%	0.2056	0.1094	54.31%	1.97E-03	420.0	40.97%	0.1611	0.0695	45.35%	1.92E-03
2.16%						1.64%					

Table C-5: Kinetic model regression results for additional vanadium extraction experiments at 15 g and 5 mL/min.

200 °C, 5mL/min, 15g, +250µm -500µm						200 °C, 5mL/min, 15g, +500µm -1mm					
σ^2					4.14	σ^2					3.08
t (min)	%Extraction	$g_{Fp}(X_i)$	$P_{Fp}(X_i)$	t/ τ	Error	t (min)	%Extraction	$g_{Fp}(X_i)$	$P_{Fp}(X_i)$	t/ τ	Error
30	9.70%	0.0334	0.0033	4.70%	2.50E-03	30	10.29%	0.0355	0.0037	4.69%	3.13E-03
60	10.56%	0.0365	0.0039	5.27%	2.80E-03	60	15.11%	0.0531	0.0082	7.83%	5.29E-03
90	16.68%	0.0590	0.0100	10.06%	4.38E-03	120	26.57%	0.0978	0.0268	18.06%	7.24E-03
120	23.68%	0.0861	0.0210	17.30%	4.06E-03	180	37.37%	0.1444	0.0566	31.88%	3.01E-03
180	31.39%	0.1180	0.0385	27.75%	1.32E-03	240	43.24%	0.1721	0.0786	41.45%	3.21E-04
240	35.49%	0.1359	0.0504	34.49%	9.99E-05	300	45.75%	0.1844	0.0895	46.05%	8.58E-06
360	38.55%	0.1498	0.0606	40.11%	2.43E-04	360	48.03%	0.1960	0.1002	50.51%	6.12E-04
420	41.59%	0.1641	0.0719	46.21%	2.14E-03	420	49.87%	0.2056	0.1094	54.31%	1.97E-03
					1.75%						2.16%

200 °C, 7mL/min, 15g, +250µm -500µm						200 °C, 7mL/min, 15g, +500µm -1mm					
σ^2					2.61	σ^2					3.66
t (min)	%Extraction	$g_{Fp}(X_i)$	$P_{Fp}(X_i)$	t/ τ	Error	t (min)	%Extraction	$g_{Fp}(X_i)$	$P_{Fp}(X_i)$	t/ τ	Error
30	13.76%	0.0481	0.0067	6.57%	5.16E-03	30	13.1%	0.0456	0.0060	6.76%	3.96E-03
60	19.87%	0.0712	0.0145	10.90%	8.04E-03	60	19.8%	0.0709	0.0144	12.35%	5.55E-03
120	30.97%	0.1162	0.0374	21.39%	9.17E-03	120	26.3%	0.0969	0.0264	19.33%	4.92E-03
180	35.02%	0.1338	0.0490	26.18%	7.81E-03	180	33.9%	0.1290	0.0456	29.59%	1.88E-03
240	48.29%	0.1974	0.1015	46.26%	4.11E-04	240	38.8%	0.1508	0.0614	37.53%	1.51E-04
300	51.76%	0.2157	0.1195	52.83%	1.13E-04	300	41.5%	0.1637	0.0716	42.57%	1.12E-04
360	53.67%	0.2262	0.1304	56.70%	9.18E-04	360	43.2%	0.1716	0.0783	45.79%	6.93E-04
420	55.14%	0.2345	0.1392	59.83%	2.20E-03	420	44.3%	0.1774	0.0833	48.20%	1.49E-03
					3.38%						1.87%

Table C-6: Kinetic model regression results for additional vanadium extraction experiments at 50 g and 5 mL/min.

200 °C, 5mL/min, 50g, +250µm -500µm						200 °C, 5mL/min, 50g, +500µm -1mm					
σ^2					5.30	σ^2					6.20
t (min)	%Extraction	$g_{Fp}(X_i)$	$P_{Fp}(X_i)$	t/ τ	Error	t (min)	%Extraction	$g_{Fp}(X_i)$	$P_{Fp}(X_i)$	t/ τ	Error
30	0.0562	0.0191	0.0011	2.48%	9.85E-04	30	5.3%	0.0181	0.0010	2.42%	8.56E-04
60	0.0898	0.0309	0.0028	4.57%	1.94E-03	60	8.8%	0.0301	0.0027	4.66%	1.68E-03
90	0.1595	0.0563	0.0091	10.48%	3.00E-03	120	12.9%	0.0448	0.0058	8.11%	2.25E-03
120	0.2266	0.0821	0.0191	18.34%	1.86E-03	180	16.7%	0.0590	0.0100	12.12%	2.07E-03
180	0.2786	0.1031	0.0297	26.07%	3.19E-04	240	21.0%	0.0757	0.0163	17.69%	1.12E-03
240	0.2981	0.1113	0.0344	29.38%	1.89E-05	300	24.9%	0.0912	0.0234	23.65%	1.66E-04
360	0.3235	0.1222	0.0411	34.02%	2.80E-04	360	27.9%	0.1034	0.0299	28.86%	8.80E-05
420	0.3397	0.1292	0.0458	37.19%	1.04E-03	420	31.0%	0.1163	0.0374	34.83%	1.48E-03
					0.94%						0.97%

65

200 °C, 7mL/min, 50g, +250µm -500µm						200 °C, 7mL/min, 50g, +500µm -1mm					
σ^2					5.58	σ^2					5.03
t (min)	%Extraction	$g_{Fp}(X_i)$	$P_{Fp}(X_i)$	t/ τ	Error	t (min)	%Extraction	$g_{Fp}(X_i)$	$P_{Fp}(X_i)$	t/ τ	Error
30	0.0581	0.0197	0.0012	2.62%	1.02E-03	30	6.7%	0.0228	0.0015	3.06%	1.32E-03
60	0.0921	0.0317	0.0029	4.82%	1.93E-03	60	11.2%	0.0387	0.0044	6.07%	2.59E-03
120	0.1498	0.0527	0.0080	9.75%	2.74E-03	120	16.2%	0.0573	0.0095	10.51%	3.28E-03
180	0.1955	0.0700	0.0140	14.81%	2.25E-03	180	23.7%	0.0864	0.0211	19.25%	2.01E-03
240	0.2347	0.0853	0.0206	20.02%	1.19E-03	240	28.5%	0.1060	0.0313	26.36%	4.76E-04
300	0.2738	0.1011	0.0286	26.09%	1.66E-04	300	31.7%	0.1192	0.0393	31.68%	9.62E-09
360	0.3155	0.1187	0.0389	33.60%	4.19E-04	360	33.8%	0.1285	0.0453	35.63%	3.35E-04
420	0.3308	0.1253	0.0432	36.63%	1.26E-03	420	35.3%	0.1350	0.0497	38.52%	1.06E-03
					1.10%						1.11%

Determination of the kinetic rate constant(s) for vanadium experiments

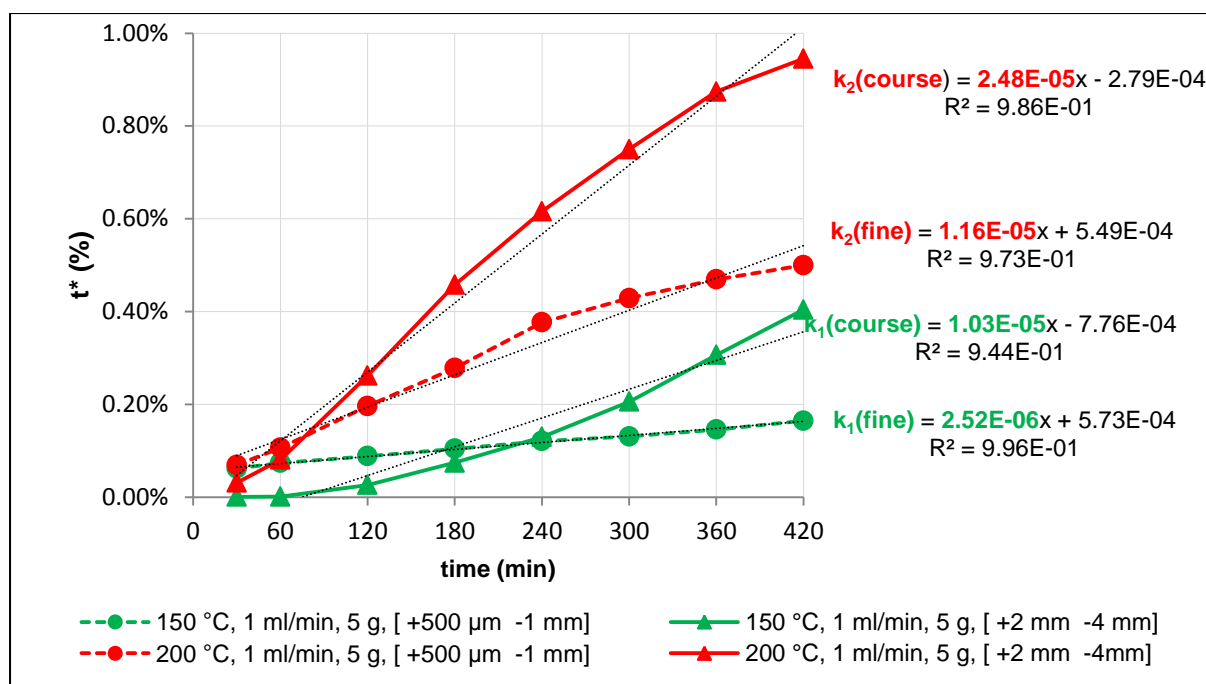


Figure C-1: Kinetic model regression curves for vanadium extraction experiments at 5 g and 1 mL/min.

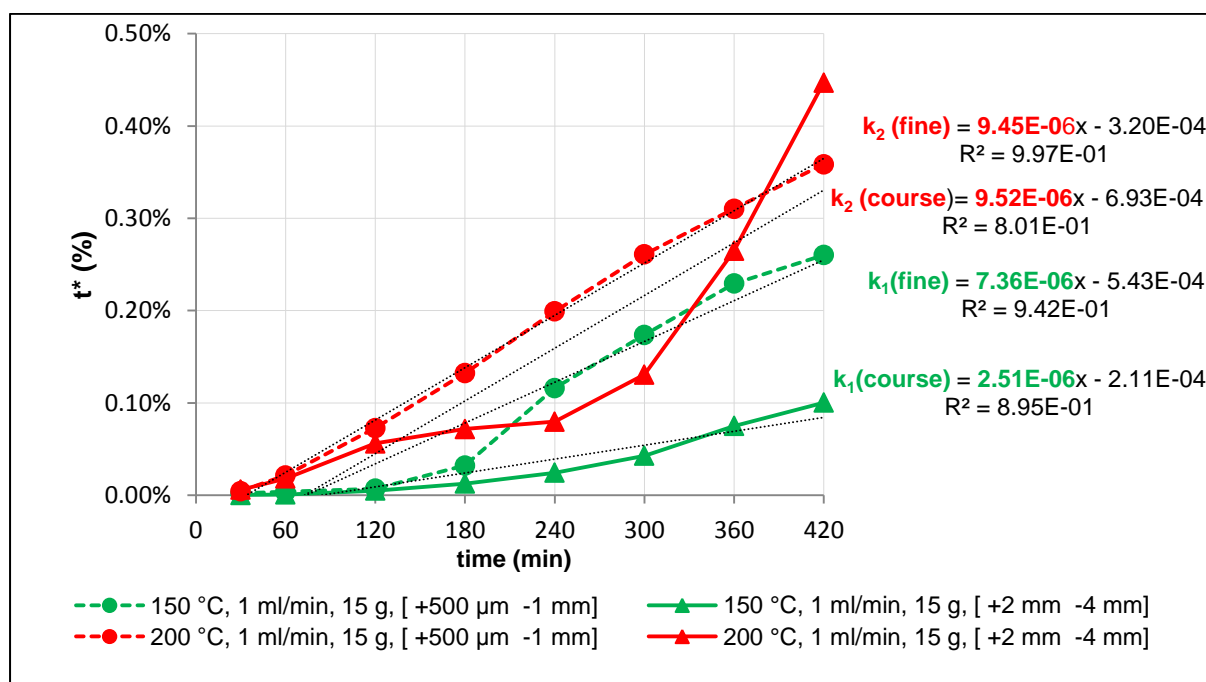


Figure C-2: Kinetic model regression curves for vanadium extraction experiments at 15 g and 1 mL/min.

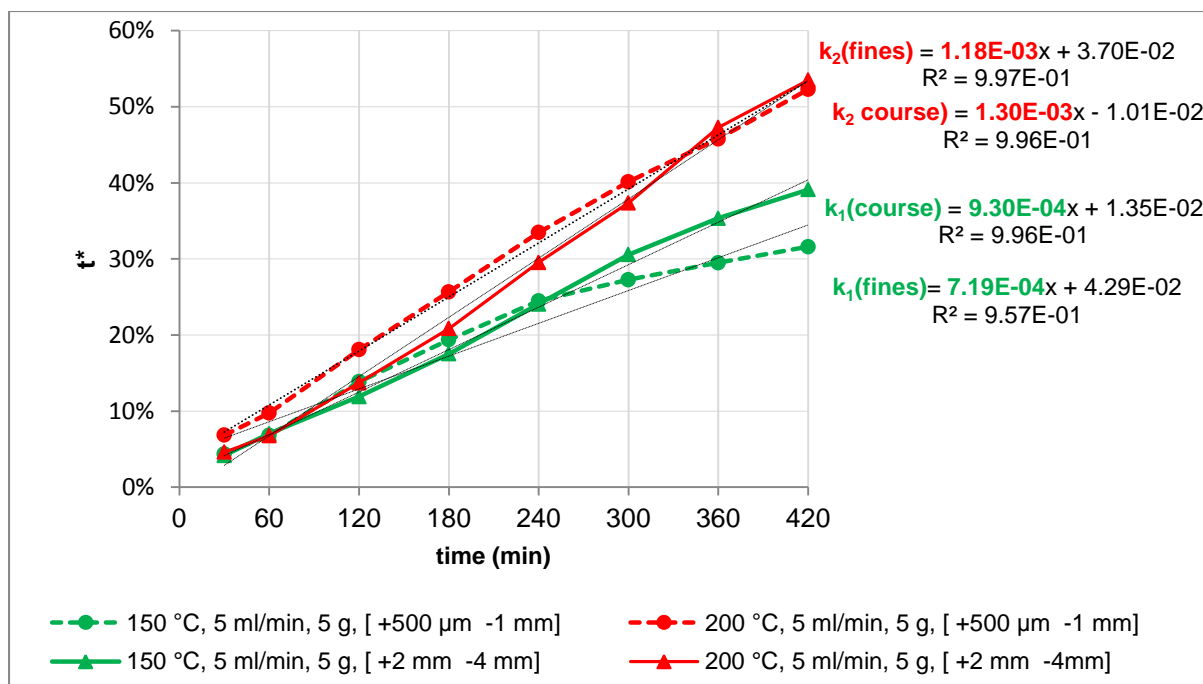


Figure C-3: Kinetic model regression curves for vanadium extraction experiments at 5 g and 5 mL/min.

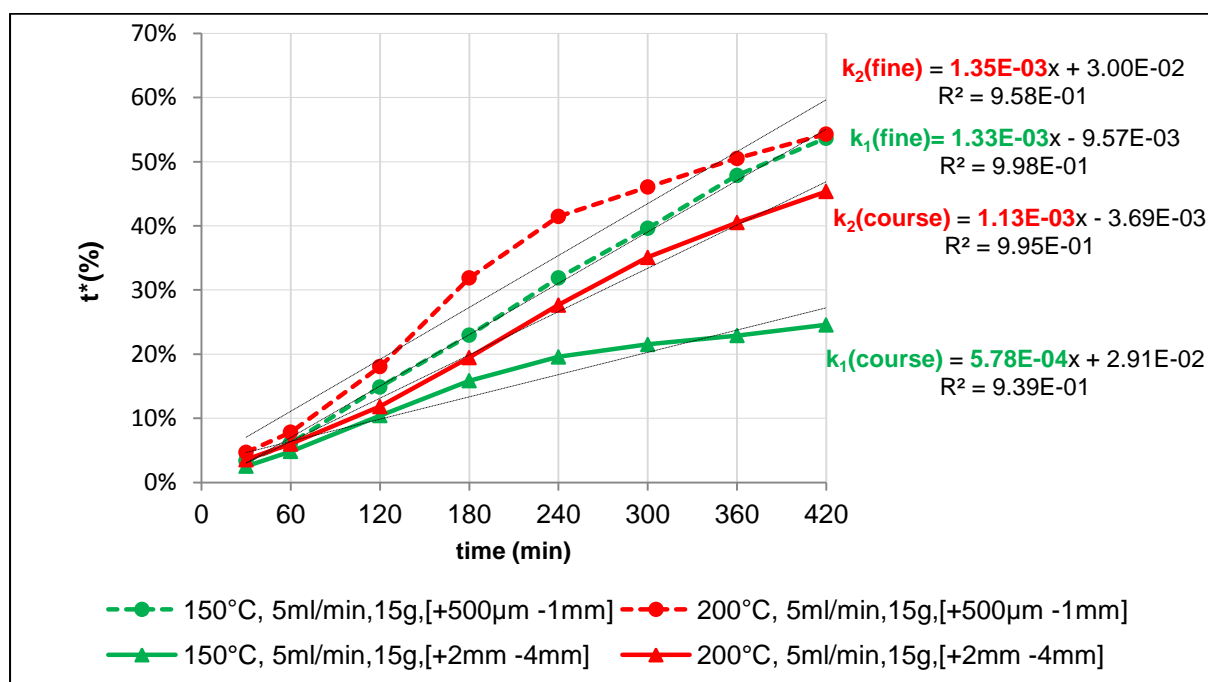


Figure C-4: Kinetic model regression curves for vanadium extraction experiments at 15 g and 5 mL/min.

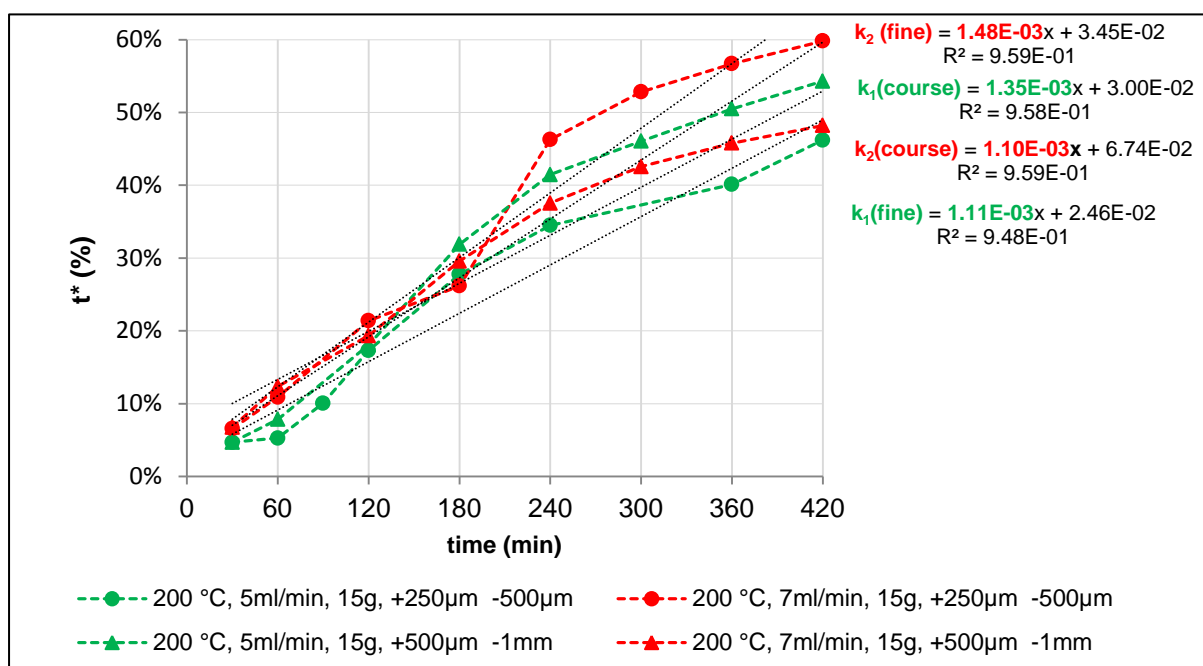


Figure C-5: Kinetic model regression curves for additional experiments at 15 g and 7 mL/min.

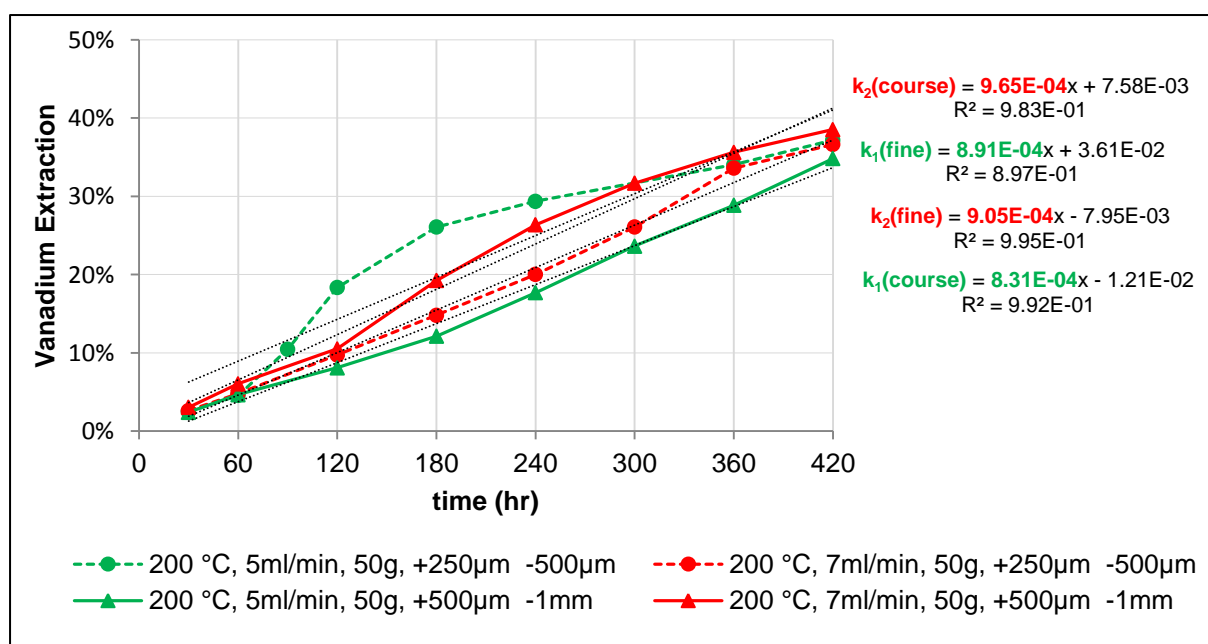


Figure C-6: Kinetic model regression curves for additional experiments at 50 g and 7 mL/min.

APPENDIX D: KINETIC ANALYSIS –TANTALUM EXTRACTION EXPERIMENTS

Model Fitting Results for Tantalum Extraction Experiments

Table D-1: Regression results of kinetic model fitting for tantalum extraction experiments at 15 g and 3 mL/min.

150°C, 3 mL/min, 15 g, 2 wt%						150°C, 3 mL/min ,15 g, 10 wt%					
σ^2 15.24						σ^2 50.93					
t (min)	%Extraction	$g_{Fp}(X_i)$	$P_{Fp}(X_i)$	t/ τ	Error	t (min)	%Extraction	$g_{Fp}(X_i)$	$P_{Fp}(X_i)$	t/ τ	Error
30.0	0.75%	2.51E-03	1.88E-05	0.28%	2.22E-05	30.0	0.18%	6.01E-04	1.08E-06	0.07%	1.31E-06
60.0	1.60%	5.35E-03	8.55E-05	0.67%	8.66E-05	60.0	0.42%	1.40E-03	5.88E-06	0.17%	6.23E-06
90.0	2.76%	9.29E-03	2.57E-04	1.32%	2.07E-04	90.0	1.01%	3.37E-03	3.40E-05	0.51%	2.48E-05
120.0	3.79%	1.28E-02	4.88E-04	2.02%	3.13E-04	120.0	1.47%	4.92E-03	7.23E-05	0.86%	3.70E-05
180.0	6.21%	2.11E-02	1.32E-03	4.13%	4.33E-04	180.0	2.36%	7.93E-03	1.88E-04	1.75%	3.74E-05
240.0	8.29%	2.84E-02	2.38E-03	6.47%	3.31E-04	240.0	3.70%	1.25E-02	4.63E-04	3.61%	8.22E-07
300.0	13.70%	4.79E-02	6.67E-03	14.96%	1.59E-04	300.0	4.29%	1.45E-02	6.27E-04	4.64%	1.22E-05
0.16%						0.01%					

200°C, 3 mL/min,15 g, 2wt%						200°C, 3 mL/min,15 g, 10 wt%					
σ^2 8.29						σ^2 32.44					
t (min)	%Extraction	$g_{Fp}(X_i)$	$P_{Fp}(X_i)$	t/ τ	Error	t (min)	%Extraction	$g_{Fp}(X_i)$	$P_{Fp}(X_i)$	t/ τ	Error
30.0	1.20%	4.02E-03	4.83E-05	0.44%	5.75E-05	30.0	0.41%	1.37E-03	5.60E-06	0.15%	6.49E-06
60.0	2.30%	7.74E-03	1.79E-04	0.92%	1.91E-04	60.0	1.03%	3.44E-03	3.54E-05	0.46%	3.25E-05
90.0	3.62%	1.22E-02	4.43E-04	1.59%	4.12E-04	90.0	1.60%	5.36E-03	8.58E-05	0.81%	6.16E-05
120.0	5.02%	1.70E-02	8.58E-04	2.41%	6.78E-04	120.0	1.84%	6.16E-03	1.14E-04	0.98%	7.28E-05
180.0	8.96%	3.08E-02	2.79E-03	5.40%	1.27E-03	180.0	2.87%	9.65E-03	2.78E-04	1.87%	1.00E-04
240.0	19.18%	6.85E-02	1.34E-02	17.99%	1.41E-04	240.0	4.67%	1.58E-02	7.43E-04	3.99%	4.62E-05
300.0	22.81%	8.27E-02	1.94E-02	24.32%	2.29E-04	300.0	6.74%	2.30E-02	1.56E-03	7.36%	3.86E-05
0.30%						0.04%					

Table D-2: Regression results of kinetic model fitting for tantalum extraction experiments at 50 g and 3 mL/min.

150°C, 3 mL/min, 50 g, 2 wt%						σ^2	45.77	150°C, 3 mL/min ,50 g, 10 wt%						σ^2	41.34		
t (min)	%Extraction	$g_{Fp}(X_i)$	$P_{Fp}(X_i)$	t/t	Error	t (min)	%Extraction	$g_{Fp}(X_i)$	$P_{Fp}(X_i)$	t/t	Error	t (min)	%Extraction	$g_{Fp}(X_i)$	$P_{Fp}(X_i)$	t/t	Error
30.0	0.81%	2.72E-03	2.21E-05	0.37%	1.94E-05	30.0	0.15%	5.09E-04	7.78E-07	0.05%	9.72E-07	60.0	0.29%	9.52E-04	2.72E-06	0.11%	3.20E-06
60.0	1.56%	5.24E-03	8.22E-05	0.90%	4.41E-05	60.0	0.29%	9.52E-04	2.72E-06	0.11%	3.20E-06	90.0	0.38%	1.26E-03	4.80E-06	0.15%	5.41E-06
90.0	2.10%	7.06E-03	1.49E-04	1.39%	5.13E-05	90.0	0.38%	1.26E-03	4.80E-06	0.15%	5.41E-06	120.0	0.46%	1.55E-03	7.21E-06	0.18%	7.82E-06
120.0	2.43%	8.17E-03	1.99E-04	1.73%	4.94E-05	120.0	0.46%	1.55E-03	7.21E-06	0.18%	7.82E-06	180.0	0.64%	2.12E-03	1.35E-05	0.27%	1.35E-05
180.0	3.22%	1.08E-02	3.50E-04	2.68%	2.83E-05	180.0	0.64%	2.12E-03	1.35E-05	0.27%	1.35E-05	240.0	0.81%	2.69E-03	2.17E-05	0.36%	1.99E-05
240.0	4.26%	1.44E-02	6.15E-04	4.26%	4.02E-12	240.0	0.81%	2.69E-03	2.17E-05	0.36%	1.99E-05	300.0	0.97%	3.23E-03	3.12E-05	0.45%	2.64E-05
300.0	4.99%	1.69E-02	8.48E-04	5.57%	3.43E-05	300.0	0.97%	3.23E-03	3.12E-05	0.45%	2.64E-05						
					0.02%						0.01%						

200°C, 3 mL/min,50 g, 2wt%						σ^2	45.16	200°C, 3 mL/min,50 g, 10 wt%						σ^2	87.64		
t (min)	%Extraction	$g_{Fp}(X_i)$	$P_{Fp}(X_i)$	t/t	Error	t (min)	%Extraction	$g_{Fp}(X_i)$	$P_{Fp}(X_i)$	t/t	Error	t (min)	%Extraction	$g_{Fp}(X_i)$	$P_{Fp}(X_i)$	t/t	Error
30.0	0.16%	5.40E-04	8.75E-07	0.06%	1.08E-06	30.0	0.10%	3.47E-04	3.61E-07	0.04%	4.38E-07	60.0	0.21%	7.11E-04	1.52E-06	0.08%	1.66E-06
60.0	0.73%	2.44E-03	1.78E-05	0.32%	1.64E-05	60.0	0.21%	7.11E-04	1.52E-06	0.08%	1.66E-06	90.0	0.31%	1.03E-03	3.18E-06	0.13%	3.16E-06
90.0	1.35%	4.53E-03	6.14E-05	0.73%	3.88E-05	90.0	0.31%	1.03E-03	3.18E-06	0.13%	3.16E-06	120.0	0.65%	2.18E-03	1.42E-05	0.34%	9.58E-06
120.0	1.86%	6.23E-03	1.16E-04	1.15%	5.05E-05	120.0	0.65%	2.18E-03	1.42E-05	0.34%	9.58E-06	180.0	1.25%	4.18E-03	5.22E-05	0.87%	1.39E-05
180.0	2.82%	9.50E-03	2.69E-04	2.16%	4.33E-05	180.0	1.25%	4.18E-03	5.22E-05	0.87%	1.39E-05	240.0	1.93%	6.47E-03	1.25E-04	1.74%	3.45E-06
240.0	3.75%	1.27E-02	4.77E-04	3.42%	1.09E-05	240.0	1.93%	6.47E-03	1.25E-04	1.74%	3.45E-06	300.0	2.54%	8.54E-03	2.17E-04	2.76%	4.84E-06
300.0	5.00%	1.69E-02	8.52E-04	5.54%	2.95E-05	300.0	2.54%	8.54E-03	2.17E-04	2.76%	4.84E-06						
					0.02%						0.004%						

Table D-3: Regression results of kinetic model fitting for tantalum extraction experiments at 15 g and 5 mL/min.

150°C, 5 mL/min, 15 g, 2 wt%						150°C, 5mL/min ,15 g, 10 wt%					
σ^2 2.52						σ^2 33.72					
t (min)	%Extraction	$g_{Fp}(X_i)$	$P_{Fp}(X_i)$	t/ τ	Error	t (min)	%Extraction	$g_{Fp}(X_i)$	$P_{Fp}(X_i)$	t/ τ	Error
30.0	3.94%	1.33E-02	5.28E-04	1.47%	6.14E-04	30.0	0.63%	0.0021	0.0000	0.25%	1.40E-05
60.0	9.68%	3.34E-02	3.26E-03	4.16%	3.04E-03	60.0	1.13%	0.0038	0.0000	0.52%	3.71E-05
90.0	15.76%	5.56E-02	8.92E-03	7.81%	6.32E-03	90.0	2.17%	0.0073	0.0002	1.27%	8.24E-05
120.0	20.62%	7.41E-02	1.57E-02	11.36%	8.58E-03	120.0	2.85%	0.0096	0.0003	1.89%	9.34E-05
180.0	33.08%	1.25E-01	4.32E-02	23.43%	9.32E-03	180.0	4.86%	0.0165	0.0008	4.36%	2.50E-05
240.0	51.11%	2.12E-01	1.16E-01	50.49%	3.87E-05	240.0	5.71%	0.0194	0.0011	5.70%	8.25E-09
300.0	56.44%	2.42E-01	1.47E-01	61.35%	2.42E-03	300.0	6.48%	0.0221	0.0014	7.07%	3.50E-05
3.03%						0.03%					

200°C, 5 mL/min, 15g, 2wt%						200°C, 5 mL/min, 15g, 10 wt%					
σ^2 2.96						σ^2 42.97					
t (min)	%Extraction	$g_{Fp}(X_i)$	$P_{Fp}(X_i)$	t/ τ	Error	t (min)	%Extraction	$g_{Fp}(X_i)$	$P_{Fp}(X_i)$	t/ τ	Error
30.0	3.53%	1.19E-02	4.22E-04	1.31%	4.90E-04	30.0	1.09%	3.65E-03	3.98E-05	0.54%	3.07E-05
60.0	5.26%	1.79E-02	9.46E-04	2.07%	1.02E-03	60.0	1.82%	6.09E-03	1.11E-04	1.08%	5.34E-05
90.0	10.18%	3.52E-02	3.62E-03	4.59%	3.13E-03	90.0	2.47%	8.29E-03	2.05E-04	1.71%	5.72E-05
120.0	13.48%	4.71E-02	6.45E-03	6.62%	4.71E-03	120.0	2.64%	8.89E-03	2.36E-04	1.90%	5.50E-05
180.0	22.06%	7.97E-02	1.81E-02	13.31%	7.66E-03	180.0	3.46%	1.17E-02	4.06E-04	2.91%	3.04E-05
240.0	40.75%	1.60E-01	6.87E-02	36.31%	1.96E-03	240.0	4.70%	1.59E-02	7.52E-04	4.83%	1.56E-06
300.0	51.23%	2.13E-01	1.17E-01	55.78%	2.07E-03	300.0	5.27%	1.79E-02	9.48E-04	5.86%	3.52E-05
2.10%						0.03%					

Table D-4: Regression results of kinetic model fitting for tantalum extraction experiments at 50 g and 5 mL/min.

150°C, 5 mL/min, 50 g, 2 wt%						150°C, 5mL/min ,50 g, 10 wt%					
σ^2 12.32						σ^2 172.03					
t (min)	%Extraction	$g_{Fp}(X_i)$	$P_{Fp}(X_i)$	t/ τ	Error	t (min)	%Extraction	$g_{Fp}(X_i)$	$P_{Fp}(X_i)$	t/ τ	Error
30.0	3.23%	1.09E-02	3.54E-04	1.53%	0.03%	30.0	0.23%	7.83E-04	1.84E-06	0.11%	1.56E-06
60.0	5.41%	1.84E-02	9.99E-04	3.07%	0.05%	60.0	0.46%	1.53E-03	7.03E-06	0.27%	3.41E-06
90.0	8.43%	2.89E-02	2.46E-03	5.92%	0.06%	120.0	0.61%	2.05E-03	1.26E-05	0.42%	3.69E-06
120.0	10.74%	3.72E-02	4.04E-03	8.70%	0.04%	180.0	0.81%	2.72E-03	2.21E-05	0.65%	2.59E-06
180.0	12.21%	4.25E-02	5.26E-03	10.72%	0.02%	240.0	1.07%	3.57E-03	3.81E-05	1.01%	3.00E-07
240.0	15.27%	5.37E-02	8.35E-03	15.66%	0.00%	300.0	1.22%	4.08E-03	4.98E-05	1.26%	2.06E-07
300.0	17.17%	6.09E-02	1.07E-02	19.22%	0.04%	360.0	1.32%	4.41E-03	5.83E-05	1.44%	1.58E-06
0.25%						0.001%					

200°C, 5 mL/min, 50 g, 2wt%						200°C, 5 mL/min, 50 g, 10 wt%					
σ^2 17.36						σ^2 211.94					
t (min)	%Extraction	$g_{Fp}(X_i)$	$P_{Fp}(X_i)$	t/ τ	Error	t (min)	%Extraction	$g_{Fp}(X_i)$	$P_{Fp}(X_i)$	t/ τ	Error
30.0	0.98%	3.28E-03	3.21E-05	0.38%	3.56E-05	30.0	0.11%	3.66E-04	4.03E-07	0.05%	4.19E-07
60.0	1.22%	4.08E-03	4.99E-05	0.49%	5.26E-05	60.0	0.13%	4.18E-04	5.25E-07	0.05%	5.26E-07
90.0	1.60%	5.35E-03	8.56E-05	0.68%	8.34E-05	90.0	0.27%	9.06E-04	2.46E-06	0.14%	1.66E-06
120.0	3.07%	1.03E-02	3.18E-04	1.58%	2.20E-04	120.0	0.46%	1.54E-03	7.13E-06	0.31%	2.45E-06
180.0	6.98%	2.38E-02	1.67E-03	5.29%	2.85E-04	180.0	0.68%	2.28E-03	1.56E-05	0.56%	1.55E-06
240.0	10.19%	3.52E-02	3.63E-03	9.81%	1.41E-05	240.0	0.87%	2.90E-03	2.52E-05	0.82%	1.90E-07
300.0	11.96%	4.16E-02	5.04E-03	12.91%	9.03E-05	300.0	1.09%	3.63E-03	3.95E-05	1.20%	1.32E-06
0.08%						0.001%					

Determination of kinetic rate constants for tantalum experiments

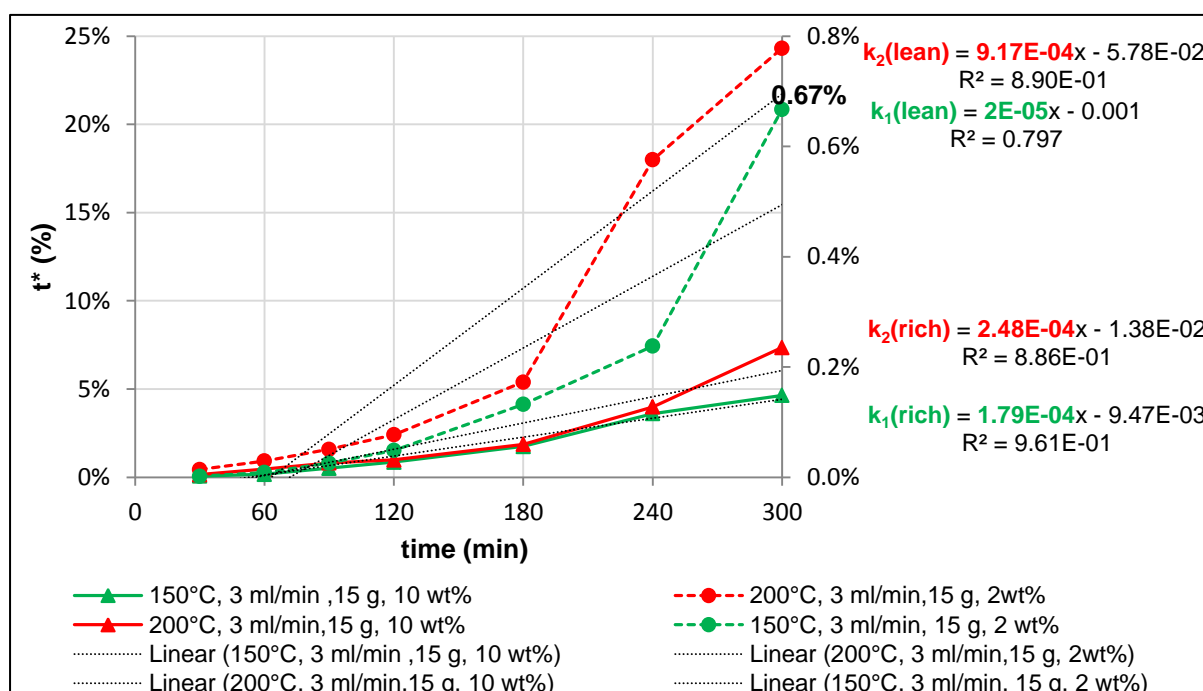


Figure D-1: Kinetic model regression curves for tantalum extraction experiments at 15 g and 3 mL/min.

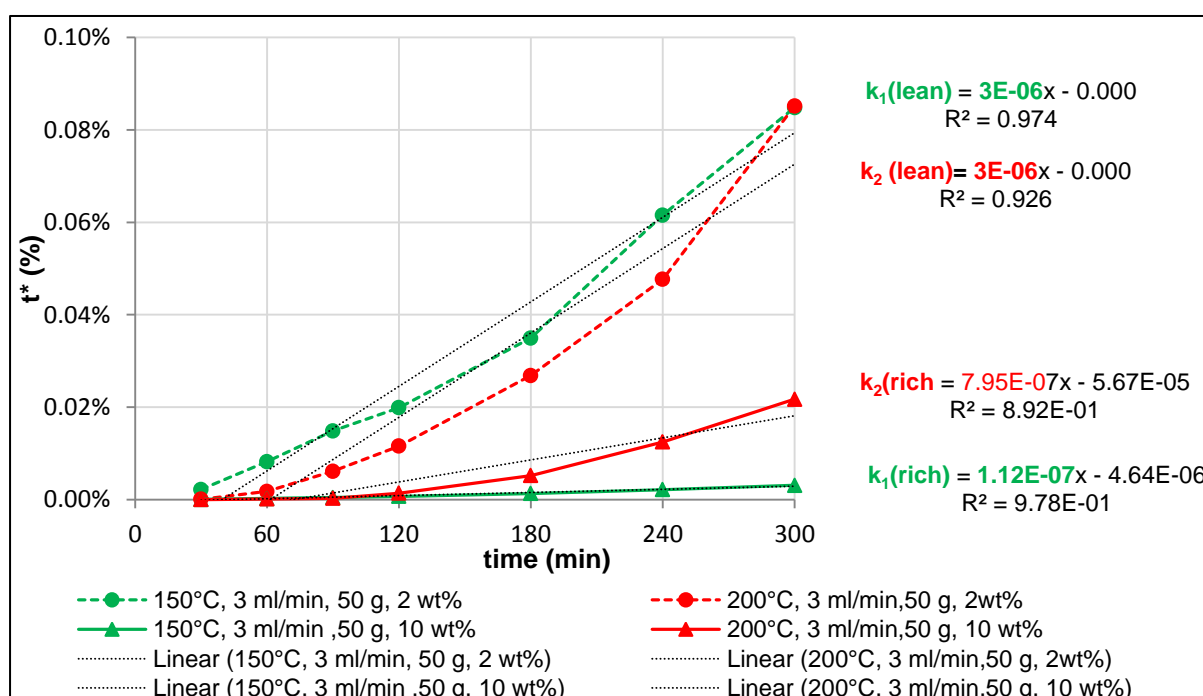


Figure D-2: Kinetic model regression curves for tantalum extraction experiments at 50 g and 3 mL/min.

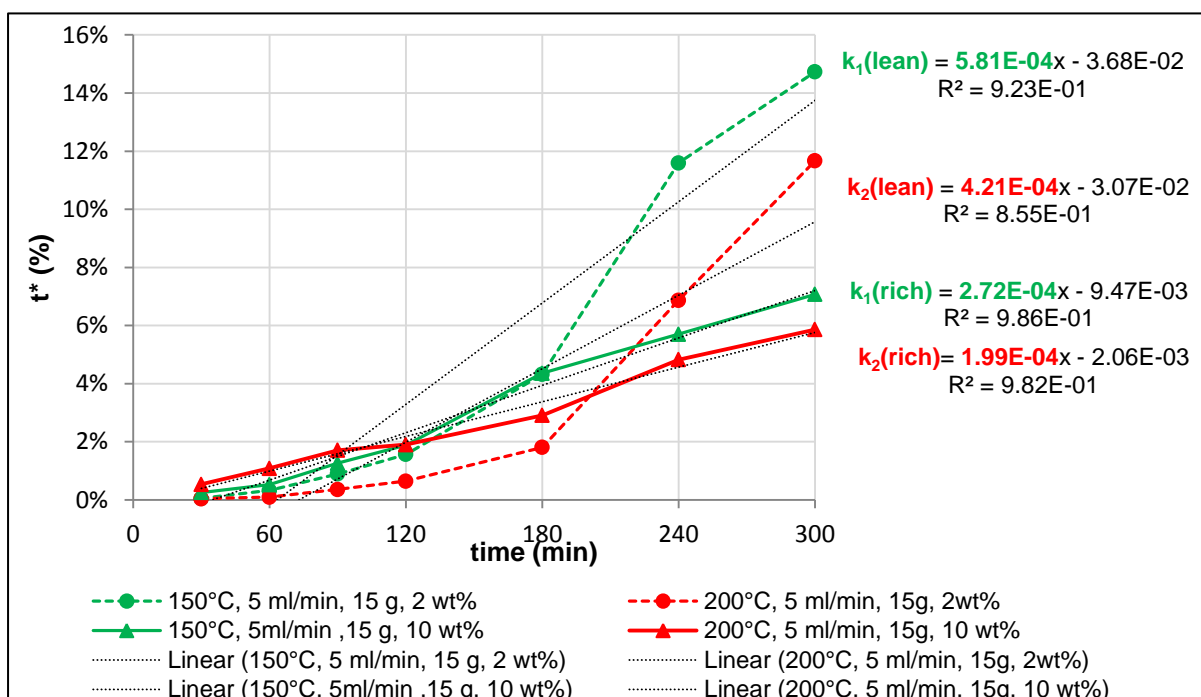


Figure D-3: Kinetic model regression curves for tantalum extraction experiments at 15 g and 5 mL/min.

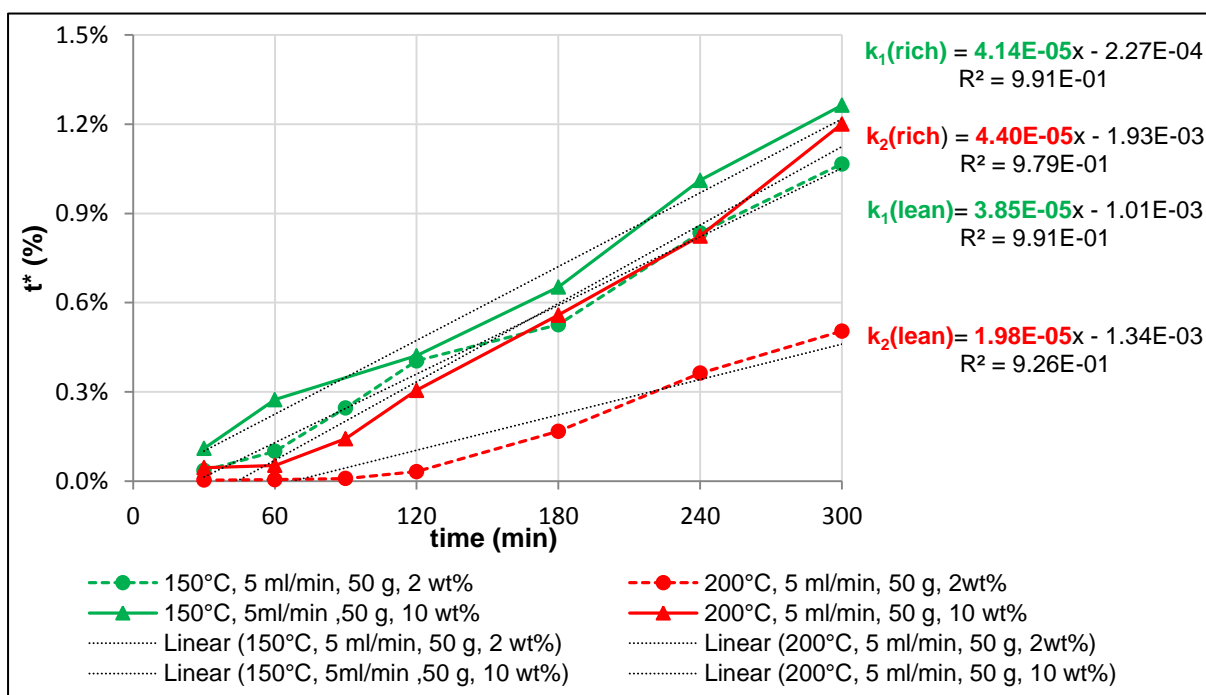


Figure D-4: Kinetic model regression curves for tantalum extraction experiments at 50 g and 5 mL/min.